On the importance of benzo(a)pyrene induced paternal DNA damage for the pre-implantation embryo

Tonje Danielsen Rongved

Master thesis in Toxicology

Department of Toxicology

Institute of Biology

UNIVERSITETET I OSLO

September 2011

Acknowledgements

The work that is presented in this master thesis is accomplished at the Department of Chemical Toxicology (MIKT), Division of Environmental Medicine at the Norwegian institute of public health (NIPH) in the time period from 08.2009 – 09.2011. My primary supervisor has been Birgitte Lindeman PhD and my co-supervisor has been Christine Instanes PhD. Professor Steinar Øvrebø PhD at the Department of Toxicology and Ecophysiology, Institute of Biology, University of Oslo has served as my inside supervisor at the University.

The choice of subject for this master thesis was mainly because of my interest in human toxicology and the field of reproduction has always captured my admiration. I would like to thank Gunnar Brunborg PhD for letting me perform my master thesis at his laboratory. My thanks also go to everyone at the MIKT department for a warm and welcoming environment, and for assist in the lab.

Thank you Birgitte, for all your help, your knowledge is irreplaceable. Thank you for being so supportive, and for never giving up on me or the project.

Thank you Christine, because you answer all my questions with always reasonable answers, and also because you are so kind and caring.

Thank you Nur, for always being there when questions needs to be answered.

Thank you Pappa, for your time, love and knowledge.

Thank you Mamma and Ingvild, for always being there for me.

Thank you Inger Lise, for being my best friend.

Thank you Lars, because you are you.

Oslo, August 2011

Tonje Danielsen Rongved

Table of contents

Abstract

Humans are under a constant influence from a vast number of environmental mutagens. Many of these are genotoxic, and therefore a constant threat to the integrity of the human genome. A reduced fertility potential has been observed in couples from industrialised areas, and Norwegian and Danish men have shown to have a reduced sperm quality compared to men in other countries from the Northern Europe. A connection between this reduced fertility and a continuous exposure to environmental mutagens may be expected.

The ubiquitous environmental mutagen Benzo(a)pyrene (BaP) has been studied in this master thesis, with the aim to examine potential genotoxic damage in male reproductive cells and the possible transmission of such damage to the embryo. Paternal exposure to BaP is embryo-toxic, and the sperm chromatin structure assay (SCSA) has been used to examine if there were enhanced levels of DNA damage in sperm cells from mice exposed to BaP *in vivo* (150 mg/kg i.p.). The use of knock out ($Ogg1^{-/-}$) mice compared to wild type animals was proposed as a model for human toxicological testicular responses. Studies has shown that sperm cells hold a high amount of 7,8-diol-9,10-epoxide (BPDE)-DNA adducts after BaP-exposure. However, the SCSA showed no statistical significant differences in the amount of DNA damage between BaP-exposed, vehicle and control animals. This indicates that BaP-exposure does not induce sperm DNA strand breaks and that the SCSA is an unsuited assay for measuring BaP-induced DNA alterations. A study has shown that sperm BPDE-DNA adducts may persist during the first embryonic cell divisions. Work with verifying this observation required a procedure for staining of BPDE-DNA adducts and a method for handling embryos before staining of potential adducts. This latter procedure was challenging and gave poor results, although the procedure and method is improved for future work with immunostaining of embryos.

Somatic mutagens are considered mutagenic also to male germ cells if the substance reaches testicular tissue. An *in vivo* somatic mutation assay called the Pig-a assay has also been a part of this master project. Establishment of this assay has included a positive control experiment with N-ethyl-N-nitrosourea (ENU) exposed mice. The assay proved to be sensitive for detecting somatic mutations in blood samples from mice, and suggestions for improvements has been made. Further work with the Pig-a assay seems promising, and the assay may have great potential in regulatory toxicology studies on chemical agents.

Abbrevations

8-oxoG	7,8-dihydro-8-oxodeoxyguanosine
AhR	Aryl Hydrocarbon receptor
AKR	Aldo-Keto Reductase
AO	Acridin Orange
ANOVA	Analysis of Variance
APC	Allophycocyanin
ARNT	Aryl hydrocarbon receptor nuclear translocator
ATP	Adenosine triphosphate
BaP	Benzo(a)pyrene
BER	Base excision repair
BSS	Buffered salt solution
Bw	Bodyweight
BPDE	7,8-diol-9,10-epoxide
BSA	Bovine Serum albumin
Comet	Single Cell Gel Electrophoresis
CYP	Cytochrome p-450
ddH20	Double distilled water
DFI	DNA fragmentation index
DMSO	Dimethyl sulphoxide
DNA	Deoxyribonucleic acid
DsDNA	Double stranded DNA
EDTA	Ethylenediaminetetraacetic acid
EH	Epoxide hydrolase
ENU	N-ethyl-N-nitrosourea
FCS	Fetal bovine serum
FITC	Fluorescein isothiocyanate
FSH	Follicle stimulating hormone
GPI	Glycosylphosphatidylinisotol
GST	Glutathione-S-transferase
HCG	Human Chorionic Gonadotropin
HCl	Hydrogen Chloride
ICC	Immunocytochemistry

i.p.	Intraperitoneal
IVF	In vitro fertilization
KO	Knock out
KSOM	Potassium simplex optimisation medium
LDLo	Lethal Dose Low
MEM	Minimum essential medium
MIKT	Department of chemical toxicology
MgCl	Magnesium chloride
MRNA	Messenger ribonucleic acid
NADPH	Nicotinamide adenine dinucleotide phosphate
NER	Nucleotide excision repair
NIPH	Norwegian Institute of Public Health
OGG1	8-oxoguanine-DNA glycosylase
PAH	Polycyclic aromatic hydrocarbon
PBS	Phosphate buffered saline
PE	Phycoerythrin
Pig-a	phosphatidylinositol glycan anchor biosynthesis, class A
PMSG	Pregnant Mare Serum Gonadotropin
PMT	Photomultiplier tube
RBC	Red blood cell
RET	Reticulocyte
RNA	Ribonucleic acid
ROS	Reactive oxygen species
SCSA	Sperm Chromatin Structure Assay
SD	Standard deviation
SE	Standard Error
SsDNA	Single stranded DNA
TUNEL	Terminal deoxynucleotidyl transferase dUTP nick end labelling
WT	Wild type
XRE	Xenobiotic responsive element

1. Introduction

1.1 General background

Reproduction is an important element in life for most humans and for the evolutionary history of all species. In the last decades infertility has become a growing problem. Especially in the Western World an increasing amount of couples have difficulty with conceiving or complete the gestation and hence this has become a public health issue. The increasing infertility is caused by both female and male factors and to establish the background for this essential biological concern, insight and determined research is needed. In developed countries in the European Union, birth rates have decreased continuously during the past half century (Barratt *et al*., 2010). Scandinavian men have been found to have reduced scores in semen quality compared to men in other European countries. In a fertility study including men from the Northern Europe, Norwegian and Danish men had the lowest sperm concentrations, while Finnish and Estonian men had the highest sperm counts (Jørgensen *et al*., 2006) The risk for testicular cancer is also higher in Norway and Denmark compared to other European countries (Giwercman and Giwercman 2011; Jørgensen *et al*., 2006). Testicular cancer typically arises from the germ cells in testis, and a correlation between infertility and testicular germ cell tumour has been observed (Hotaling and Walsh 2009). The incidents of testicular cancer are generally increasing, especially among young men from 15 to 35 years. The occurrences are assumed to double every 15 to 25 years (Adami *et al*., 1994).

There are numerous and complex causes for this observed direction of decreased fertility. A generally higher age of both men and woman when conceiving is observed and believed to be a contributing cause (Kidd *et al*., 2001). However, environmental and lifestyle factors are believed to have vast impact on both semen quality and testicular cancer. People in the Western world are daily exposed to a high number of toxicants from the approximately 70.000 chemicals used in commerce (Anastas and Williamson 1996). Only a few of these chemicals have been evaluated in particular for their potential to cause sperm DNA damage and affect sperm cells (Barratt *et al*., 2010).

Air pollution is a major contributor to human exposure of chemicals. Polycyclic aromatic hydrocarbons (PAHs), nitrated and halogenated organic compounds and metals are all present in the ambient air and can affect human health (Wolterbeek 2002). PAHs are some of

the most potent human carcinogens and many of them are also complete carcinogens with ability to both initiate and promote cancer (Boström *et al*., 2002). The use of cigarettes is still widely distributed although more than 60 carcinogens have been detected in mainstream and side stream cigarette smoke and tobacco has proved to be highly carcinogenic (Hecht 2003; Lewtas 2007). PAHs are one of the important groups of carcinogenic compounds in cigarette smoke, and cigarette smoke is therefore a significant exposure source of PAHs to humans (Pfeifer *et al*., 2002). PAHs stimulate oxidative stress and have mutagenic and carcinogenic activity in human cells (Boström *et al*., 2002). These damaging effects may reduce human fertility, and are important to evaluate both in somatic cells and germ cells.

Smoking may affect the fertility potential in both males and females, and smoking during gestation is a well known risk factor for damage and alterations of the offspring's fitness and genetic integrity (Vine 1996; Zenzes *et al*., 1999a; Zenzes 2000). The maternal influence and input to the genetic composition of the embryo have for a long time been the main health focus before and during gestation. The fact that both sperm and egg contributes equally with 50 % of the genes to the embryo, has given the paternal influence more attention (Delbes *et al*., 2010; Ji *et al*., 1997; Olsen *et al*., 2005; Zenzes 2000). Paternal smoking has proven to give a genetic transmission of modified DNA to the embryo, in the manner of detectable DNA adducts (Zenzes *et al*., 1999b).

A broad assortment of studies has confirmed that toxicants in cigarettes affect the sperm cells in men by reduced sperm count, motility and an increase in sperm with abnormal morphology (Künzle *et al*., 2003; Vine 1996). One of these studies showed that heavily smoking men had a 19 % lower mean sperm concentration, and a 13 % lower mean percentage of motile sperm than non-smoking men (Ramlau-Hansen *et al*., 2006). In a study using *in vitro* fertilisation (IVF) it was shown that the number of clinical pregnancies was significantly reduced (40%) in smoking compared to non-smoking men (Zitzmann *et al*., 2003). The DNA integrity of sperm cells can potentially be a valuable and independent indicator for infertility.

1.2 Male reproduction

1.2.1 The male reproductive organ

Sperm production (spermatogenesis) takes place in small seminiferous tubules of the testis which are all bounded by a basal membrane. Each tubule contains a fluid filled lumen that harvests the spermatozoa. The wall consists of developing germ cells and a permanent population of somatic Sertoli cells (Bellve *et al*., 1977; Borg *et al*., 2010). The Sertoli cells extend from the basal membrane out to the core of the lumen and are joined together in tight junctions that form the basis of the blood-testis barrier. The barrier controls the free exchange of endogenous substances as well as chemicals and drugs between the blood and fluid inside the seminiferous tubules. Degree of lipid solubility, size and ionisation are factors that determine whether a substance can penetrate the barrier or not. Small ionised hydrophobic substances most easily pass the barrier. Sertoli cells also provide nutrients, endocrine and paracrine substances and organise the delivery of mature spermatides into the tubular lumen (Borg *et al*., 2010; Holstein *et al*., 2003; Vander *et al*., 2001b). An interstitial space surrounds the seminiferous tubules and consists of connective tissue with Leydig cells, blood vessels and immune cells. Leydig cells are the most numerous cell type and a major producer of androgens and especially testosterone (Borg *et al*., 2010).

The numerous seminiferous tubules gathers in a network called the rete testis. The small ducts are then called efferent ductules and leave the rete testis in one single duct. This gathers into the epididymis, which is loosely attached to the testis. The epididymis is divided into a head (caput), body (corpus) and tail (cauda). The epididymis from each testis leads to the vas deferens, which is a thick walled tube behind the urinary bladder bound together with blood vessels and nerves in the spermatic cord. Ducts from two seminal vesicles connect the vas deferenses and form two ejaculatory ducts that join the urethra out of the penis. Substance from the prostate gland is added during ejaculation to enhance the motility of the sperm (Vander *et al*., 2001b). Figure 1.1 shows the anatomy of the testis.

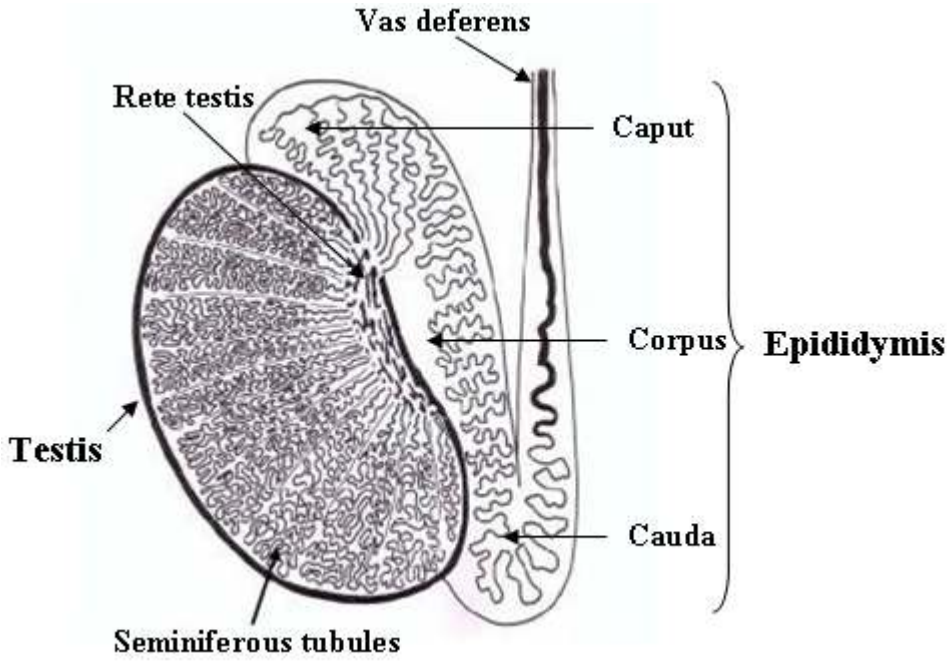

Figure 1.1 Anatomy of the human testis. The seminiferous tubules in testis are connected in the rete testis, which leads to the epididymis. Maturation of the spermatozoa occurs during transit through the caput, corpus and cauda epididymis (modified from Holstein *et al.*, 2003).

1.2.2 Spermatogenesis

Spermatogenesis is the constant development of germ cells into mature sperm cells. The development includes series of events with establishment of a stem cell population, mitosis, meiosis and morphogenesis of the haploid germ cell (Borg *et al*., 2010). Already in the male embryo the testes contain germ cells that differentiate into spermatogonia. Spermatogonia multiply continuously in successive mitosis, and can be divided into a type A and type B. Type A belongs in the stem cell pool and type B starts the development towards future spermatides. The spermatogenesis first begins at puberty when type B spermatogonia differentiate into primary spermatocytes. These are developed to secondary spermatocytes in a first meiotic cell division and then into haploid spermatides in a second meiotic division. This is called the spermiogenesis and reduces the chromosome number from diploid (2n) to haploid (n) (figure 1.2). Spermiation is the transfer of spermatides by Sertoli cells out from the germinal epithelium and in to the lumen of the seminiferous tubule. Spermatozoa are then transferred into the rete testis and further into the epididymis (Campbell and Reece 2005; Holstein *et al*., 2003).

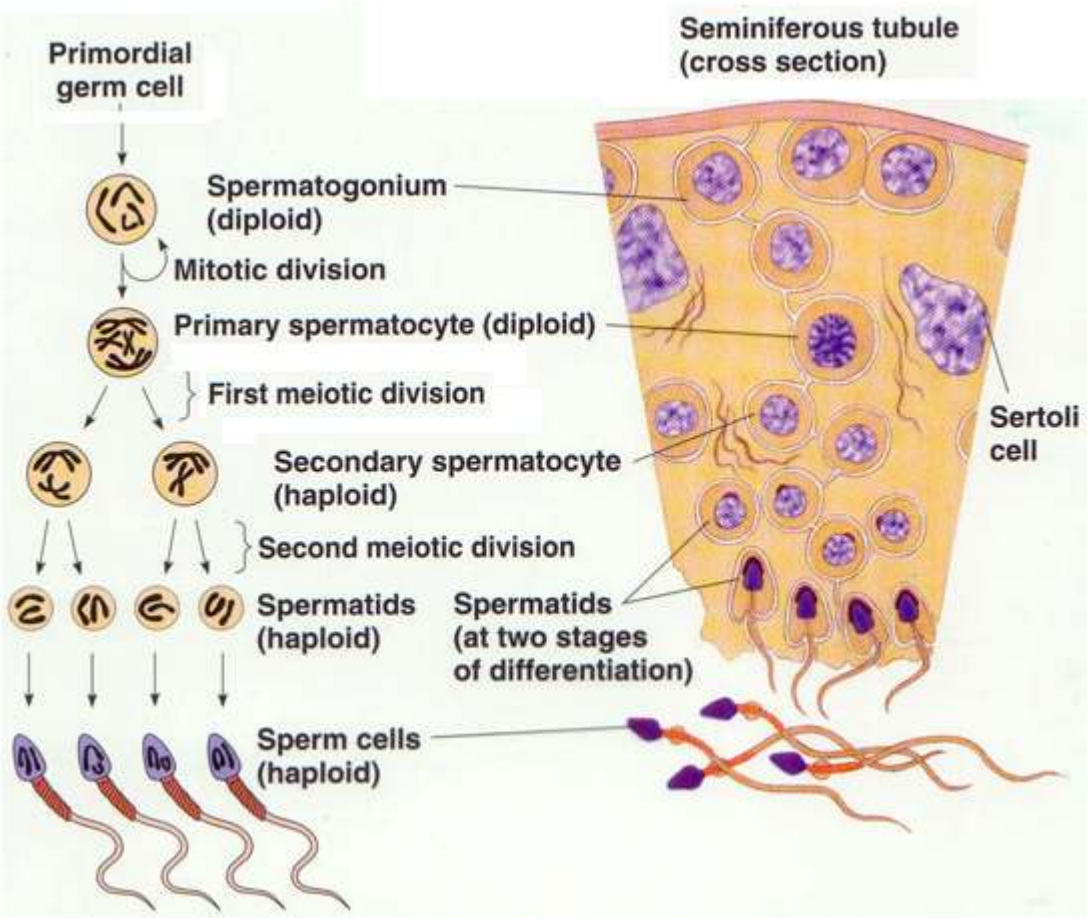

Figure 1.2 Spermatogenesis in seminiferous tubules of the testis. Germ cells are present in the wall of the seminiferous tubules together with somatic Sertoli cells. Germ cells differentiated into spermatogonia proliferates by mitotic divisions, and some of them differentiate into primary diploid spermatocytes. The first meiotic cell division produce two secondary spermatocytes, which undergo a second meiotic division into four haploid spermatides that are released into the lumen of the seminiferous tubules for transfer to the rete testis (modified from Campbell and Reece 2005).

The spermatozoa in rete testis are structurally complete, although functionally still immature. The caput and corpus areas of the epididymis are adapted to give spermatozoa a further maturation and modification, which is essential for the sperm for fertilisation of the oocyte. The main function of the caudal part of the epididymis is sperm storage (Bedford 1994; Borg *et al*., 2010). Modifications during transfer in the epididymis include morphological changes, stabilisation of the chromatin and changes in membrane composition (Borg *et al*., 2010; Dadoune 2003). Spermatozoa gain an increase in potential for forward motility, which is essential for reaching the female reproductive tract. Capability to recognise, bind and fuse with the oocyte also arises in the epididymis, via increased ability to undergo acrosome reaction. All these modifications participate in a full maturation of the spermatozoa (Moore 1998). The spermatogenesis in humans takes approximately 64 days (Heller and Clermont

1963). Additional 2-6 days is needed for the sperm to pass along the epididymis, and normal storage capacity in the cauda is 3-4 days (Moore 1998; Rowley *et al.*, 1970). Spermatogenesis in mice takes approximately 35 days (Oakberg 1956), with an additional 7-10 days for passage of sperm along the epididymis (Oakberg and Diminno 1960). There are several stages in the process of spermatogenesis and transfer through the epididymis that are sensitive for interfering agents and toxicants.

1.2.3 The sperm cell

The sperm cell is divided into a head and tail. The nucleus with condensed chromatin linked by protamines is localised in the head with a nuclear envelope and a perinuclear theca that forms a firm shell of proteins that covers the nucleus. The acrosome is localised in the apical part of the sperm cell, and contains enzymes needed for penetration of the oocyte. A mitochondrial sheath is present behind the head and provides adenosine triphosphate (ATP) for movement of the sperm cell. Behind the mitochondrial sheath is the tail or flagellum, which is composed of microtubules connected by dynein arms and generates motility (figure 1.3) (De Jonge and Barratt 2006). The sperm cells in rodent and humans have different morphology, with a hook-shaped head in rodents and a spatula-shaped head in humans (De Jonge and Barratt 2006). Sperm cells could be an efficient way for studying exposure of environmental toxicants in humans, and variation in quality between populations or individuals could be linked to external environmental and lifestyle factors. Establishment of a complete relationship with sperm integrity and human fertility must be the ultimate goal (Sipinen *et al*., 2010).

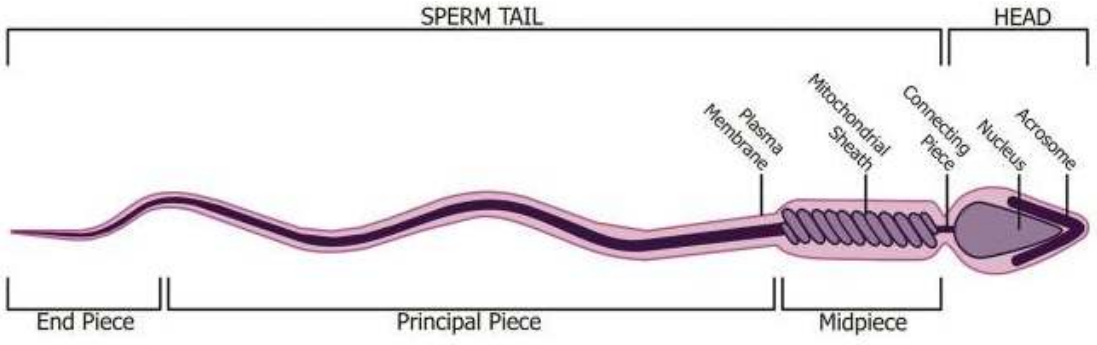

Figure 1.3 Schematic illustration of the anatomy of the sperm cell. The head is covered by an acrosome that facilitates binding to the oocyte. The head contains the nucleus with DNA. Behind the head is a mitochondrial sheath that provides ATP for movement of the flagellum (tail) (Borg *et al.*, 2010).

1.2.4 DNA packing in sperm cells

In the early stages of spermiogenesis, the chromatin in germ cells is arranged in the same way as somatic cells, with nucleosome core particles in histones that make transcription achievable. During development of the sperm cells in the spermiogenesis, the sperm chromatin modifies to a more resistant and compact structure. The histones get hyper-acetylated and the nucleosomes are disassembled. Transcription stops when the enzyme Topoisomerase II unwinds the DNA helix, and transition proteins bind DNA. At the end of spermiogenesis, the transition proteins are replaced by small proteins called protamines, enabling a high degree of chromatin condensation (Oliva 2006). During maturation of sperm cells in the epididymis, formation of disulphide bonds stabilises the nucleoprotamine complex. The DNA and protamines are coiled into compact toroides that contains about 50 kb of DNA (D'Occhio *et al*., 2007). About ninety percent of mature sperm chromatin is bound to protamines, while the remaining 10 % is still linked by histones (Barratt *et al*., 2010). During fertilisation and before the first cleavage division of the zygote, the nucleoprotamine structure is unpacked and restructured into nucleosomes. This is to obtain a looser chromatin configuration for DNA replication in the first mitotic division of the embryo (Oliva 2006). The protamine configuration in sperm cells give higher motility and protect the genetic material from external stress and physical disruption during transfer through the epididymis and female reproductive tract (Perreault 1992).

1.3 Female reproduction

1.3.1 The female reproductive organ

The ovaries produce eggs and are located in the pelvis at each side of the uterus, and also secrete oestrogen and progesterone out in the blood stream. In humans the oviduct is divided into three parts named the Infundibulum, Ampulla and Isthmus. During ovulation the ovary releases a secondary oocyte into the Infundibulum. The oocyte is surrounded by a zona pelludica, corona radiate and nourishing cumulus cells. The oocyte complex travels into the Ampulla where fertilisation may occur. After fertilisation, the pre-implant embryo undergoes cleavages and is transported through the Isthmus to the uterus where it becomes implanted in the endometrium (figure 1.4) (Talbot and Riveles 2005).

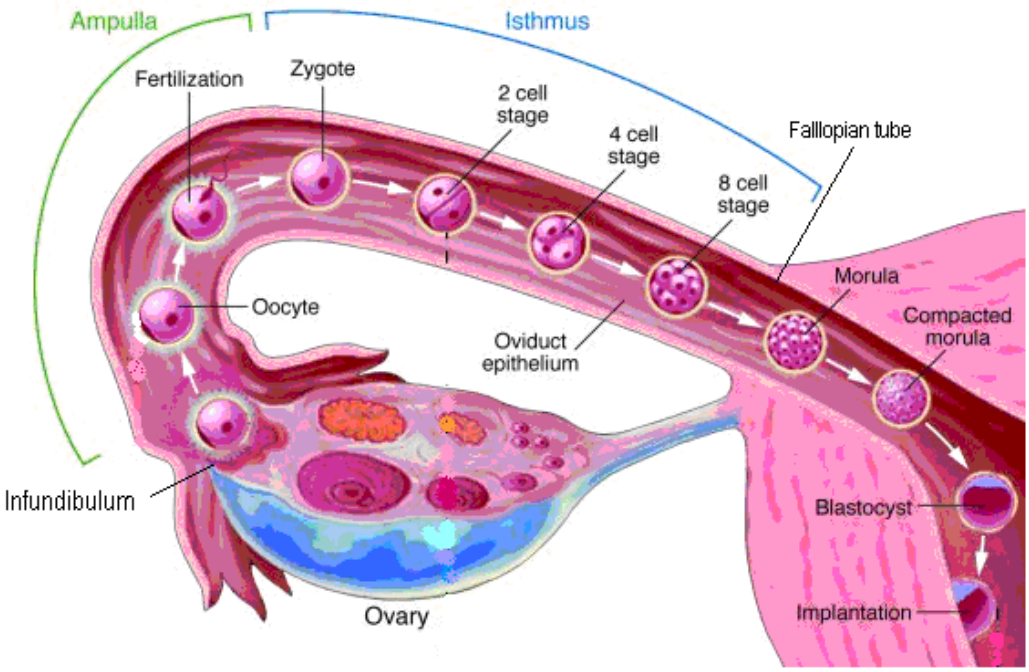

Figure 1.4 Anatomy of the uterus, oviduct and ovary. The ovary produces eggs that are released one at the time as secondary oocytes into the Infundibulum, and transported further into the Ampulla for fertilisation. After fertilisation, the pre-implantation embryo travels down the Isthmus while it undergoes cell divisions. The pre-implantation embryo reaches a compact morula stage and becomes a blastocyst before implantation in the uterus (Schuel 2006).

1.3.2 Oogenesis

Oogenesis is the production of an ovum that can be fertilised by a sperm cell. Differentiation of germ cells into ovary specific stem cells called oogonia already begins in the female embryo. Oogoniums proliferate by mitosis and starts meiosis, however, the progression arrests at prophase I. The cells are now called primary oocytes and will settle in ovary follicles until puberty. When puberty is reached, hormones including the follicle stimulating hormone (FSH) stimulate the primary oocytes. Meiosis I is completed and meiosis II starts, before another arrest at metaphase II. The primary oocytes have now developed into secondary oocytes with a first polar body. The oocytes are released one at the time as the follicles breaks open under ovulation each month. Meiosis carries on when a sperm fertilize the secondary oocyte in the Ampulla, and the oogenesis is accomplished when an ovum is produced, which is a haploid female reproductive gamete. All the meiotic events involve unequal cytokinesis and the smaller cells become polar bodies (Campbell and Reece 2005; Jaroudi and SenGupta 2007).

1.4 Fertilisation

Fertilisation in mammals occur when the membranes of spermatozoa and oocyte fuses and the sperm cell enters the oocyte. The sperm cell must bind the zona pellucida and cumulus cells surrounding the oocyte. This event is irreversible and initiates a calcium dependent transduction pathway that results in exocytosis of the sperm acrosome. Hydrolytic enzymes are released and facilitate breakthrough of the sperm in the zona pellucida (Borg *et al*., 2010). Following fertilisation, the oocyte completes meiosis and becomes a zygote where the oocyte and sperm chromosomes are captured in the female and male pro-nuclei. The chromosomes are replicated before the first cleavage of the zygote. The zygote starts the travel down the oviduct, and undergoes mitosis into smaller daughter cells called blastomers. Roughly around the 16-cell stage, the oocyte is called the morula and has a fluid filled cavity that is transformed to a blastocyst. The blastocyst has an inner and outer cell mass celled the embryoblast and thropoblast, respectively. The inner mass gives rise to the embryo while the outer mass is the source of the placenta (figure 1.5). The blastocyst is released from the zona pellucida when the embryo reaches the uterus, and the embryo interacts with the endometrium for implantation (Jaroudi and SenGupta 2007). Spermatozoa with DNA damage may be capable of fertilizing an oocyte, however, development and survival of the embryo is highly related to integrity of the genetic material (Ahmadi and Ng 1999).

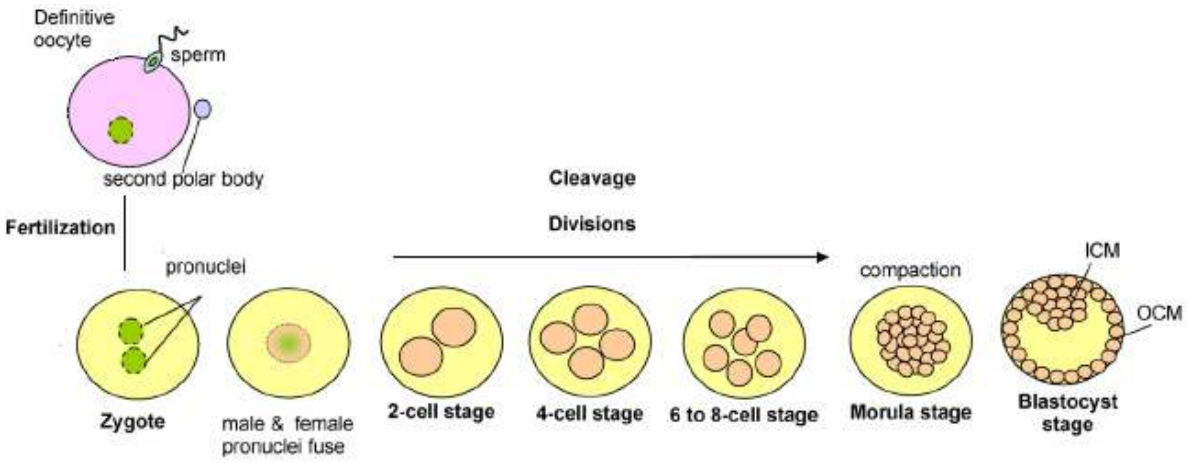

Figure 1.5 Fertilization and development of the pre-implantation embryo(modified from Jaroudi and SenGupta2007).

1.5 *In vitro* fertilisation (IVF)

In vitro fertilisation (IVF) is fertilisation of oocytes by sperm cells outside the body.
The history of IVF dates back to experiments in the 1800 century with successful transfer of embryos from an oviduct in rabbit to the uterus in hare. The first successful completed IVF was carried out with rabbit oocytes in 1959 (Chang 1959; Zhao *et al*., 2011). Experiments with human strategies for IVF were improved, and in 1978 the first successful human test tube baby was born (Steptoe and Edwards 1978). The IVF technique is now well established and is applied for production of embryos to research experiments, treatment of human infertility, enhancing productivity of domestic animals and for conservation of endangered animals. IVF protocols are now available for most species, including mice, and can produce fertilized ova and viable offspring after transfer to recipient females (Bavister 2002).

1.6 Polycyclic aromatic hydrocarbons with focus on Benzo(a)Pyrene

1.6.1 Properties of BaP

Benzo(a)pyrene (BaP) is a PAH in the class of benzopyrenes, which is composed of a benzene ring fused with a pyrene molecule. BaP consists of five benzene rings ($C_{20}H_{12}$) and have a molar mass of 252.31. The melting and boiling points are 179°C and 495°C respectively. BaP is lipophilic with a LogP of 6.19 and the estimated half lives are <1-6 days in the atmosphere, <1-8 hours in water, 5-10 years in sediment and >14-16 months in soil (Spectrum Laboratories 2000).

The mutagenic and carcinogenic potential of BaP is caused by arrangement of the benzene rings in a bay region (figure 1.6). Carbon 9-12 is considered to be the bay region and carbon 10 is regarded as an active centre (Miller and Ramos 2001). The bay region in BaP is a sterically hindered cup-shaped area. Thus, oxidation or radical formation occurs more easily, while detoxification and conjugation is impeded because of the bay region structure. Binding of an epoxide in this area makes BaP a diol epoxide, which is an ultimate carcinogen (Conney 1982; Dabestani and Ivanov 1999; Sims *et al*., 1974). The BaP molecule also contains a K-region in carbon 4 and 5, with high electron density and therefore high metabolic activity (Miller and Ramos 2001).

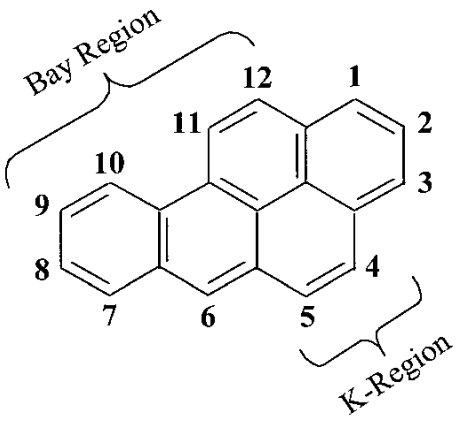

Figure 1.6 The structure of Benzo(a)pyrene (Miller and Ramos 2001)

1.6.2 Occurrence and sources of PAH and BaP

PAHs are formed during incomplete combustion of organic material at 300-600°C. Sources to PAHs are diesel engine emission, automobile exhaust, cigarette smoke, oil and coal, smoke formed by heating with wood and fried food (Boffetta *et al*., 1997; Boström *et al*., 2002; Lewtas 2007). A part of the PAHs in the atmosphere also arises from natural combustion in forest fires and volcanic eruptions (Nikolaou *et al*., 1984). During the past centuries, especially in industrialised countries, the occurrence and emission of PAHs have increased dramatically. This development is due to the abundant use of fuels for industrial applications, heating, transport and many other purposes, and as a consequence, the levels of PAHs in cities are higher than in rural areas. The total quantity of PAHs in the environment is not easy to measure due to various sources, mixtures and differences between areas. The most significant source of PAHs in countries like United States and Sweden is residential burning of wood. In the cities however, working machinery and vehicle exhaust contributes to the major part of the PAH emission (Boström *et al*., 2002). PAHs are ubiquitous and genotoxic and are therefore a constant threat to the integrity of our genomes.

BaP is the most well known and studied PAH (Boffetta *et al*., 1997; Jeffrey 1985; Verhofstad *et al.*, 2011). There is no commercial production or use of BaP, but all the mentioned sources releases BaP to the air where it may bind to particular matter. Ultraviolet radiation may catalyse oxidation and degradation of PAHs, and give dry deposition to land and water (Boström *et al*., 2002). In the last 30 years, the levels of BaP in the air have decreased significantly. In 1960 the BaP levels in some European cities approached 100 ng/m^3. Today the concentrations in Europe are often below 1 ng/m^3 at background stations and between 1-5 ng/m^3 in areas close to traffic (Boström *et al*., 2002). This development is

due to a reduction in the use of coal and open burning, and an increase in use of oil and natural gas energy sources ,as well as improved combustion technology (Baek *et al*., 1991).

1.7 Metabolism of BaP

1.7.1 Bioactivation

Xenobiotics including PAHs are often hydrophobic and non-polar and may accumulate in cells because the environment is more hydrophilic. Metabolism of PAHs occurs in general in all tissues of the human body, with liver as the main organ for bioactivation due to the high amount of required enzymes. The large cytochrome p450 (CYP) family together with several other enzymes participate in the metabolism (Conney 1982; Kemper *et al*., 2008). Phase I enzymes for metabolism of BaP includes several CYP p450 enzymes, epoxide reductase (ER) and epoxide hydratase (EH). Primary metabolites of BaP are epoxides, dihydrodiols, phenols, and quinones (Gelboin 1980; Selkirk 1977). Phase II conjugating enzymes includes glutathione-S-transferases (GST), UDP-glucurosyltransferases (UGT) and sulfotransferases (SULT) (Gelboin1980). Secondary metabolites of BaP are formed following further enzymatic attack of primary metabolites, and the enzymes can react with available hydrogen molecules in BaP. Both phase I and phase II enzymes have the purpose of altering BaP to intermediates with higher hydrophilicity, for easier elimination from the organism. BaP is metabolised to numerous metabolites, with three main pathways for bioactivation as reviewed by Xue and Warshawsky in 2005.

In BaP, the bay region dihydrodiol epoxide pathway starts when oxygen is introduced at a double bond by CYP1A1/ 1A2/1B1 and creates BaP-7,8-oxide. Hydrolysis of BaP-7,8-oxide by epoxide hydrolase (EH) generates BaP-7,8-dihydroxy-7, 8-dihydrodiol (BaP-7,8-diol). Another CYP mediated oxidation at the double bond next to the diol group generates BaP-7,8-dihydroxy-9,10-epoxid (BaP-7,8-diol-9,10-epoxide, BPDE) (figure 1.7). BPDE can react and from stable adducts in the DNA (Conney 1982; Sims *et al*., 1974; Xue and Warshawsky 2005). Of all primary and secondary metabolites of BaP, the diol epoxides are the most mutagenic, cell-transforming, and carcinogenic metabolites (Pelkonen and Nebert 1982). Four isomeric BaP-7,8-diol-9,10-epoxides (± *anti* and ± *syn*) may be formed during activation of BaP (Baird *et al*., 2005). The (+) anti-BPDE isomer is referred to as an ultimate carcinogen, and it is also the most abundant of the four isomers (Takemura *et al*., 2010; Xue and Warshawsky 2005).

In the radical cation pathway peroxidase activity of CYP forms a BaP radical cation in a one-electron mediated oxidation (figure 1.7). The radical cations are electrophilic and have potential to interact with nucleophilic cores in cellular macromolecules like DNA. The electrophilic charge is generally localised at carbon 6 and 10 in BaP (Xue and Warshawsky 2005).

Reactive PAH-*ortho*-quinones may be formed when dihydrodiol dehydrogenase (DD) from the aldo-keto-reductase family (AKRs) competes with the CYP-enzymes and oxidise BaP-dihydrodiols (Penning 2004). The reaction is $NADP^+$ dependent, and forms a ketol that spontaneously rearrange to an unstable catecol, and becomes an electrophilic o-quinone by auto-oxidation (Smithgall *et al*., 1988). The o-quinones can be reduced to catecol again or they might form oxidative DNA adducts. Auto-oxidation subsequently generates radicals due to the redox cycle that generates reactive oxygen species (ROS) multiple times (Penning 2004; Xue and Warshawsky 2005). Quinone formation can account for a large metabolic yield of BaP in a variety of tissues (Lesko and Lorentzen 1985).

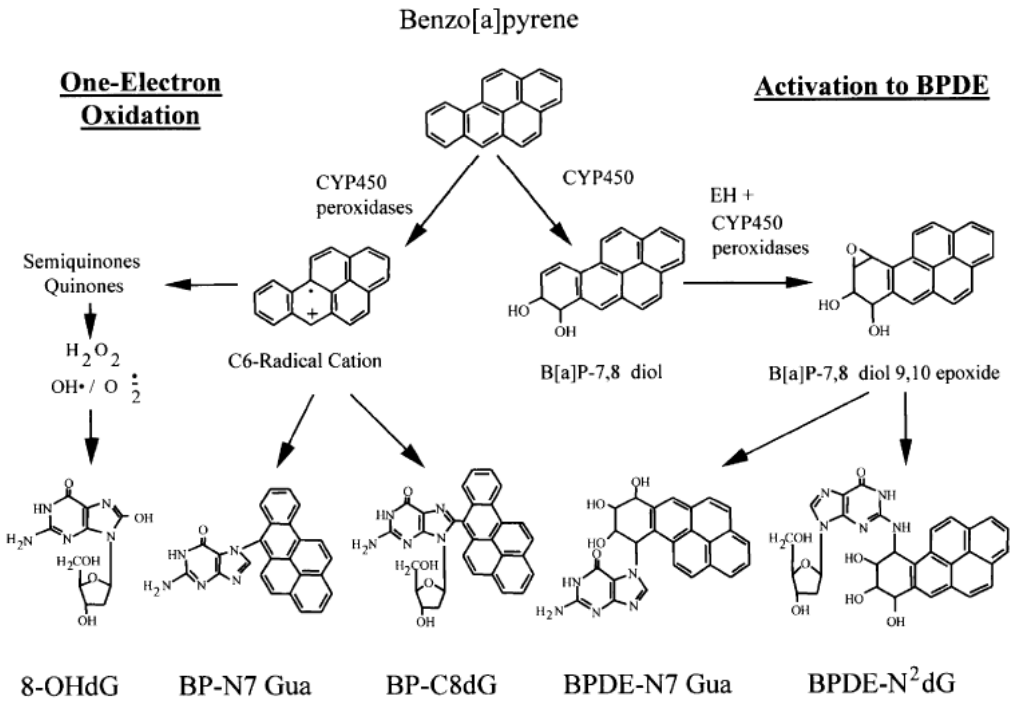

Figure 1.7 Pathways for BaP-induced DNA-adduct formation. BaP can form radical cations by one-electron mediated oxidation that produce adducts at position N7 and C8 in guanine. Toxic quinones may form the common 8-OHdG adduct, which may be transferred to 8-oxoG. The bioactivation of BaP to the reactive metabolite BPDE may form DNA-adducts, including BPDE-N^2-dG or BPDE-N7Gua (Godschalk *et al.*, 2003).

CYP1A1/1A2/1B1 enzymes are induced through the aryl hydrocarbon receptor (AhR) pathway. BaP binds to AhR in the cytoplasm of cells, which changes the receptors configuration and mediates active transport into the nuclei. AhR associates with Ah nuclear translocator protein (ARNT), and the complex binds to a xenobiotic response element (XRE) in the DNA which induces enhanced transcription of genes for the CYP enzymes (Kemper *et al*., 2008; Takemura *et al*., 2010; Tarantini *et al*., 2011).

1.7.2 Detoxification

Despite formation of potentially damaging intermediates that may promote cellular injury and toxicity, the purpose of oxidative metabolism of BaP is detoxification and elimination from the body (Roth and Vinegar 1990). The conjugating phase II enzymes attach functional groups to parts of the BaP molecule to increase their hydrophilic character. The initial metabolism of BaP through the CYP p450 monooxygenase system generates several oxide intermediates, including 7,8-oxide. These oxides can rearrange spontaneously to phenols, be hydrolysed to trans-dihydrodiols or react covalently with glutathione either spontaneously or catalysed by glutathione-S-transferases. Phenols, quinones and dihydrodiols can be conjugated to water-soluble compounds by either sulphation or glucuronidation (Gelboin1980). BaP phenols are the preferred substrates for UDP-glucuronyl transferases. Glutathione, glucuronide and sulphate conjugates are formed both *in vitro* and *in vivo* and glutathione conjugations are the most important pathway for detoxification of BaP. Excretion through hepatobiliary route and faeces is the most important route for elimination (Plummer *et al*., 1980).

1.8 Human exposure and toxicokinetics of BaP

Humans may be exposed to BaP via inhalation, oral intake through the gastrointestinal (GI) tract or dermally through the skin (Boffetta *et al.*, 1997; Boström *et al.*, 2002). These pathways give a distribution of BaP throughout the body, dependent on the administered route. PAHs including BaP generally enter lipophilic tissue in the body. BaP can pass over plasma membranes in cells due to its lipophilic properties, and associate with hydrophobic molecules that may distribute BaP throughout intracellular compartments (Miller and Ramos 2001). BaP tend to be accumulated in the kidneys, liver, and fatty tissue while smaller amounts are stored in the spleen, adrenal glands, and ovaries. The excretion depends on the route of administration, but is generally rapid within a few days (ATSDR 1995). The highest

non-occupational intake of BaP is through diet and represents for non-smokers 70 % of the total BaP-exposure (Phillips 1999).

BaP present in the air are usually bound to particles. The pulmonary absorption of BaP is therefore influenced by the solubility of the carrier particles. Inhaled PAHs may be absorbed via the mucous lining of the bronchi in lungs (ATSDR 1995). After inhalation of a single dose BaP (1µg/kg) in rats, 21 % was available in the liver within 10 minutes (Weyand and Bevan 1986). BaP inhalation in rats give high levels in the lungs, liver, kidney, gastrointestinal tract, esophagus, small intestine and blood (Sun *et al*., 1982). Generally, liver and bile is the major elimination route of PAHs in animals following inhalation exposure (ATSDR 1995).

Humans may be exposed to BaP orally by intake of fried and charcoal-grilled food, contaminated vegetables and crops, and contaminated drinking water (Boström *et al.*, 2002). Absorption of substances after oral intake in humans is dependent on lipophilicity of the compounds. Ingested PAHs may be absorbed in the GI in fat-soluble compounds. Absorption of BaP following ingestion is relatively low in humans (ATSDR 1995). BaP is distributed to the liver, lung, and kidneys after oral administration (Yamazaki *et al*., 1987). In a study with oral exposure to BaP (1µg BaP/kg) in rats there was some evidence of enterohepatic recirculation. Six hours after exposure, 53 % of the administered dose was excretes into intestine contents of the animals lacking a bile cannula. 77 % of the administated dose was recovered in bile, intestines and intestine contents of animals with a bile cannula over the same period (Weyand and Bevan 1986). After oral BaP-exposure in rats, elimination via faeces dominates in early excretion and urinary route dominates later (Ramesh *et al*., 2001).

Dermal exposure to BaP can occur through contact with soil that contains high levels of the toxicant, including petroleum products like soot and tars. Dermal absorption of PAHs appears to be rapid in both humans and animals, however, the extent of absorption is variable and affected by the vehicle used for administration. Dermal absorption occurs through passive diffusion (ATSDR 1995). Elimination of BaP after percutaneous exposure in rats occurs relatively rapid in the urine and faeces (Yang *et al*., 1989).

1.9 Toxicity

BaP toxicity is mediated by the reactive intermediates formed by oxidative metabolism. These intermediates may react with macromolecules in cells and give structural and functional alterations (Miller and Ramos 2001). The acute and sub-chronic toxic effects of BaP are relatively low. LDLO (lethal dose low) for mouse after intraperitoneal (i.p.) administration is 500 mg/kg bodyweight (Epstein *et al*., 1972). However, the chronic effects from low doses of BaP are of great concern. BaP toxicity may occur in cells (cytotoxicity), immune system, liver, hematopoietic system, the reproductive system and kidneys. A study has indicated that male rats are more sensitive for damage than female rats (ATSDR 1995; Knuckles *et al*., 2001). Inhalation of BaP may result in toxicity of the respiratory tract and lungs (ATSDR 1995).

1.10 Reproductive toxicity

BaP have potential to affect the reproductive system in both males and females. Exposure to BaP in mice is linked with early ovarian failure, destruction of oocytes and reduced fertility (Mattison *et al*., 1980). A study with administration of BaP by gavage in mice for ten days during gestation gave a reduced percentage of females able to bring forth progeny at the highest dose tested (160 mg/kg bw/day). The lowest dose tested (10 mg/kg bw/day) also gave reduced fertility, associated with alterations in gonadal morphology and germ cell development. Treatment with higher doses resulted in total sterility (MacKenzie and Angevine 1981).

The spermatogenesis in males may be susceptible for damage by toxicants in mitotic spermatogonia, meiotic germ cells, post meiotic spermatids and spermatozoa under maturation in the epididymis. This may affect the production and integrity of the mature sperm, and both double and single stranded breaks may occur in the DNA (Ahmadi and Ng 1999; Delbes *et al*., 2010). BaP-exposure to sperm cells give rise to bulky DNA adducts and potential transfer of these to embryonal DNA following fertilisation. In smoking couples, the amount of BaP related DNA-adducts in the embryo seemed more dependent on paternal than maternal smoking (Zenzes *et al*., 1999b). Smoking also has a dose related association to low quality of spermatozoa (Ahmadi and Ng 1999; Vine 1996). DNA integrity of sperm cells is essential for fertilisation and normal embryonal development (Barratt *et al*., 2010; Gaspari *et al*., 2003). Dominant lethality studies of mice may be performed for evaluation of

reproductive toxicity (Epstein *et al*., 1972; Generoso *et al*., 1982). Exposure of male mice to a high dose of BaP resulted in dominant lethal effects, indicated by a decreased number of living embryos due to high incidents of pre and post implantation losses (Generoso *et al*., 1982; Shukla and Taneja 2001).

1.11 Carcinogenesis

BaP is referred to as a pro-carcinogen and requires metabolic activation to become carcinogenic (Conney 1982). BaP is known as a complete carcinogen because it can facilitate carcinogenesis via its own metabolism (Baird *et al*., 2005). Previously BaP was placed in group 2B (possible carcinogenic to humans) on the list from International Agency for Research on Cancer (IARC), but extensive research have moved BaP to group 1 (carcinogenic to humans) (IARC 2011; Takemura *et al*., 2010).

In the early 1900s it became generally known that soot, coal and tar are carcinogenic to humans. Experiments with rabbits in 1915 proved carcinogenicity when this PAH containing material caused tumours at the site of application. In the early 1930, BaP was shown to cause tumours in rodents, and the use of BaP as a model for PAHs originates from this observation (Boström *et al*., 2002). Since then there has been a substantial number of studies on BaP and its carcinogenic potential. BaP produce tumours in experimental animals after administration via oral, skin and intratracheal routes. The carcinogenic effects of BaP are both local and systemic, and has shown to be carcinogenic in single-dose experiments (IARC 1973). Exposure to BaP is believed to cause tumours in a diverse range of human tissue, including lungs, skin, esophagus and colon, pancreas, bladder and breasts in woman. The effect is dependent on exposure route (Boström *et al*., 2002). Lung tumours have been identified following inhalation, i.p. injection and oral administration in rats. Oral exposure to BaP also induces stomach tumours while skin tumours have been observed after topically administration (Qu and Stacey 1996). The most significant health effect caused by inhalation of BaP in humans is lung cancer (Boffetta *et al*., 1997; Nielsen *et al*., 1996; Qu and Stacey 1996).

1.12 DNA damage

DNA damage is alteration of the genetic material in cells, and the main contributing factor to mutagenesis, carcinogenesis and aging. DNA damage may arise from exposure to exogenous agents like radiation and chemicals or be the result of metabolic endogenous processes. Hydrolysis and generation of ROS or reactive metabolites may all generate DNA damage in cells (De Bont and van Larebeke 2004). BaP have the potential to cause DNA damage in both somatic cells and germ cells. Several metabolites of BaP may form DNA-adducts and give mutagenic and carcinogenic effects if not repaired. The ability for reaction with DNA could be influenced by the availability of detoxifying enzymes like glutathione (Jeffrey 1985). However, many of the BaP metabolites manage to escape defence mechanisms, and generate DNA adducts immediately after metabolism.

As described in chapter 1.7.1, the BaP metabolite BaP-7,8-diol-9,10-epoxide (BPDE) has proven to be the most tumorgenic metabolite (Conney 1982; Takemura *et al*., 2010; Xue and Warshawsky 2005). The epoxide group in the bay-region makes the epoxide resistant for hydrolysation by epoxide hydrolase, and susceptible for nucleophilic attack. BPDE-DNA adducts occur primarily through covalent linkage of carbon 10 at the epoxide and the amino groups of deoxyadenosine and deoxyguanosine DNA residues (Szeliga and Dipple 1998). The major part of the epoxides forms guanine residues at the N^2 position of guanine and produces N^2-deoxyguanosine(dG)adducts (BPDE-N^2-dG) (Chary *et al*., 1995). Several of the BaP metabolites have genotoxic properties, including semiquinone intermediates formed during redox-cycling of quinones which can bind directly to the DNA. BaP-quinone metabolites can also form unstable DNA adducts. These and generation of ROS during metabolism, may induce oxidative DNA damage (Devanesan *et al*., 1996; Miller and Ramos 2001). Figure 1.7 shows some of the pathways for formation of BaP-induced DNA adducts.

A relatively high dose of coal tar (0.2 g/100g meal) over a time period of 28 days, give detectable BPDE-N^2-dG adducts in the liver, lung, and fore stomach of mice. The highest amount of adducts were present in the liver (Culp and Beland 1994). BPDE-DNA adducts were also present in lungs, liver, spleen and peripheral blood in rats after i.p. injections of 10 mg/kg bw BaP three times a week for two weeks. The highest amount of adducts were present in the lungs (Qu and Stacey 1996). This indicates that the administration route of BaP has influence on absorption and toxicity. There may be various consequences of an increased amount of BPDE-DNA adducts in cells. Commonly the outcome is mutations that

alter the integrity of the genome. The male germ cells are target for BaP metabolites. Smoking men have a higher degree of DNA adducts, including BPDE, in their sperm DNA compared to non-smoking men (Zenzes *et al*., 1999a), and this may be a link to a reduced fertility observed in smoking men (Vine 1996; Zenzes *et al*., 1999a). The reduced fertility can also be caused by abnormal protamine expression, excessive generation of reactive oxygen species (ROS) and abortive apoptosis during spermatogenesis (Barratt *et al*., 2010). Genotoxic environmental mutagens are also a serious threat to the DNA integrity of somatic cells (Peruzzi *et al*., 2010).

1.12.1 Reactive oxygen species

Oxidative stress is a condition where an increased rate of cellular damage occurs, induced by oxygen or oxygen-derived oxidants (ROS). A background level of oxidative stress are normal in cells, however, this level may be amplified by chronic disease stages, aging or toxin exposure. ROS are generated in cells by external factors or internal metabolic and biochemical reactions, and are highly reactive and oxidising agents in the class of free radicals. The most common types of ROS are superoxide (O_2^-), hydrogen peroxide (H_2O_2), hydroxyl radicals ($OH^\bullet$) and singlet oxygen ($^1O_2$) which all have the ability to oxidise the DNA (De Bont and van Larebeke 2004; Halliwell 1991; Miller and Ramos 2001; Sikka *et al*., 1995). ROS may generate genotoxic oxidative DNA damage including oxidised bases and single or double stranded breaks in the DNA. Damage may also occur in proteins and lipids and ROS mediated cellular DNA damage is the most common type of damage in cells (De Bont and van Larebeke 2004). The mitochondria consume most of the cells oxygen in production of adenosine triphospate (ATP), and a high flux of radicals is generated with potential for creating DNA damage (Richter *et al*., 1988; Richter 1995). Mitochondria may be cellular targets of BaP. Cytotoxicity from BaP-quinone is observed with a decrease in cellular ATP content. This induce mitochondrial morphological changes which can create loss of cell survival (Zhu *et al*., 1995).

Guanine has low energetic properties and is therefore the most vulnerable base for oxidative attack from radicals, and the most common mutagenic lesion formed by oxidative stress is 7,8-dihydro-8-oxoguanine (8-oxoG) (figure 1.8). This oxidised guanine base have mutagenic and miscoding properties (Cheng *et al*., 1992; Larsen *et al*., 2004). In rats exposed to BaP, an increased level of oxidative damage like 8-OhdG were observed in the liver, kidneys and lungs (Kim and Lee 1997), and sperm cells with enhanced levels of 8-oxoG has shown

correlation with decreased sperm concentration in humans (Ni *et al*., 1997). It is unclear whether BaP-exposure induces oxidative DNA-lesions in sperm. However, as mentioned in chapter 1.13, a transgenic mouse ($Ogg1^{-/-}$) is used by the Department of Chemical Toxicology (MIKT) as a model for human toxicological responses in the testis.

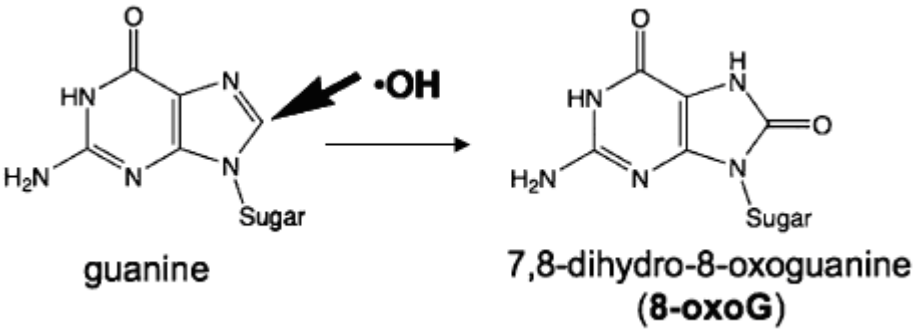

Figure 1.8 Formation of 7,8-dihydro-8-oxoguanine (8-oxoG) (modified from Wells *et al.*, 2009).

1.13 Repair of BaP-induced DNA lesions in testicular cells

Repair systems are present in all cell types of the human body. DNA repair is necessary for survival, although some mutations are essential for evolution. The constant DNA damage provided by endogenous and exogenous sources requires constant replacement of damaged nucleotide residues. Repair of common DNA lesions lower the potential for mutagenic and cytotoxic events, although the DNA repair pathways are not absolutely exact. On of the main pathways for DNA repair is base excision repair (BER). BER normally repairs common DNA lesions caused by exogenous and endogenous agents, including ROS-induced DNA lesions like 8-oxoG. Nucleotide excision repair (NER) mainly repair helix-disorting damage caused by environmental mutagens, including bulky BPDE-DNA adducts. NER recognise altered DNA lesions and makes an incision of the DNA strand containing the lesion. DNA synthesis and ligation replaces the deleted oligo-nucleotide (Lindahl and Wood 1999; Olsen *et al*., 2005).

The population of stem cells in testis is under a constant attack from DNA damaging agents through the whole adult life. A repair system is necessary for removal of DNA lesions that are induced every day, and for removal of the high level of mutations that otherwise could be transferred to the zygote (Olsen *et al*., 2005; Sipinen *et al*., 2010). The different stages of spermatogenesis have different capacity for removal of DNA adducts. Removal of DNA-

lesions in elongated spermatozoa is generally low due to the condensed chromatin in sperm cells, and removal of BPDE-N^2-dG following BaP-exposure is poor in meiotic and post-meiotic stages. When differentiating spermatogonia is exposed to BaP, these adducts does not persist to the spermatozoa stage, indicating a higher repair capacity in early stages (Olsen *et al*., 2010). However, a successful fertilisation and further embryonal development is dependent on the level of DNA damage in sperm, and the oocytes ability to repair DNA damage. Damage above a certain level may result in fragmentation of embryos or a low rate of embryonal development (Ahmadi and Ng 1999).

Differences in repair capacity are observed between rodents and humans. This includes the 8-oxoG lesions, where humans exhibit a lower capacity of repair than mice (Olsen *et al*., 2003). Such differences are important to consider when evaluating results from animal experiments. Eukaryotic cells use a specific DNA glycosylase, a product of the OGG1 gene, to excise 8-oxoG from DNA (Klungland *et al*., 1999). A transgenic mouse model with destruction of the murine OGG1 gene for the DNA glycosylase, generates homozygous Ogg1 null mice ($Ogg1^{-/-}$) for repair of this lesion. The $Ogg1^{-/-}$ mice accumulate an increased level of 8-oxoG in the genome. (Klungland *et al*., 1999) These mice are viable and fertile, and show only a moderate increase in spontaneous mutations in the liver. This was not observed in the testis, and the mice show no striking pathological alterations (Klungland *et al*., 1999). Due to the decreased repair capacity, the testicular cells in $Ogg1^{-/-}$ mice may have a more similar capacity to humans than $Ogg1^{+/+}$ mice. This is valuable when studying genotoxic effects from environmental mutagens in male germ cells.

1.14 Methods for measuring DNA damage in sperm cells

Studies have shown that increased sperm DNA fragmentation is associated with reduced fertility potential (Ahmadi and Ng 1999; Delbes *et al*., 2010). There are several methods available for measuring such DNA damage in sperm cells. The in situ nick translation assay applies fluorescence microscopy to quantify the insertion of marked nucleotides at single stranded DNA breaks in a reaction catalyzed by a template dependent enzyme. The Terminal deoxynucleotidyl transferase dUTP nick end labelling (TUNEL) assay uses another enzyme to recognize the same incorporation in double stranded DNA. The latter method can be applied in both fluorescence microscopy and flow cytometry. The Single Cell Gel Electrophoresis (Comet) assay is applied to a great extent at the MIKT-lab, and a modified

version quantifies single or double stranded DNA breaks in sperm DNA. This is achieved by single cell electrophoresis of spermatozoa stained with a fluorescent DNA binding dye (Barratt *et al*., 2010; Erenpreiss *et al*., 2006).

The sperm chromatin structure assay (SCSA) assay is used in the present study, and is a well established and standardised method for examining chromatin integrity in sperm cells. The SCSA has been applied for both research and clinical use as a male fertility assay. The increasing use of assisted conception requires analysis of DNA integrity and a test like the SCSA is therefore valuable for human fertility assistance. The method is based on flow cytometry and is a technique used for both rodent and human samples (Evenson and Jost 2000; Evenson *et al.*, 1980). Results with toxicants have shown a high dose-response relationship and the SCSA results have been well repeatable. The principle for the SCSA is the extent of denaturation of sperm DNA after a short lasting acid treatment *in situ*. The denaturation occurs preferentially at sites of pre-existing DNA strand breaks. The sperm cells are stained with acridine orange (AO) to detect green fluorescence as a measure of intact double stranded DNA, and red fluorescence as a measure of denatured DNA (Evenson and Jost 2000). Each of the mentioned techniques for measuring sperm chromatin integrity has advantages and limitations. However, they give no or little information as to the nature of the DNA-damage.

1.15 Pig-a assay for measuring somatic mutations *in vivo*

Identification of human genotoxic compounds is an important step in risk assessment of chemicals. Generally, somatic genotoxicity compounds are assumed to be genotoxic also to male germ cells if the active metabolite can reach the testis. It is of interest to know to what degree mutagenicity in somatic cells are predictive for germ cell mutagenicity. The Pig-a assay is a relatively new and promising method that is developed for quantifying somatic mutations *in vivo* (Bryce *et al*., 2008). The Pig-a assay is best established and described using blood samples in rat (Miura *et al*., 2008; Phonethepswath *et al*., 2010), although the assay is also used for analysing blood samples in mice (Phonethepswath *et al*., 2008). PIG-A (phosphatidylinositol glycan, Class A) is a gene located on the X-chromosome. The gene product is a catalytic subunit with a central role in initial biosynthesis of glycosylphosphatidyl inositol (GPI)-anchors (Kawagoe *et al*., 1994). GPI-anchors are important glycolipids that attach membrane proteins on the cell surface. This is achieved by

a phospholipid tail attached in the cytoplasmic membrane and a short glycan structure that extend out in the extracellular environment. These anchors attach membrane proteins in a covalent binding (Dobrovolsky *et al*., 2010; Low 1989).

There are several genes that influence the GPI-anchor synthesis, however, PIG-A is believed to be the only one of these that is located on the X-chromosome. Thus, only a single copy of the PIG-A gene is active in somatic cells. Only one mutation in this gene can restrain the synthesis of the GPI-anchors, with the consequence that the cell is unable to attach different surface proteins that relay on GPI (Dobrovolsky *et al*., 2010). This has created the hypothesis that absence of the GPI-anchor is a phenotypic marker for a mutation in the PIG-A gene (figure 1.9) (Dobrovolsky *et al*., 2010; Phonethepswath *et al*., 2008). By using a fluorophore labelled antibody towards one of the surface proteins that relay on the GPI-anchor, a mutation in the PIG-A gene can be recognised as cells that are unable to attach the antibody. PIG-A mutations in human cells is believed to be linked with the hematopoietic disease Paroxysmal nocturnal hemoglobinuria (PNH). Patients with this acquired disease have an abnormal population of blood cells, due to a deficiency in the GPI-anchor synthesis caused by a mutation in the PIG-A gene (Takeda *et al*., 1993).

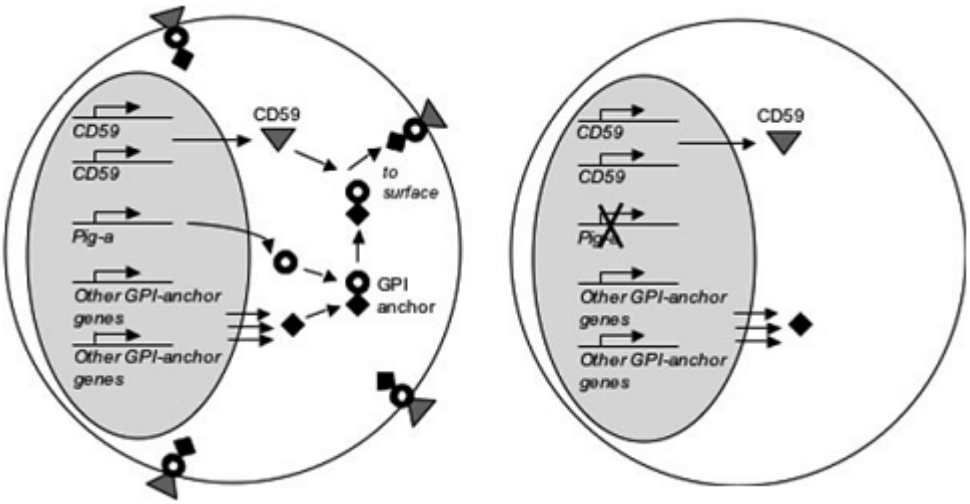

Figure 1.9 Schematic illustrations of rat cells with and without a mutation in the Pig-a gene. The cell to the left has a functional PIG-A gene, and is therefore able to express the surface protein CD59. The cell to the right have a mutation in the PIG-A gene with the consequence of a deficient GPI-anchor, that are unable to attach CD59 on the cell surface (Bryce *et al.*, 2008)

Human blood consists of reticulocytes, mature erythrocytes and leukocytes suspended in plasma which is composed mainly of water, ions, glucose, hormones and thrombocytes (platelets) (Vander *et al*., 2001a). Red blood cells, white blood cells and platelets are

continuously renewed in the bone marrow from the hematopoietic stem cells. Stem cells form populations of multipotent progenitor cells that give rise to the major cell lines in the bone marrow, which are erythroid, myeloid, megakaryocytic and lymphoid (Riley *et al*., 2001). Reticulocytes (RETs) are immature red blood cells. They are anuclear and slightly larger than mature red blood cells (RBCs). The youngest RETs in the bone marrow have a dense mass of RNA, mitochondria, ribosomes, centriole and remnants of the Golgi apparatus. These cellular organelles are progressively lost during maturation together with ability of hemoglobin synthesis (Gasko and Danon 1974). After normally 2 days in the bone marrow the RETs are released into the peripheral blood stream and undergo final maturation. The RNA becomes less dense and only scattered remnants of RNA remains in the most mature RETs and this is also lost when they becomes mature RBCs. RETs becomes mature RBCs after about three days in the peripheral blood. The number and character of RETs in the blood stream reflects the activity of the bone marrow (Gasko and Danon 1974; Geminard *et al*., 2002; Patel and Lodish 1984; Riley *et al*., 2001). Red blood cells isolated from whole blood in mice were used in the present master thesis for evaluation of mutation load in somatic cells by the Pig-a assay. The aim is to relate mutation frequency in somatic and germ cells following BaP-exposure in mice. However, as the technique is new, N-ethyl-N-nitrosourea (ENU) was used as a positive control (chapter 1.15.1).

1.15.1 N-ethyl-N-nitrosurea (ENU)

N-ethyl-N-nitrosourea (ENU) is a laboratory-synthesised compound with the highest mutation rate of any germ line mutagen tested in mice (figure 1.10). It causes random single base pair mutations in a wide variety of organisms. ENU acts directly through alkylation of nucleic acids without need for any metabolic activation. The compound has an ethyl group that can be transferred to oxygen or nitrogen radicals in several reactive sites identified both *in vivo* and *in vitro*. These transferred groups of ethyl causes DNA adducts, which may give miss pairing during DNA replication (Noveroske *et al*., 2000). ENU is a strong mutagen with fairly cytotoxic effects (Goth-Goldstein and John Burki 1980).

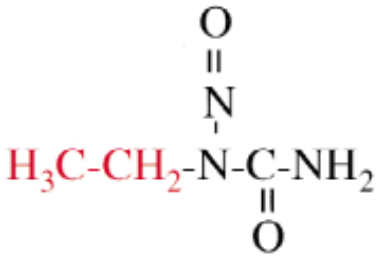

Figure 1.10 N-ethyl-N-nitrosourea (ENU) with an ethyl group (Noveroske et al., 2000).

1.16 Mouse as a model organism

Effects of drugs and chemicals are to a large extent based on extrapolation from animal data, and animal studies are essential to our understanding of basic biological mechanisms and disruption in human key processes (Barratt *et al*., 2010). The field of reproduction is well studied and crucial time spots and appearance of the different stages of sperm cell development is well defined (Bellve *et al*., 1977; Borg *et al*., 2010). Mice are widely used in reproduction studies for several reasons. Experiments in mice are possible to conduct after a relatively short time period and a great number of genes are also conserved between man and mouse. Mice are also relatively cheap to house and the use of transgenic mouse lines are of great advantage. However, there are great differences between man and mice and results from animals studies must be handled with caution and cannot be directly transferred to humans. In the present master, the Ogg1$^{-/-}$ mouse has been used as a model for BaP effects in human testicular cells.

1.17 Aims

The overall goal in the present work has been to study the role of environmental mutagens on male reproductive health. Exposure of male mice to BaP has been shown to reduce sperm quality and to induce an increase in pre- and post-implantation losses of embryos. We wanted to achieve a better understanding of the mechanisms responsible for male mediated reproductive toxicity of BaP and related environmental mutagens.

Specific aims:

- **Analyse effects of *in vivo* BaP-exposure of mice on sperm chromatin integrity**

Analyses of sperm DNA damage is a challenge due to the highly compact nature of sperm DNA. Analytic measurements have shown that BaP may induce sperm BPDE-DNA adducts. We wanted to test whether the sperm chromatin structure assay (SCSA) was able to detect sperm DNA damage following BaP-exposure in mice.

- **Examine if Ogg1$^{-/-}$ mice are more sensitive to BaP-induced sperm DNA damage than Ogg1$^{+/+}$ mice**

The Ogg1$^{-/-}$ mice are proposed as a model for human responses to testicular toxicants. SCSA results were used to compare the response of BaP-exposure in Ogg1$^{-/-}$ mice to the response in wild type mice.

- **Examine if sperm BPDE-DNA adducts persist in mice embryo**

One study suggests that sperm BPDE-DNA adducts may persist past the first embryonal cell divisions (Zenzes *et al*., 1999b). We wanted to verify this finding in a mouse model when only the father was exposed to BaP.

a) Set up an immunological method to detect cellular BPDE-DNA adducts.
b) Establish a handling procedure for adduct detection in pre-implantation embryos.
c) Immunological staining for BPDE-DNA adducts in two and four cell embryos.

- **Establish the Pig-a assay for analysis of *in vivo* induction of somatic mutations**

The Pig-a assay is currently characterised and optimised by the Litron Laboratories. One of the aims of this project was to set up the Pig-a assay at the Department of Chemical Toxicology (MIKT) lab. This included testing of the assays performance in mice exposed to the potent mutagen ENU *in vivo*.

2. Materials and methods

All solutions and chemicals used in these experiments are listed in the Appendix.

2.1 Mice

2.1.1 Animals and genotypes

In the BaP experiment, male Ogg1$^{+/+}$ C57BL/6J BomTac mice obtained from Taconic in Ejby, Denmark were used together with C57BL/6 Ogg1$^{-/-}$ mice. Ogg1$^{-/-}$ mice were bred at the Norwegian Institute of Public Health (NIPH), Oslo, Norway as described in chapter 2.1.2. The mice from Taconic acclimatised for a week after arrival. Two to five mice (9-11 weeks) were housed per cage and individually marked by ear punching. Groups of 7-10 mice were treated with BaP, corn oil or remained untreated. All animals in the BaP-experiment were sacrificed ten days after exposure (chapter 2.2.1). Strains of Ogg1$^{+/+}$ and Ogg1$^{-/-}$ mice were a part of the experimental design, however, a mistake with the genotyping of animals occurred at the laboratory. This was first discovered after the experiment and many of the Ogg1$^{-/-}$ animals were actually Ogg1$^{+/+}$ or Ogg1$^{+/-}$ (heterozygous).

Male B6D2F1 (8-12 weeks) and female B6D2F1 (4-6 weeks) mice, both obtained from Charles River Laboratories were used in the *in vitro* fertilisation (IVF) experiments. C57BL/6J male mice obtained from Taconic in Ejby, Denmark were used in the Pig-a experiment. Random unexposed mice obtained from the NIPH, were used in immunostaining and Pig-a experiments when establishing and testing the procedures.

2.1.2 Breeding and care

Ogg1$^{-/-}$ mice were housed in air flow IVC racks (Thoren Maxi-Miser System) and filter cabinets (Scantainer, Scanbur BK AS, Nittedal, Norway) in plastic disposable cages on Nestpack (Datesand Ltd., Manchester, UK) bedding. They were exposed to a 12/12 h light/dark cycle, 6-10 air changes per hour, room temperature (20 ± 2 °C) and controlled relative humidity (55±5 %). Diet and water were given *ad libitum*. The mice were given a breeding/maintenance diet (2018SX Teklad Global 18% Protein Extruded Rodent Diet, Harland Teklad, Madison, Wisconsin, USA). All research was performed in conformity with the laws and regulations for experiments with live animals in Norway.

2.2 Sacrificing animals, organ removal and sperm isolation

2.2.1 BaP experiment

Mice were sacrificed by CO_2 gas when establishing a reference sample and a positive control for the sperm chromatin assay (SCSA). Due to animal welfare, cervical dislocation was used in all subsequently experiments. Epididymis and selected tissues was surgically removed from the male mice ten days after BaP-exposure, immediately frozen on dry ice and stored at -80°C. A chirurgic scissor was used to make an opening in cauda epididymis and a bended needle was used to put on gentle pressure to release sperm cells. The squeezing was performed in phosphate buffer (PBS), deoxyribonuclease (DNase) buffer or TNE buffer depending on the different experiments.

2.2.2 *In vitro* ferilisation (IVF)

Egg-clutches with 10-20 oocytes surrounded by cumulus cells were removed surgically from each oviduct in female mice and transferred to Eppendorf tubes with M2 medium before IVF. Cauda sperm for fertilisation were made available as described above (chapter 2.2.1).

2.2.3 Pig-a experiments

Blood was collected from mice in the Pig-a experiments. The saphenous vein was incised with a surgical blade and blood was transferred directly to heparin coated capillary tubes (size 400-600µl). For the experiment with platelets and lymphocytes, four mice was anesthetised by intraperitoneal (i.p.) injection (ZRF-coctail with Zoletil, Rompun and Fentanyl as used by the animal department at NIPH) and heart punctured with a heparin coated needle for draining of blood. Blood was transferred to heparin coated tubes (BD Vacutainer 13 x10 mm). Mice were sacrificed directly afterwards by cervical dislocation. Handling of animals was performed by trained personnel.

2.3 Benzo(a)Pyrene

2.3.1 Dissolving BaP in corn oil

BaP is lipophilic and almost insoluble in water. Corn oil was therefore used as a solvent. BaP is toxic and carcinogenic and all the required precautions were taken. Hence, a ventilation cabinet, glows and a safety mask were used.

Procedure:

1. A 100 mg vial of BaP was used. In a biohazard bench, BaP was transferred to a sterile glass Erlenmeyer flask, and corn oil was added to obtain a concentration of 7.5 mg BaP/ml corn oil.
2. The Erlenmeyer flask was placed in a water bath at 30°C with shaking for about 1 hour to dissolve.
3. Remaining undissolved material was dissolved by placing the Erlenmeyer flask with BaP on a magnetic stirrer for 1 hour.
4. The BaP solution was transferred to a sterile glass vial and covered with aluminium foil to shield from light. The vial was stored in the dark at room temperature inside a dry and ventilated security cabinet.

2.3.2 Exposure of mice to BaP

BaP dissolved in corn oil (chapter 2.3.1) was administered to the male mice via i.p. injection by trained personnel. Mice weighted from 21-25 g and were injected with 0.4 – 0.5 ml BaP in corn oil. The mice were administered a single dose of 150 mg BaP/kg bodyweight (bw), or the vehicle (corn oil). One group of animals stayed untreated as an additional control.

2.3.3 Exposure of mice to N-ethyl-N-nitrosurea (ENU)

N-ethyl-N-nitrosourea (ENU) dissolved in PBS was administered to mice via i.p. injection by trained personnel as a positive control for the Pig-a assay. Mice were injected three times over a period of five days (day, 1, 3, 5) with single doses of 40 mg/kg bodyweight for each animal. The mice were administered a total dose of 120 mg/kg bodyweight, or the vehicle (solvent). Two animals stayed untreated as an additional control.

2.4 Sperm chromatin structure assay (SCSA)

The sperm chromatin structure assay (SCSA) was introduced by Evenson in 1980 as a method to determine sperm DNA integrity, and how sperm DNA damage is related to fertility (Evenson *et al*., 1980). The assay characterises irregular chromatin structure in sperm cells via increased susceptibility of DNA to acid induced denaturation *in situ*. The SCSA is a standardised procedure with a detailed protocol described by Evenson and Jost (Evenson and Jost 2000). Sperm samples isolated in TNE-buffer as described in 2.2.1 were

denaturised in 30 seconds with an acid-detergent treatment, and then coloured with acridine orange (AO) which is a DNA intercalating dye. AO stains both single and double stranded DNA. Green fluorescence indicates double stranded DNA (native), while red fluorescence marks the single stranded and damaged DNA (figure 2.1). The principle for SCSA is that sperm DNA that already contains nicks, due to for instance destructive agents, is more susceptible for denaturation than undamaged DNA and thus have a higher red and a reduced green fluorescence signal. Accurate denaturation time and optimal pH conditions is essential for correct and comparable results. BD FACSDiva software (v 6.1.2) for the flow cytometer was used to obtain all data and cytograms from sperm samples. The program FCS express (v 3.00.0821) was used for handling and calculation of data.

A cytogram of green versus red DNA fluorescence (figure 2.1) was used to measure sperm DNA quality. The parameter Alpha t is the relationship between red (ss DNA) and total green and red (ss + ds DNA) fluorescence. Alpha t was used to detect sperm cells with increased red fluorescence and separate these from the main population of cells. The percentage of sperm that falls outside this main population in a sample is called the DNA fragmentation index (% DFI), and represents cells with increased level of single stranded DNA. % High green represents cells with increased green fluorescence, and are shown to be cells with an incomplete chromatin condensation like that present in immature cells. Mean Alpha t, % DFI and % High green were parameters used for analysing the SCSA result.

A reference sample with unexposed sperm cells was used in the assay before running the actual samples, as a calibration sample for the flow cytometer. A reference sample sets the red and green photomultiplier tube (PMT) voltage, to yield the same mean green and red fluorescence levels for each sample in the experiment and functioned as a standard to observe where a main population of untreated sperm cells was located. This was used to define gates in the cytogram that separated the main cell population from cells in the % DFI or % High green areas. In the preliminary SCSA experiments, the reference samples were made by sperm cells in caudas from two untreated mice. The cells were allocated in Eppendorf tubes and stored at -80°C. Sperm cells from three $Ogg1^{+/+}$ untreated control animals were squeezed and pooled in 800 µl cold 1x TNE buffer and used as a reference sample in the BaP experiment. The reference samples were not used more than once and were not saved for more than 1 hour at 4°C.

A positive control with caudal sperm and a high dose of DNase was also prepared for the SCSA. DNase is a nuclease enzyme that catalyses the hydrolytic cleavage of phosphodiester linkages in the DNA backbone. The positive control was used to make sure that the denaturation and staining of DNA with AO worked. The positive control is not described in the original SCSA manual, but was included in the procedure by the MIKT-lab. Sperm cells from caudas in an untreated control mouse were squeezed (chapter 2.2.1) in DNase buffer with 1% Triton X-100 to permeabilize the cell membrane. DNase (200 U/ml) for degradation of DNA was added to the sperm cells and the cells were incubated at 37°C for 1 hour and then centrifuged (Eppendorf centrifuge 5810R) at 288 x *g* for 5 min. Supernatant was aspirated and the pellet was re-suspended in 1x TNE buffer. Samples were allocated in Eppendorf tubes and stored at -80°C. Figure 2.1 shows sperm cells in a reference sample and a positive control with images obtained by flow cytometry.

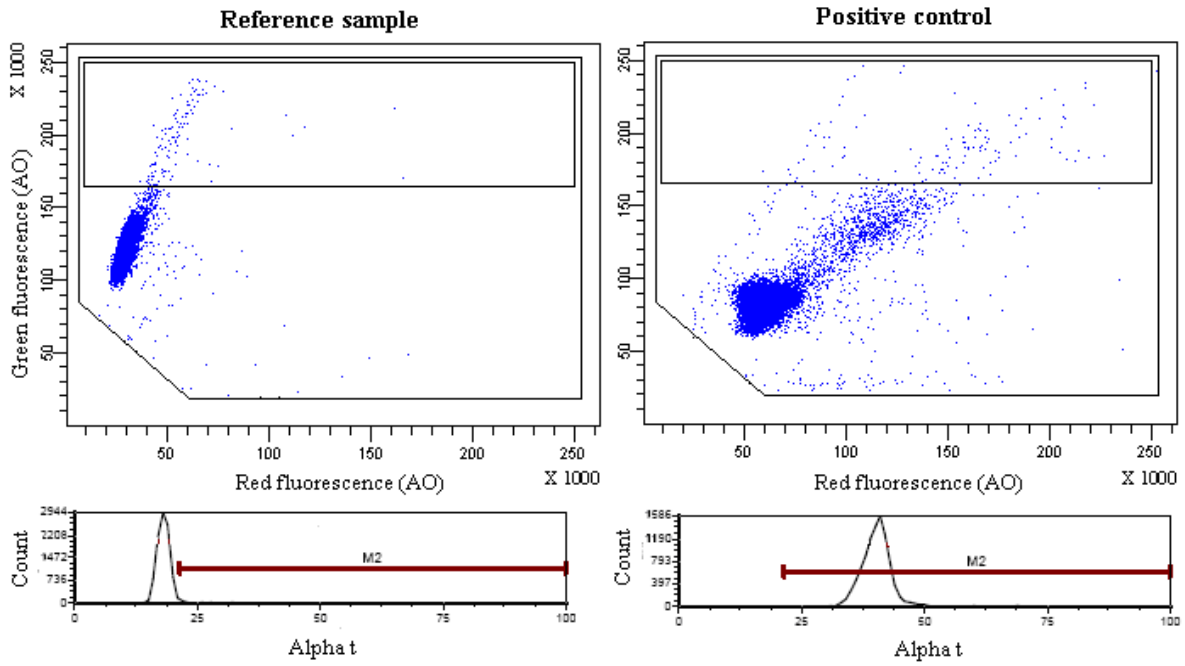

Figure 2.1 SCSA cytograms (top) of a reference sample and a positive control. Green fluorescence on the y-axis represents double stranded DNA and red fluorescence on the x-axis represents single stranded DNA. A gate is placed around the population of sperm cells to eliminate debris, and the upper gate is for detection of % High green. The two lower diagrams shows the Alpha t populations in the reference (left) and positive control (right). The red M2 line represents cells outside the normal population of cells, meaning cells with a higher mean value of Alpha t than observed in the reference sample.

A dose-response analysis with DNase exposed sperm cells was performed to test the sensitivity of the different parameters measured. A dilution series with DNase in DNase buffer was prepared using the same protocol as the positive control, and mixed with sperm

cells from an untreated mouse. The samples were run through the flow cytometer in order of the most diluted sample first, to avoid contamination from DNase in the more concentrated samples. Table 2.1 shows the different concentrations for the dilution series with DNase that were mixed with sperm cells in DNase buffer.

Table 2.1 Concentrations of DNase (U/ml) in the dose-response experiment with sperm cells.

Sample	DNase (U/ml)
a	0
b	0.2
c	2
d	20
e	200

Sperm cells from BaP exposed, vehicle (corn oil) and unexposed animals were analysed by the SCSA to study if the treatment groups showed any difference in degree of DNA damage.

SCSA procedure:

1. The flow cytometer (BD LSRII) was prepared:

    a) Lasers in the cytometer needed 20 min for warming up.
    b) A test tube containing ddH20 was run through the cytometer.
    c) A standard solution with 350 µl PBS and roughly two drops of BDTM cytometer setup and Tracking beads (Lot id 66656) was run through the cytometer to quality check the laser settings. The rate was set at approximately 100 events pr. second.
    d) The cytometer needed adjustments before SCSA analysis:
        - The blue laser (488, 10-30 mW) was used for excitation
        - Emission is detected through filter (630-650 nm) for red fluorescence (ss DNA) and filter (515-530 nm) for green fluorescence (ds DNA).

2. A test tube with AO equilibration buffer (400µl acid-detergent solution and 1.2 ml AO colour solution) was run through the cytometer for 15 min. Since AO is toxic, precautions when handling the solutions were needed.
3. 200 µl from the reference sample with sperm from three pooled $Ogg1^{+/+}$ control mice was transferred to a cold test tube and 400 µl cold acid-detergent solution was added and

mixed carefully. After exact 30 seconds, 1.2 ml cold AO staining solution was added to the tube and after 3 min the sample was run through the cytometer.

4. The event rate was set at approximately 200 cells pr. second and the PMT were adjusted to the right voltage. The sperm population in the reference sample was used to make a gate for excluding debris and gates for detection of cells in the High green area. Number of cells counted for each sample was 10 000.
5. A test tube with AO equilibration buffer was run through the cytometer before the first sample.
6. Caudas were collected from the freezer and brought to the laboratory on dry ice. Sperm cells were squeezed on a cold plate in a petri dish with 800 µl cold TNE buffer for each cauda, immediately before flow cytometric analysis. The sperm cells in buffer were transferred to Eppendorf tubes through a filter for removal of cell lumps and debris.
7. 200 µl of the sperm samples was transferred to a cold test tube and 400 µl cold acid-detergent solution was added and mixed carefully. After exact 30 seconds, 1.2 ml cold AO staining solution was transferred to the tube and the samples were run through the cytometer. Data was recorded 3 min after adding the acid-detergent.
8. A test tube with AO equilibration buffer was run through the cytometer between all samples to maintain AO equilibration conditions in the instrument and to flush the previous sample.

2.5 *In vitro* fertilisation (IVF) in mice

The *In vitro* fertilisation (IVF) procedure described in the present project is well established in mice (Nagy *et al*., 2003). We used IVF for generation of embryos to the immunostaining experiments. Sperm cells from BaP exposed male mice *in vivo* were used to fertilise oocytes from unexposed female mice. Embryos could then be inspected for BPDE-DNA adducts to examine if paternal BaP-exposure gave detectable adducts in embryonal DNA. Occurrence of BPDE-DNA adducts in the one, two and four cell stages of the embryo should be examined. The female mice went through a super ovulation procedure to induce maturation and increase the number of released oocytes. The males were exposed to BaP by i.p. injections (chapter 2.3.2) 4 days before IVF. A light microscope was used for visualisation of sperm and oocytes, and cells were handled on a heating block at 37ºC. A cell incubator was used for culturing of cells to maintain optimal conditions. The oocytes and embryos were transferred by using a mouth pipette with a thin glass tip. Oocytes from one side of the

female were mixed with sperm from BaP exposed males, while oocytes from the other side were combined with sperm from unexposed males. This assures that oocytes from all the females are present in both BaP exposed group and control group. IVF was accomplished with help from trained personnel at the MIKT-lab. This part of the experiment was performed as a part of a larger post doc project (Asgeir Brevik), and the embryos were also used in gene expression studies. Although the fertilisation and development of embryos was successful, we experienced some challenges with immunostaining of these embryos.

IVF procedure:

1. Day 4 before IVF: Male mice were exposed with i.p. injections of BaP in corn oil or injected only with vehicle (corn oil) (chapter 2.3.2).
2. Day 3 before IVF: Female mice were injected i.p. with 5 international units (IU) of the pregnant mare serum hormone gonadotropin (PMSG).
3. Day 1 before IVF: Female mice were injected i.p. with 5IU of the human chorionic gonadotropin (HCG).
4. Day of IVF: Male and female mice were sacrificed by cervical dislocation. Caudas and oviducts were surgically removed (chapter 2.2.2) and collected in Eppendorf tubes containing M2 medium that were kept in room temperature.
5. Micro scissor were used to make incisions in cauda and the sperm dispersed for 10 min in 250 µl human tubal fluid (HTF) medium under liquid paraffin. Egg clutches with 10-20 oocytes in cumulus cells were removed from each oviduct.
6. Sperm cells and oocytes were transferred to IVF dishes and incubated in 250 µl of HTF medium under liquid paraffin for 4.5 hours at 37ºC.
7. The fertilized oocytes (zygotes) were washed 5 times in 150 µl potassium simplex optimisation medium (KSOM) for removal of cumulus and sperm cells and transferred to 150 µl KSOM in a petri dish under liquid paraffin.
8. Embryos from the first cell stage were collected immediately and the rest was grown and harvested to later developmental stages.

2.6 Immunostaining of BPDE-DNA adducts

Immunocytochemistry (ICC) is broadly applied in research and has great versatility in extensive number of fields. The method use antibodies to detect antigens in tissue preparations or isolated cells. High affinity and selectivity of the antibody towards the epitope on the antigen is necessary, and a fluorophore attached to the antibody (primary or secondary) are needed to generate fluorescence signal (Parham 2009). The main adducts after BaP-exposure *in vivo* are the BPDE-DNA adducts (chapter 1.7.1). An antibody towards BPDE-DNA adduct was used in the immunostaining experiments. The primary monoclonal antibody BPDE, clone 5D11 from mouse IgG_{2a} was used (Nordic BioSite AS) (Santella *et al.*, 1984; Santella *et al.*, 1988). A secondary antibody, donkey anti-mouse labelled with fluorophore Alexa 488 (Invitrogen), was used to visualise binding of the primary antibody.

Murine hepatoma cells (Hepa1c1c7, obtained from the MILS department at NIPH) were exposed to a high dose of BPDE *in vitro* and used as a positive control for the optimisation of the staining procedure. Cells were transferred to slides and tested with different concentrations of the antibodies. DNA denaturation with Hydrogen chloride (HCl) was a part of the immunostaining procedure to denaturise DNA and thus increase the availability of the DNA adducts to antibody recognition. Different concentrations of HCl were tested to the specimens to optimise the staining procedure (denaturation conditions and antibody concentrations).

Embryos from BaP exposed fathers were obtained by IVF, but there were some difficulties with the preparations during the immunostaining procedure. The challenge was to obtain a technique where a few embryos could be stained and visualised without being lost during the procedure. Embryos placed directly on slides were easily lost. Fibrinogen clots that captured the embryos were therefore assessed, as this procedure is used for normal embryo-immunostaining studies in the lab. A few embryos were transferred to 20 µl fibrinogen (solved in KSOM) and added thrombin to solidify. However, the clot and embryos did not tolerate the acid denaturation step in the procedure. Subsequently, a clot with embryos inside 1 % agarose in PBS with EDTA was tried. This composition tolerated the denaturation step. However, staining results were poor when examined by fluorescence microscopy for unknown reasons. Solutions and chemicals were prepared and ordered fresh before additional experiments. Oocytes were easier to obtain than embryos, and for further testing

of the procedure oocytes were exposed to a high dose (10 µM) BPDE *in vitro* as a positive control for staining of BPDE-DNA adducts. Oocytes were removed from mice in the same way as for IVF (chapter 2.2.2). The procedures for exposure *in vitro* and capture in agarose clots were similar for oocytes and embryos. The only difference was removal of cumulus cells with Hyase before exposure of the oocytes. Somatic testicular cells from an unexposed mouse were also exposed to a high dose of BPDE *in vitro* when staining results were weak in embryos and oocytes. This was to examine if there was something in the embryos, oocytes or the agarose clot that did not allow staining or if the procedure unexpectedly did not work. Somatic testicular cells were expected to have the same response as hepatoma cells to a high dose of BPDE *in vitro*. Unfortunately, some methodological problems occurred that were not solved due to the time limits of this master thesis.

The immunostaining procedure was mutual for all cell types, with different exposure and preparation techniques. Hepatoma cells, testicular cells and oocytes were only exposed to BPDE *in vitro*, whereas embryos were exposed both *in vitro* as a positive control and *in vivo* through BaP-exposure of the father. The procedure for embryos is described with use of the agarose clot, and denaturation concentration is 2 N HCl. Preparations, exposure and fixation of the individual cells are described first, followed by the general procedure for immunostaining. Unexposed control cells were prepared for all experiments and all precautions for handling BPDE were followed.

2.6.1 Preperation of hepatoma and testicular cells and BPDE exposure *in vitro*

Procedure hepatoma cells:

1. Murine hepatoma cells (Hepa1c1c7) were grown in four petri dishes in serum-free Minimum Essential Medium (MEM) Alpha medium inside a cell incubator to maintain optimal conditions. 3 ml fresh medium was transferred to the cells before exposure of BPDE.
2. Two of the petri dishes were exposed to 3.5 µl (1 mM) BPDE to a final concentration of 1.2 µM, and the other two dishes were added 3.5 µl DMSO (control). The dishes were gently mixed. Sterile pipette tips were used and the exposure was performed in a biohazard bench.
3. Cells were incubated at 37°C in 1 hour.

4. The medium was aspirated and cells were washed two times with 3 ml PBS. 1 ml Trypsin was transferred to each dish to detach the cells, and cells were incubated at 37°C in 2 min.
5. Each dish were added 3 ml fresh MEM Alpha medium and mixed gently.
6. The medium with cells (1ml) from each dish were transferred to four Eppendorf tubes and centrifuged (Eppendorf centrifuge 5415R) at 288 x *g* in 5 min at room temperature.
7. The supernatants were aspirated and the pellets were re-suspended in 1 ml PBS and 200 µl fetal calf serum (FCS).

Procedure testicular cells:

1. Testes were surgically removed from an unexposed control mouse and placed in an Eppendorf tube with PBS.
2. The internal spermatic fascia (membrane around the testis) and blood vessels were removed by a chirurgical scissor and the testis were placed in a small petri dish with 1.5 ml PBS.
3. The testis was incised with a surgical scissor approximately 100 times followed by a filtration through a 55 µm filter into an Eppendorf tube. This is a rough method to separate individual cells from the testis.
4. Cells were exposed to 5 µl (1 mM) BPDE in Eppendorf tubes to a final concentration of 10 µM and control cells were added 5 µl PBS. Sterile pipette tips were used and the exposure was performed in a bio hazard bench.
5. The cells were incubated at 37 °C in 1 hour and centrifuged (Eppendorf centrifuge 5415R) at 288 x *g* in 5 min at room temperature.
6. The supernatants were aspirated and the pellets were resuspended in 200 µl PBS and 100 µl FCS.

Fixation procedure for hepatoma and testicular cells:

1. Hepatoma or testicular cells in PBS (7.5 µl) were transferred to slides and air dried.
2. The cells were fixed for 3 min in 150 ml cold 70 % methanol in a slide container.
3. The cells were then transferred to a slide container with 150 ml cold Acetone for 30 seconds.
4. The slides were air dried and stored at -20°C.

5. An ImmEdge pen (Vector Laboratories Inc) was used to encircle the cells for a more restricted area for incubation of the antibodies.
6. The general immunostaining procedure was then followed for hepatoma cells and testicular cells.

2.6.2 Preperation of embryos and BPDE exposure *in vitro*

Procedure for preparation and fixation:

A stereo microscope (Olympus) was used for visualisation of oocytes and embryos, and handling was performed on a heating block at 37ºC. A mouth pipette with a thin glass tip was used for transfer of the oocytes and embryos, and they were kept in a cell incubator between all steps in the procedure to maintain optimal conditions before fixation.

1. Female super-ovulated mice were killed by cervical dislocation and oviducts were surgically removed and collected in Eppendorf tubes with M2 medium and kept in room temperature.
2. Egg clutches with 10-20 oocytes surrounded by cumulus cells were removed from each oviduct.
3. IVF was performed as described in chapter 2.5.
4. Gel film placed on 37°C was added 20 µl 1 % low melting point agarose in PBS with 10 mM EDTA. 3 µl KSOM with 5-10 embryos obtained by IVF were transferred to the agarose clot using a 0.5–10 µl pipette with thin tip.
5. The agarose clots with embryos on gel film were placed on a cold plate to make the agarose solidify.
6. The agarose clots on gel film were placed in a dish and fixated in 50 ml 70 % cold methanol for 3 min. The general immunostaining procedure was then immediately followed.

Procedure for BPDE exposure to embryos and oocytes *in vitro*:

1. Embryos obtained by IVF were washed 5 times in drops of 150 µl KSOM under liquid paraffin.
2. In a biohazard bench, a drop with 495 µl KSOM and 5 µl (1 mM) BPDE to a final concentration of 10 µM was prepared in a petri dish under liquid paraffin. The embryos were transferred and incubated at 37 °C in 1 hour.

3. The embryos were washed 3 times in drops of 150 µl KSOM and transferred to agarose clots and fixed as described above. The general immunostaining procedure was then immediately followed.

2.6.3 General procedure for immunostaining of BPDE-DNA adducts

The volumes described in the different steps of the immunostaining procedure were added to one clot with embryos or oocytes, or one ring made by the ImmEdge pen around hepatoma cells and testicular cells.

1. Cells were washed 2 x 5 in PBS on a tilt board and then rinsed quickly in ddH20.
2. RNA in cells was removed by adding 20 µl RNase-it (2 mg/ml RNase A and 5000 U/ml Rnase T1 in 50 mM Tris-HCl (pH 7.4), 50% glycerol). This is to enable visualisation of mitochondria and nuclear DNA staining. Cells were incubated at 37°C for 1 hour and then washed 1 x 5 min in PBS. Slides or gel film with cells were air dried.
3. To digest proteins and reduce background, 20 µl Proteinase K (10 µg/ml Tris buffer) was added to the cells for 5 min. Proteinase K also inactivates nucleases that otherwise could degrade the nuclear acids in DNA.
4. Cells were then washed 3 x 5 min in PBD (PBS with 0.1 % Triton X-100) and transferred to PBS before a quick rinse in ddH20.
5. The cells were denaturised in 2N HCl in 10 min to obtain a more open configuration of DNA, and then neutralised in Tris base solution in 10 min. Cells were washed 2 x 2 min in PBS.
6. To block unspecific binding of the antibody, 20 µl blocking solution (5 % bovine serum albumin (BSA) in PBS) was added for 1 hour and the cells were then rinsed quickly in PBS.
7. Cells were incubated overnight at 4°C with 20 µl primary antibody (BPDE 5D11) in a 1:200 dilution with 1 % BSA in PBS.
8. The morning after, cells were washed 3 x 3 min in PBD and added 20 µl secondary Alexa 488 labelled antibody in a 1:1000 dilution with 1 % BSA in PBS. Cells were kept in the dark for 30 min and then washed 2 x 10 min in PBD.
9. The cells were carefully transferred to a glass container with 1500 µl hoechst 33342 in 150 ml PBD. Since hoechst is toxic, this glass container was specifically used for

this purpose and a biohazard bench was used. Hoechst is a DNA intercalating agent and stains nuclei.

10. The cells were rinsed quickly in ddH2O, then air dried and a drop of Dako cytomation fluorescence medium was added. Cover glasses were placed over the cells and excess air bubbles was removed with a pipette tip. The cells on slides or gel film were stored at 4°C until examination by fluorescence microscopy.

A Zeiss Axioplan 2 microscope (5883) equipped with FITC and UV blocks was used for visualisation of Alexa 488 and hoechst staining, respectively. A Spot RT3 Slider digital camera and Spot advanced software from Diagnostic Instrument Inc., was used for capturing images. Immersol® (1-2 drops) was added to the slides for improved resolution in oil immersion objectives.

2.7 Pig-a assay for measuring *in vivo* somatic mutations

The Pig-a assay for measuring somatic mutations *in vivo* is described and established by Litron Laboratories (Bryce *et al*., 2008). The procedure is still in a process of optimisation and characterisation and the MIKT-lab is a part of this work. The assay uses blood samples collected during the experiment, the volume needed is low and blood withdrawal do not affect the animals. The first step in the Pig-a assay was separation of red blood cells from other components in the blood stream, achieved by optional gradient centrifugation (leukodepletion) (figure 2.2). Different leukodepletion solutions including Nycoprep, Lymphoprep and Lympholyte were tested. Separation of the cells with Lympholyte gave a distinct pellet of red blood cells that was easier to work with compared to the other separation solutions. The isolated red blood cells were then incubated with a phycoerythrin (PE) labelled antibody, specific for the cell surface protein CD24 in mice (antiCD24-PE). Further incubation with the nucleic acid dye Syto13, made it possible to identify reticulocytes (RETs) due to the messenger ribonucleic acid (mRNA) content in RETs. Syto13 emits green fluorescence in the Fluorescein isothiocyanate (FITC)-channel. Flow cytometry with BD FACSDiva (v 6.1.2) software was used to analyse the blood samples.

Fig 2.2 Basic steps of the pig-a assay. Blood are collected from mice before a leukodepletion of red blood cells for separation from other components in the blood. The assay continues with antibody labelling (antiCD24-PE) and incubation with a nucleic acid dye (Syto13). Samples are then analysed by flow cytometry (Dobrovolsky *et al.*, 2010).

A calibration standard was used before every experiment to calibrate the flow cytometer and adjust gates in the cytogram that distinguish mutated and non-mutated RETs and RBCs (figure 2.3). The standards were made of blood from untreated control mice and followed the Pig-a procedure in parallel with the other samples. The volume withdrawn from these mice was doubled compared to the other samples. Half of the native cells were then labelled with the antibody to CD24, while the other half remained unlabelled. The cells that were unlabelled imitate the phenotype of cells with a mutation in the Pig-a gene, and are referred to as “mutant mimics”. The calibration standard was also treated with Syto13. Compensation was performed to avoid overlapping of the two fluorescence emissions (PE and Syto13).

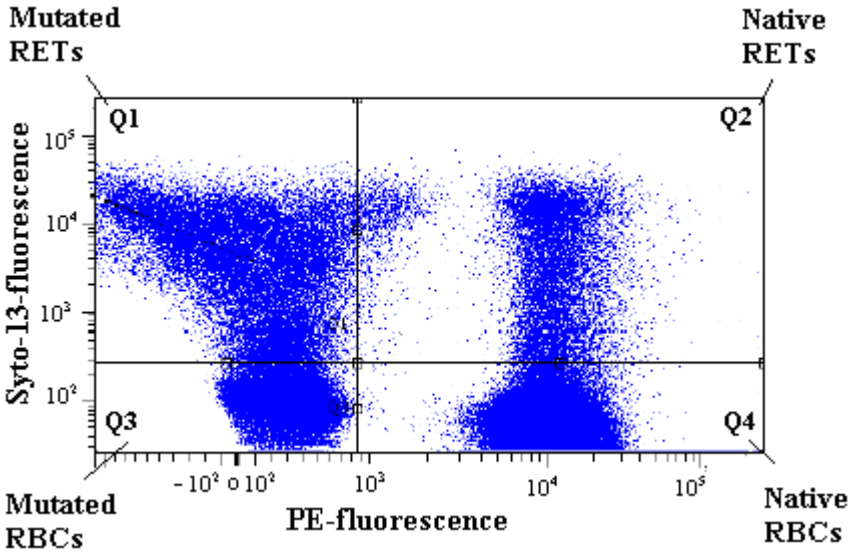

Figure 2.3 Cytogram obtained by flow cytometry showing a calibration standard for the Pig-a assay. The main cell population to the right is treated with the antibody towards CD24 (antiCD24-PE), while the population to the left is untreated and referred to as "mutant mimics". Syto13-fluorescence on the y-axis distinguishes reticulocytes (RETs) and mature red blood cells (RBCs). PE-fluorescence represents cells with attached antibody. The cytogram is divided into four quadrants and represent mutated (CD24 negative, Q1, Q3) and non-mutated (CD24 positive, Q2, Q4) RETs and RBCs.

In the pilot studies performed in the present master, the needed reagents and solutions were ordered by the MIKT-lab. When the assay demonstrated to provide sensitive and repeatable results, Litrons prototype kit containing all the required solutions were used. Standard kits make it possible to achieve a similar basis for all experiments and to compare the results with other labs. This is useful since the Pig-a assay is a relatively new and under current establishment at several laboratories. Two pilot experiments are described first, followed by the full Pig-a procedure.

2.7.1 Dose-response analysis with "mutant mimics"

A dose-response experiment with a dilution series of "mutant mimic" unlabelled cells mixed with a labelled antiCD24-PE blood sample was conducted in order to examine the performance of the assay. Blood was collected from untreated control mice, which are expected to have a natural low mutation load. Number of blood cells in a sample with isolated red blood cells was estimated by manual cell counting in a hemocytometer under light microscope. A dilution series with an estimated number of untreated blood cells were

then made. Before flow analysis, the samples from the dilution series were mixed with a sample of blood cells treated with antibody. This was to examine if the flow cytometer was able to detect the untreated cells as mutants. Solution and chemicals from the MIKT-lab were used and the number of cells counted in the flow cytometer for each sample was 10^5 cells.

Procedure:

1. Blood samples were collected from the *saphenous vein* in untreated control mice as described in chapter 2.2.3. 60-100 µl blood from each mouse was transferred directly into small heparin-coated tubes. Samples were then transferred to Eppendorf tubes with heparin in PBS (1:10) to further avoid coagulation. The pig-a assay (chapter 2.7.3) was applied for all samples including a calibration standard. Half of one of the samples was kept untreated with antiCD24-PE.
2. The untreated blood sample was used to make the dilution series of "mutant mimic" cells. First, 10 µl cells from this sample was mixed with 10 µl Tryphan blue and then diluted in PBS (1:200 total dilution) for cell counting. This was performed 3 times to achieve a mean value of cells in the sample.
3. Mean number of cells in these three samples was 1.27×10^9 cells/ml blood.
4. 100 µl unlabeled cells (1.27×10^8 cells) was incubated with 900 µl Syto13 solution. This was the first sample in the dilution series.
5. The dilution series was made by transferring 100 µl to new tubes with 900 µl Syto13 (1:10).
6. The dilution series consisted of 4 Eppendorf tubes with approximately 1.27×10^8, 1.27×10^7, 1.27×10^6 and 1.27×10^5 cells/ml in Syto13.
7. According to the cell count, 200 µl of the blood sample that was labelled with antiCD24-PE contained an approximate number of $2,54 \times 10^8$ cells.
8. 50 µl unlabelled cells from each of the four tubes was mixed with 200 µl labelled cells. The proportion of unlabelled to labelled cells was therefore approximately 1:40 ($2.54 \times 10^8/6.35 \times 10^6$), 1:400, 1:4000 and 1:40 000 in sample 1-4, respectively.
9. Since 10^5 cells were run through the cytometer, the blood samples contained an estimated number of 2500, 250, 25 and 2.5 unlabelled cells pr 10^5 labelled cells.

2.7.2 Visualisation of platelets and lymphocytes in the flow cytogram

In the Pig-a assay, it is important to avoid platelets and lymphocytes in the analysis of mutated cells. Platelets and lymphocytes were isolated from red blood cells in order to examine where these cells were localised in the flow cytograms that are used during Pig-a analyses. An allophycocyanin (APC) labelled antibody towards platelets (CD42d-APC) was used for visualisation of platelets, and Syto13 for visualisation of lymphocytes since these have a high staining as they are nucleated cells. Isolated platelets and lymphocytes were mixed with a sample of native isolated red blood cells that had followed the Pig-assay. This was to compare where the cell types were localised in the same cytogram. The sizes of the three cell types are different so it should be possible to separate the individual cell populations in forward and side scatter flow diagrams. Flow cytometry can also gate out different cell populations for a more accurate examination of number and localisation of cells. Knowledge of where platelets and lymphocytes are localised in the Pig-a cytograms would be useful to avoid contamination of these in red blood samples, which makes the assay more reliable. Two different concentrations of CD42d-APC were tested and we concluded that a 1:10 dilution gave the best visualisation. Solution and chemicals from the MIKT-lab were used.

Procedure:

1. Blood samples were collected by heart puncture in 4 untreated control mice using a heparin coated needle (chapter 2.1.2). Blood were immediately transferred to heparin coated tubes (BD Vacutainer 13 x 10 mm).
2. A volume of 1 ml blood was mixed with 1 ml PBS and gently layered on top of 1 ml Lympholyte. The sample was centrifuged (Eppendorf centrifuge 5810R) at 800 x g for 20 min in room temperature.
3. The lymphocytes and platelets were gathered in a thin grey layer on top of the Lympholyte, this layer was transferred by a pipette to an Eppendorf tube. 10 µl was transferred to a slide and examined in a light microscope to make sure that these cells were present in the sample.
4. The grey layer with cells were mixed with 1 ml PBS and centrifuged (Eppendorf centrifuge 5810R) at 300 x *g* for 10 min in room temperature. The supernatant was aspirated and the pellet was resuspended in 600 µl PBS. From now on the sample were kept on ice and protected from light until flow analyses.

5. A 1:10 dilution of CD42d-APC (2 % FCS in PBS) was prepared and 100 µl platelets and lymphocytes were transferred to 100 µl of this antibody solution and incubated in 30 min on ice in the dark.
6. The sample was mixed carefully and transferred to a new Falcon tube (15 ml) on top of 10 ml PBS before centrifugation (Eppendorf centrifuge 5810R) at 300 x g for 5 min in room temperature.
7. The supernatant was aspirated and 1.5 ml Syto13 (0.12 µM syto13 in FCS) was transferred to the tube before incubation at 37 °C in 30 min. The samples were kept on ice until flow analysis.

2.7.3 Pig-a analysis of of N-ethyl-N-nitrosourea (ENU) exposed mice *in vivo*

When a stable gating strategy of the calibration standard and the procedure for isolation of red blood cells was outlined, a long term experiment with exposure of mice to the potent mutagen N-ethyl-N-nitrosourea (ENU) was conducted in order to examine the performance of the Pig-a assay. Mice were divided into three treatment groups. These were untreated, vehicle (solvent) and ENU exposed and the mice were followed over a period of 5 weeks. The Pig-a procedure was performed on blood samples from mice pre-exposure, 2 weeks and 5 weeks after exposure. The experiments used chemicals and solutions obtained from Litrons prototype kit.

Procedure:

1. Blood samples were collected from the *saphenous vein* in mice as described in chapter 2.2.3, and transferred directly into small heparin-coated tubes. Volumes ranging from 60-100 µl were collected from each mouse.
2. Blood in volumes of 30 µl were immediately transferred to pre-labelled Eppendorf tubes with 100 µl Anti Coagulant Solution on ice. 60 µl blood from an untreated mouse was transferred to one of the Eppendorf tubes as a calibration standard.
3. Falcon tubes (15 ml) containing 3 ml Lympholyte® had been equilibrated to room temperature in advance, and 130 µl (160 µl for calibration standard) of blood in Anticoagulant Solution was gently layered on top of the Lympholyte®. The samples were centrifuged (Eppendorf centrifuge 5810R) at 800 x *g* in 20 min at room temperature.

4. The supernatants were aspirated carefully without disturbing the pellets, and the surfaces of the pellets were washed two times in 300 µl Buffered Salt Solution (BSS).
5. BSS was transferred in volumes of 155 µl (310 µl for calibration standard) to the pellets and mixed gently. From now on the samples were kept on ice and protected from light until flow analyses.
6. Blood samples were transferred to Eppendorf tubes containing 100 µl cold Working Antibody Solution (1:20 stock antiCD24-PE in 2 % FBS in BSS) in volumes of 150 µl. The calibration standard was split into two Eppendorf tubes. 150 µl was transferred to a tube with 100 µl Working Antibody Solution and 160 µl was transferred to a tube with 2 % FCS in BSS. All samples were incubated on ice for 30 min.
7. Blood samples were then resuspended by using a pipette, and the whole content in each tube was transferred to new Falcon tubes (size 15 ml) containing 10 ml BSS. Drops with blood that had missed contact with the Working Antibody Solution were not transferred. This is to avoid untreated cells that appear as mutant cells in the flow diagram. The samples were centrifuged at 300 x *g* in 5 min in room temperature.
8. The supernatants were carefully aspirated and the pellets were added 1.5 ml Working Nucleic Acid Dye Solution (0.12 µM syto13 in BSS).
9. All samples were transferred to new light protected Eppendorf tubes (1.5 ml) and incubated at 37°C in 30 min. All tubes were kept on ice until flow cytometric analysis.

2.8 Statistical analyses

Statistical analyses were conducted on data from the SCSA and Pig-a experiment, to examine if there were any statistical significant differences between the different treatment groups. For the SCSA, a power analysis was performed in advance of the experiment. This was to calculate the number of animals required to be able to detect a biological relevant increase in potential BaP-induced DNA damage. Statistical analyses were performed using Sigma Plot 11.0 software. The p-value and significance level was set at 0.05 and values below this were accepted as statistical significant.

The data in the SCSA and Pig-a experiments were initially tested for a normal distribution. This was conducted by a Shapiro-Wilk normality test, which tests the null hypothesis that a sample comes from a normal distribution. For the SCSA parameters, Q-Q (quantile-quantile) probability plots were also used to examine the ordered distribution of data (Henderson 2006). The Levene's test for homogeneity of data was also used for initial statistical analyses. Normality and an approximately equal variance are requirements for an analysis of variance (ANOVA), together with independent observations. The ANOVA tests the null hypothesis that there are no differences between group means (Festing and Altman 2002). A one-way ANOVA was conducted for the mean Alpha t and % High green parameter in the SCSA, and for the analysis of mutated RBCs in the Pig-a experiment. A one-way ANOVA can be used for comparing multiple groups with one factor variable, and because it is a robust test, small deviations from the mentioned requirements can be tolerated (Lovell and Omori 2008). An equal variance is more essential than full normality of the data.

When the parametric test (ANOVA) requirements were not met, the non parametric Kruskal-Wallis test was used. Kruskal-Wallis is the non-parametric version of the one-way ANOVA (Festing and Altman 2002). A Kruskal-Wallis test was used to test whether there were any statistical significant differences in medians for the treatment groups in the % DFI parameter in the SCSA. The Kruskal-Wallis test does not assume a normal distribution, although an identical shaped and scaled distribution for each group (except differences in medians) is assumed.

When the results from a one-way ANOVA or Kruskal-Wallis test indicated a statistical significant difference between groups, an additional post-hoc test was used. A lot of such tests are available, and they examine between which groups there were differences. The Fisher least significant difference (LSD) test for multiple pair wise comparison of groups (Meier 2006) was conducted as a post-hoc test in this statistical analyses. This was due to a relatively few groups compared, and the SCSA data also had unequal number of animals in each group (n). The non-parametric Mann-Withney test was conducted on data from the Pig-a experiment to examine whether two independent samples were statistical significant different from each other.

3. Results

3.1 Analysis of DNA damage in sperm cells by the SCSA

Paternal BaP-exposure 1-2 weeks before fertilisation is associated with embryo lethality in mice (Generoso *et al*., 1982). The SCSA is an assay for evaluation of sperm chromatin integrity in both human and animal samples, and was used in this project in order to examine if the assay was able to detect BaP-induced sperm DNA damage in mice.

3.1.1 Dose-response analalsysis of DNase exposed sperm cells by the SCSA

A dose-response analysis with exposure of sperm cells to an increasing concentration of DNase enzyme (0, 0.2, 2, 20, 200 U/ml)) was conducted in order to examine the sensitivity of the SCSA, and the performance of the mean Alpha t and % DFI parameters. Figure 3.1 shows a clear dose-dependent increase in DNA damage of sperm cells following DNase exposure. The Alpha t parameter (red/total fluorescence) seems to be fairly linear following increasing levels of DNase. The percentage of damaged cells expressed as % DFI is nearly saturated after the lowest DNase concentration (0.2 U/ml).

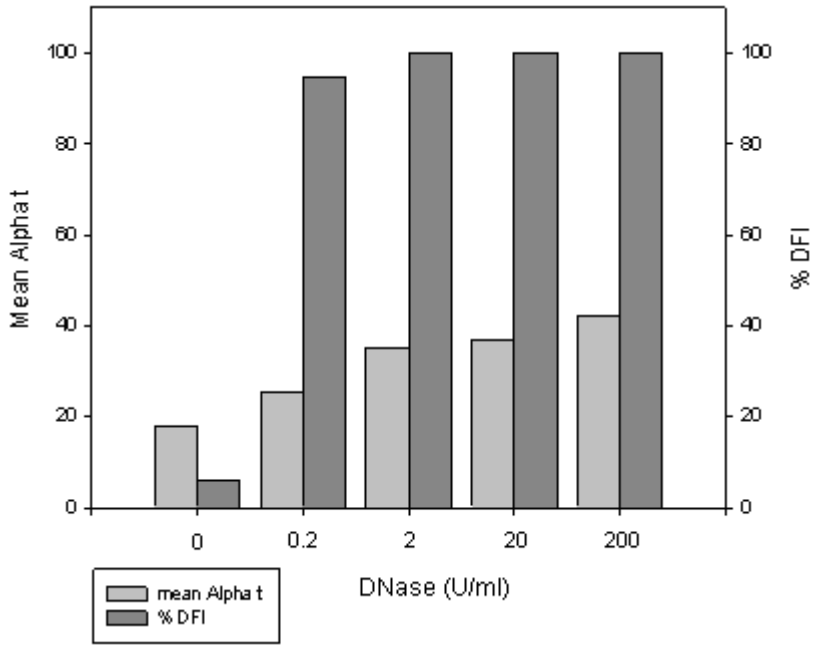

Figure 3.1 Dose-response analysis of DNase exposed sperm cells by the SCSA, showing data for the parameters mean Alpha t and % DFI (DNA fragmentation index).

Figure 3.2 shows cytograms obtained by flow cytometry of sperm cells in the dose-response analysis with DNase exposure. The main population of cells shifts towards higher red fluorescence in the diagrams following higher concentrations of DNase, indicating an increased level of single stranded DNA in cells.

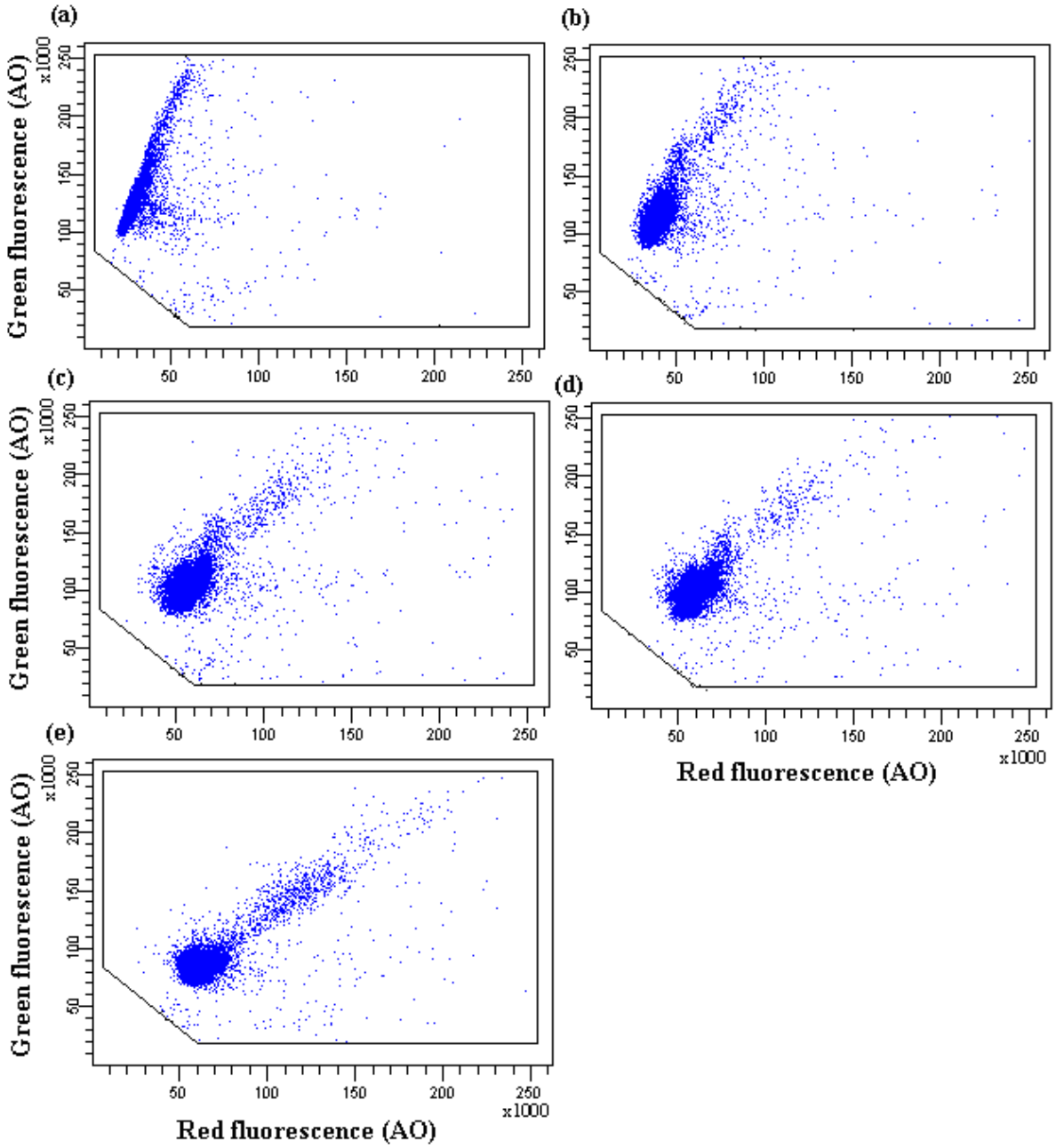

Figure 3.2 SCSA cytograms of caudal sperm cells treated with DNase enzyme. 10 000 sperm cells were stained by acridine orange (AO) and are analysed by flow the cytometer for each sample. Green fluorescence on the y-axis represents dsDNA and red fluorescence on the x-axis represents ssDNA. A gate is placed around the population of sperm cells to eliminate debris. **(a)** Sperm cells without DNase treatment (control sample) **(b)** Sperm cells treated with 0.2 U/ml DNase **(c)** Sperm cells treated with 2 U/ml DNase **(d)** Sperm cells treated with 20 U/ml DNase **(e)** Sperm cells treated with 200 U /ml DNase.

3.1.2 SCSA analysis of sperm cells from *in vivo* BaP-exposed mice

The chromatin integrity in sperm cells from mice was examined by the SCSA, ten days after administration of BaP, corn oil (vehicle control) or no exposure (control). The experiment initially included both $Ogg1^{+/+}$ and $Ogg1^{-/-}$ mice in the three treatment groups for comparison of responses in normal and repair deficient mice. However, after correcting for a mistake with genotyping of animals, several of the $Ogg1^{-/-}$ animals proved to have the genotype $Ogg1^{+/+}$ or $Ogg1^{+/-}$. $Ogg1^{+/+}$ and $Ogg1^{+/-}$ animals express the OGG1 gene for repair of 8-oxoG and have shown to have a normal repair capacity compared to the decreased repair capacity in $Ogg1^{-/-}$ animals (Personal communication, Ann Karin Olsen). $Ogg1^{+/+}$ and $Ogg1^{+/-}$ animals were therefore expected to have a similar response to the different treatments, and data from these two groups were merged together for unexposed (control) and BaP treated animals. These to genotypes together are from now on referred to as $Ogg1^{wt}$. Table 3.1 shows the composition of genotypes and treatments that were initially planned for the experiment, together with the actual genotypes of animals in the three treatments groups. The unexposed control and vehicle groups contained only two and one $Ogg1^{-/-}$ animals, respectively. Comparison of $Ogg1^{+/+}$ and $Ogg1^{-/-}$ animals in these treatment groups was therefore impossible, and there were not enough animals for a valid statistical analysis. The table also shows the genotypes of mice in the three treatment groups that were used for analysing the SCSA result.

Table 3.1 Genotypes of mice analysed by the SCSA. Nr. 1 shows genotypes in the treatment groups that were planned for the experiment, and nr. 2 show genotypes that actually were present in the three treatment groups after correcting for a mistake with genotyping of animals. Nr. 3 shows the genotypes in treatment groups that were used in the SCSA analyses after merging the $Ogg1^{+/+}$ and $Ogg1^{+/-}$ mice to $Ogg1^{wt}$. *Three used as a reference sample.

1: Planned genotypes of mice (no, mice)	**Genotype $Ogg1^{+/+}$**	**Genotype $Ogg1^{-/-}$**	**Genotype $Ogg1^{+/-}$**
(16) Control	9	7	0
(16) Vehicle	9	7	0
(19) BaP-exposed	9	10	0
2: Actual genotypes of mice (no, mice)	**Genotype $Ogg1^{+/+}$**	**Genotype $Ogg1^{-/-}$**	**Genotype $Ogg1^{+/-}$**
(16) Control	9 (6*)	2	5
(16) Vehicle	15	1	0
(19) BaP-exposed	9	7	3
3: Genotypes of mice used (no, mice)	**Genotype $Ogg1^{wt}$**	**Genotype $Ogg1^{-/-}$**	
(14) Control	14	0	
(15) Vehicle	15	0	
(19) BaP-exposed	12	7	

Figure 3.3 shows results for all genotypes, including the Ogg1$^{+/-}$ mice compared with all other groups in the three SCSA parameters before fusion with the Ogg1$^{+/+}$ mice. The figure shows some differences between the Ogg1$^{+/-}$ and Ogg1$^{+/+}$ animals. However, the observed differences were considered random variation due to small sample size. The conclusion was that a mutual repair capacity was a valid argument for merging of the two genotypes before the SCSA analysis.

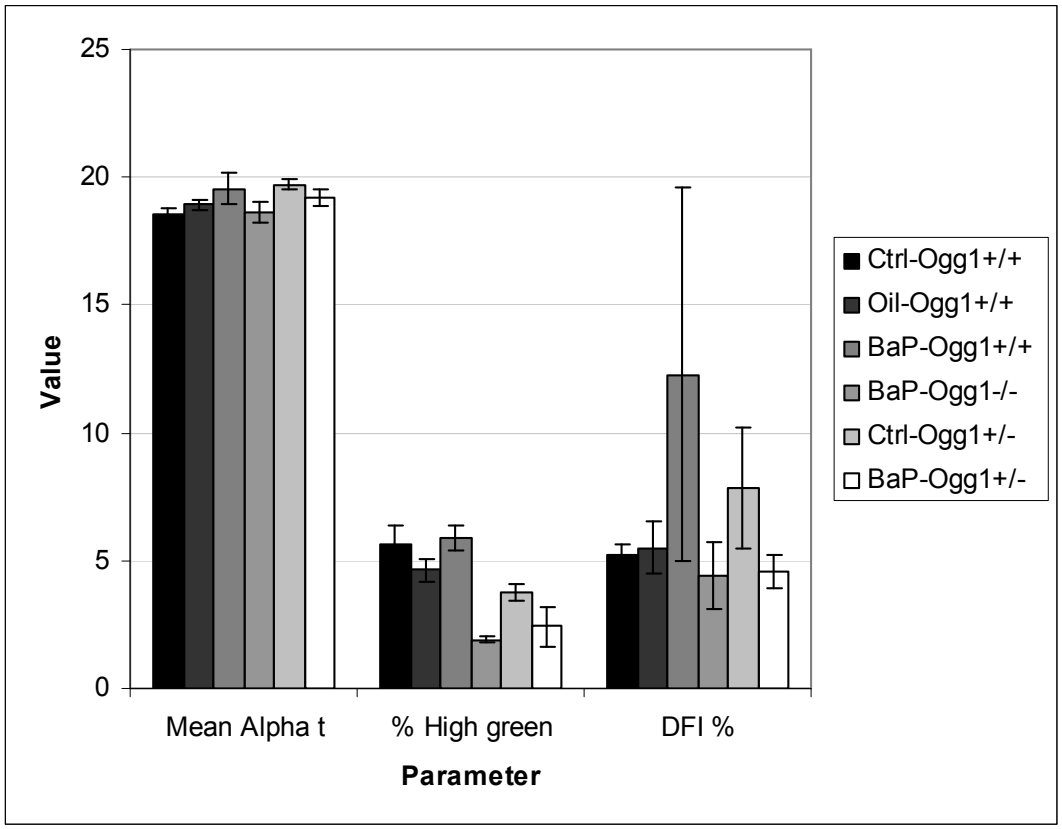

Figure 3.3 SCSA results in the mean Alpha t, % High green and % DFI parameters before merging the Ogg1$^{+/+}$ and Ogg1$^{+/-}$ animals to Ogg1^{wt}. The genotypes and treatments are Ctrl-Ogg1$^{+/+}$ (n=6), Oil-Ogg1$^{+/+}$ (n=15), BaP-Ogg1$^{+/+}$ (n=9), BaP-Ogg1$^{-/-}$ (n=7), Ctrl-Ogg1$^{+/-}$ (n=5) and BaP-Ogg1$^{+/-}$ (n=3). The error bars are the standard error of the mean (SE) for all individual groups.

Sperm cells from three of the control animals (Ctrl-Ogg1$^{+/+}$) were pooled and used as a reference sample and are therefore not included in the SCSA results. Table 3.2 shows the result in mean Alpha t, % High green and % DFI for Ogg1^{wt} and Ogg1$^{-/-}$ animals. The mean values for all three parameters (mean Alpha t, % High green and % DFI) in BaP exposed Ogg1^{wt} mice were slightly higher than in the other groups. The BaP exposed Ogg1$^{-/-}$ mice had lower mean values than the other groups. The BaP exposed Ogg1^{wt} group had one sample with a high level of damage. The SD for this group was therefore also increased, especially in the % DFI parameter. The vehicle exposed Ogg1^{wt} groups also showed an increased SD for the % DFI parameter.

Table 3.2 Results for mean Alpha t, % High green and % DFI parameters from the SCSA. Control, oil and BaP-exposed animals are shown. Ogg1^{wt} mice are represented in all treatments, while Ogg1$^{-/-}$ mice are only available in the BaP exposed group. Mean, standard deviation (SD) and minimum and maximum values were calculated, and are shown for all groups and parameters.

Parameter	Mean Alpha t			
Treatment	**Ctrl-Ogg1^{wt}**	**Oil-Ogg1^{wt}**	**BaP-Ogg1^{wt}**	**BaP-Ogg1$^{-/-}$**
	19.88	20.83	18.48	16.81
	19.15	18.98	19.63	18.08
	19.44	19.62	19.5	18.21
	20.14	17.59	24.21	19.7
	19.99	17.71	18.94	19.71
	18.89	19.21	17.54	19.66
	17.52	20.11	19.46	18.08
	19.02	19.3	18.77	
	18.52	19.15	18.63	
	18.34	19.36	19.28	
	19.01	19.23	19.45	
		18.45	19.61	
		18.58		
		19.78		
		18.68		
Mean and SD	**19.08 (SD 0.78)**	**19.11 (SD 0.84)**	**19.46 (SD 1.62)**	**18.61 (SD 1.12)**
(min - max)	**(17.52 - 20.14)**	**(17.59 - 20.83)**	**(17.54 - 24.21)**	**(16.81 - 19.71)**
Parameter	**% High green**			
Treatment	**Ctrl-Ogg1^{wt}**	**Oil-Ogg1^{wt}**	**BaP-Ogg1^{wt}**	**BaP-Ogg1$^{-/-}$**
	4.28	2.96	2.19	1.64
	3.26	2.25	3.83	1.89
	4.84	3.38	1.26	2.09
	3.25	3.32	6.64	2.28
	3.34	7.49	4.96	1.92
	9	4.89	8.02	1.35
	5.06	3.82	4.28	2.18
	5.56	3.1	5.26	
	5.28	2.55	5.26	
	4.44	3.15	8.01	
	4.55	6.33	3.98	
		4.65	6.24	
		5.17		
		4.59		
		6.48		
Mean and SD	**4.81 (SD 1.61)**	**4.28 (SD 1.56)**	**4.99 (SD 2.07)**	**1.91 (SD 0.32)**
(min - max)	**(3.25 - 9)**	**(2.25 - 7.49)**	**(1.26 - 8.02)**	**(1.35 - 2.28)**
Parameter	**% DFI**			
Treatment	**Ctrl-Ogg1^{wt}**	**Oil-Ogg1^{wt}**	**BaP-Ogg1^{wt}**	**BaP-Ogg1$^{-/-}$**
	7.87	32.59	3.59	1.5
	2.88	3	5.86	0.96
	5.01	6.99	4.3	1.65
	16.67	4.3	70.57	9.94
	6.91	3.55	2.87	8.01
	5.31	4.01	3.59	5.87
	3.46	14.94	6.14	2.92
	6.04	4.51	4.2	
	4.4	4.43	4.07	
	5.85	4.5	7.32	
	6.11	4.96	4.32	
		4.55	7.29	
		2.46		
		10.53		
		3.11		
Mean and SD	**6.41 (SD 3.70)**	**7.23 (SD 7.74)**	**10.34 (SD 19.02)**	**4.41 (SD 3.56)**
(min - max)	**(2.88 - 16.67)**	**(2.46 - 32.59)**	**(2.87 - 70.57)**	**(0.96 - 9.94)**

3.1.3 The Alpha t parameter was not influenced by BaP-exposure

Figure 3.4 shows mean and median Alpha t for control, vehicle and BaP exposed mice in the SCSA experiment.

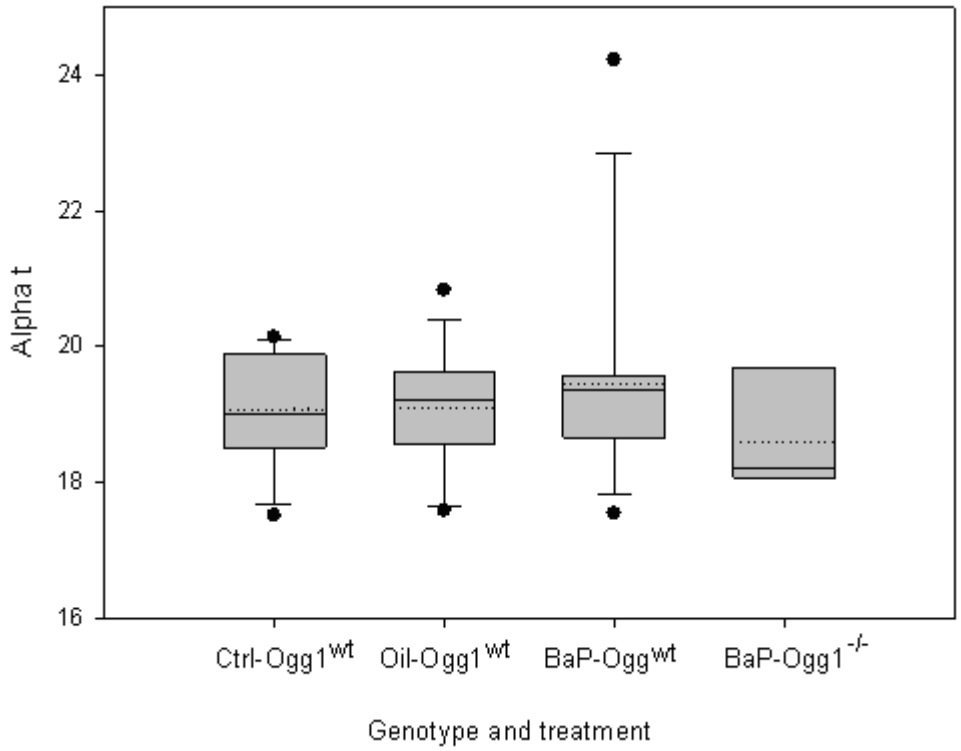

Figure 3.4 Box plot showing the result from the Alpha t parameter following analysis of sperm by the SCSA. Genotypes and treatment groups are Ctrl-Ogg1^{wt} (n=11), Oil-Ogg1^{wt} (n=15), BaP-Ogg1^{wt} (n=12) and BaP-Ogg1$^{-/-}$ (n=7). The solid lines are the median for each treatment group and the dashed lines are the mean values. The dots outside the boxes are outliers. There are few data points for the Ogg1$^{-/-}$ group, and the 10 % and 90 % percentiles were not calculated by the software (Sigma plot 11.0). Minimum and maximum values are shown in table 3.2.

The data for the mean Alpha t parameter was normally distributed in all groups except in the BaP-Ogg1^{wt} ($p<0.001$) group, and the data showed no signs of a non-constant variance ($p=0.779$). A one-way ANOVA was conducted and showed no statistical differences between the treatment groups ($p=0.477$).

3.1.4 The % DFI parameter was not influenced by BaP-exposure

Figure 3.5 shows mean and median % DFI for the control, vehicle and BaP exposed mice in the SCSA experiment.

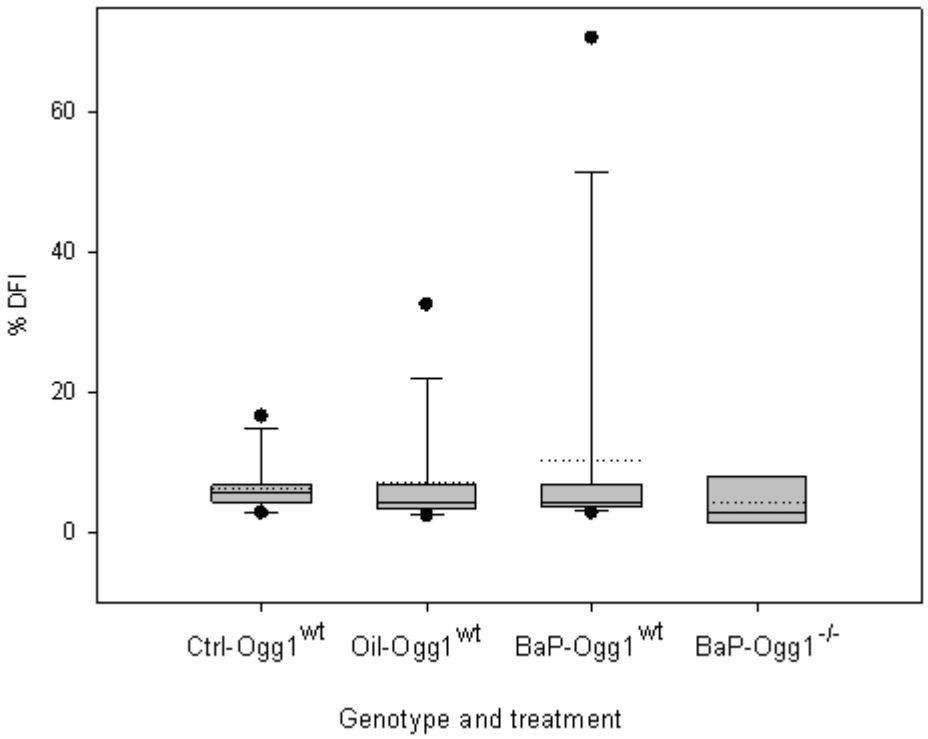

Figure 3.5 Box plot showing result from the % DFI parameter following analysis of sperm by the SCSA. Genotypes and treatment groups are Ctrl-Ogg1^{wt} (n=11), Oil-Ogg1^{wt} (n=15), BaP-Ogg1^{wt} (n=12) and BaP-Ogg1$^{-/-}$ (n=7). The solid lines are the median for each treatment group and the dashed lines are the mean values. The dots outside the boxes are outliers. There are few data points for the BaP-Ogg1$^{+/-}$ group, and the 10 % and 90 % percentiles were not calculated by the software (Sigma plot 11.0). Minimum and maximum values are shown in table 3.2.

Figure 3.5 show that the BaP-Ogg1^{wt} group had a slightly higher mean value than the other groups. The BaP-Ogg1^{wt} data also had a high dispersal of data. This may partly be due to the outlier shown in table 3.2. Data for the % DFI parameter was not normally distributed ($p<0.001$), although the data showed no signs of a non-constant variance ($p=0.826$). The non-parametric Kruskal-Wallis test for comparison of all groups against each other was conducted. There were no statistical significant differences between any of the treatment groups in the % DFI parameter in the SCSA ($p=0.532$).

3.1.5 BaP-exposed Ogg1$^{-/-}$ mice have a reduced number of immature cauda sperm

Figure 3.6 shows mean and median % High green for control, vehicle and BaP exposed mice in the SCSA experiment.

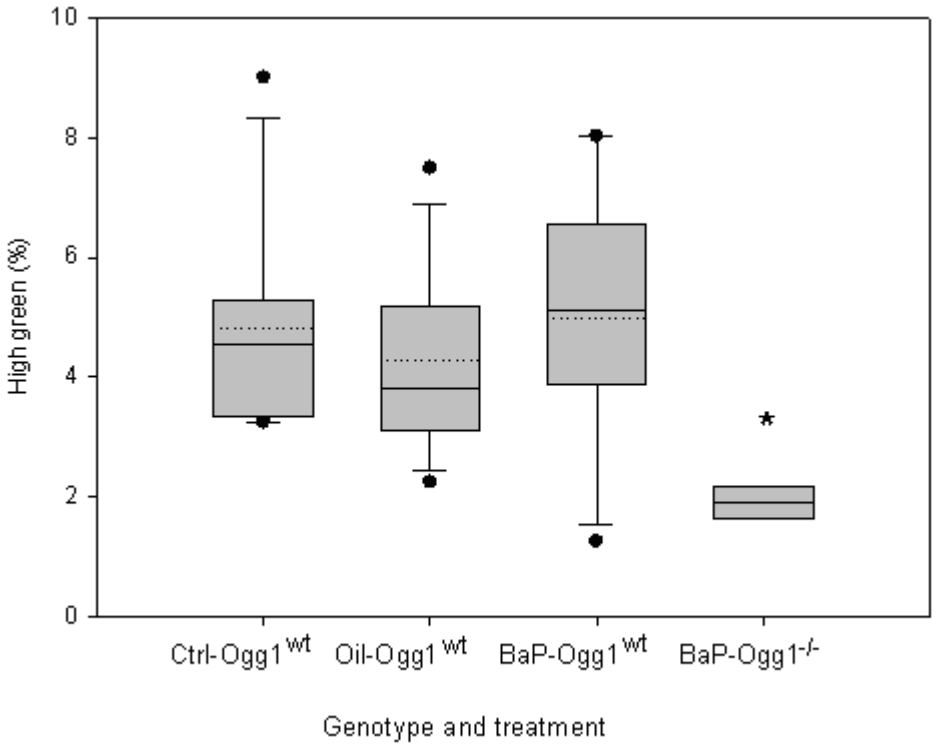

Figure 3.6 Box plot showing result from the % High green parameter following analysis of sperm by the SCSA. Genotypes and treatment groups are Ctrl-Ogg1^{wt} (n=11), Oil-Ogg1^{wt} (n=15), BaP-Ogg1^{wt} (n=12) and BaP-Ogg1$^{-/-}$ (n=7). The solid lines are the median for each treatment group and the dashed lines are the mean values. The dots outside the boxes are outliers. There are few data points for the BaP-Ogg1$^{+/-}$ group, and the 10 % and 90 % percentiles were not calculated by the software (Sigma plot 11.0). Minimum and maximum values are shown in table 3.2. (*p<0.003 compared to all Ogg1^{wt}).

Figure 3.6 shows a decreased median value in the BaP-Ogg1$^{-/-}$ group compared to the others. The data for the % High green parameter was normally distributed in all groups except the Ctrl-Ogg1^{wt} group (p=0.001). The data showed an equal variance (p=0.119), and a one-way ANOVA was conducted and showed statistical significant differences between treatment groups (p=0.002). Diagnostic plots showed some indications of a non constant variance, with an increasing variance with higher values. A non-parametric Kruskal-Wallis test was therefore also conducted, and confirmed that there were statistical significant differences between treatment groups (p=0.001). Fisher-LSD post-hoc test for all pair wise multiple

comparison was further conducted on data and showed statistical significant differences between the BaP-Ogg1$^{-/-}$ and all the Ogg1^{wt} groups (Ctrl-Ogg1^{wt} and BaP-Ogg1$^{-/-}$ ($p<0.001$), Oil-Ogg1^{wt} and BaP-Ogg1$^{-/-}$($p=0.003$), BaP-Ogg1^{wt} and BaP-Ogg1$^{-/-}$ ($p<0.001$). There were no statistical significant differences between the treatment groups in the Ogg1^{wt} animals.

3.2 Immunostaining of BPDE-DNA adducts in BaP exposed cells

To be able to measure the potential persistence of paternally transmitted BPDE-DNA adducts in embryos, a method for immuno-detection of BPDE-DNA adducts was established in our lab and modified for the purpose of labelling these adducts in mice embryo. Different concentrations of HCl (1N, 2N, 4N) for DNA denaturation and different antibody concentrations were tested.

Immunostaining of hepatoma cells exposed to a high dose of BPDE *in vitro* gave clear and detectable BPDE-DNA adducts visualised by fluorescence microscopy. Figure 3.7 shows unexposed and BPDE exposed hepatoma cells treated with 4 N HCl. Staining of the nuclei in exposed cells was observed when using 4N HCl, as shown when comparing image (b) and (c). Figure (a) shows that unexposed cells gave fluorescence signal, which further indicates a high background of unspecific binding from the antibody following denaturation with 4N HCl.

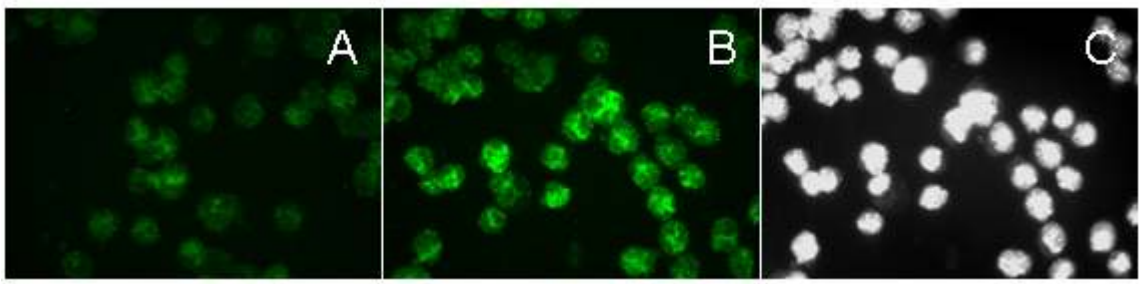

Figure 3.7 Fluorescence images of BPDE exposed hepatoma cells. All cells are denaturised with 4N HCl and treated with a 1:200 dilution of primary antibody (anti-BPDE 5D11) and a 1:1000 dilution of secondary Alexa 488 labelled antibody. Green fluorescence indicates BPDE-DNA adducts. **(a)** BPDE-staining in unexposed control cells **(b)** BPDE-staining in cells exposed to BPDE **(c)** Cells nuclei of exposed cells visualised by hoechst staining.

Denaturation with 2N HCl gave visualisation of BPDE-DNA adducts in hepatoma cells after BPDE exposure (figure 3.8 (c)). Based on experiments with 2N HCl that gave repeatable results and low background level of unspecific binding, we concluded that denaturation with

2N HCl gave the best visualisation of BPDE-DNA adducts. Figure 3.8 shows unexposed and BPDE exposed hepatoma cells treated with 2N HCl. Figure 3.8 (a) shows cells that are exposed to BPDE and labelled with secondary antibody, while untreated with primary antibody. This was to observe if the secondary antibody gave unspecific staining. Figure 3.8 (a) shows that the secondary antibody gives low unspecific background. Figure 3.8 (b) further show lack of staining of unexposed cells, while staining was clear in nuclei of BPDE-exposed cells (c).

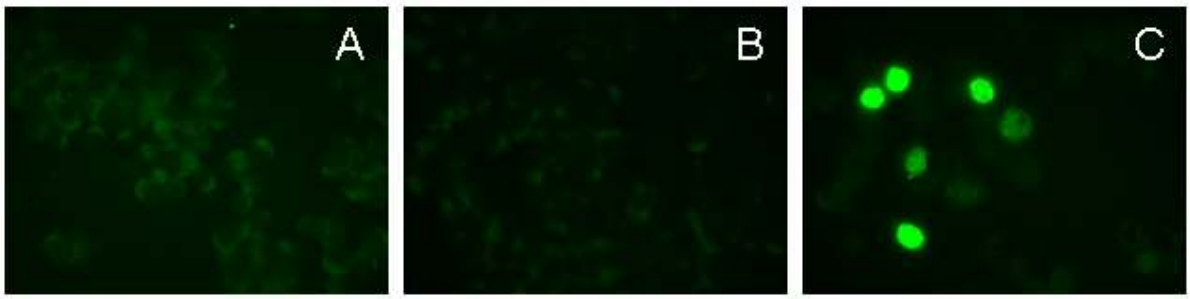

Figure 3.8 Fluorescence images of hepatoma cells. All cells are treated with 2N HCl for denaturation. A 1:200 dilution of primary antibody (anti-BPDE 5D11) and a 1:1000 dilution of secondary Alexa 488 labelled antibody are used. **(a)** Cells treated with BPDE and secondary antibody, while untreated with primary antibody **(b)** BPDE-staining in unexposed control cells **(c)** BPDE-staining in cells exposed to BPDE

To be able to stain pre-implantation embryos, the embryos needed to be captured in a matrix. The use of fibrinogen clots for capturing embryos is useful for normal immuno cytochemistry. However, denaturation with HCl dissolved the fibrinogen clots. As an alternative procedure, the embryos were embedded in clots of agarose, which tolerated the subsequent treatments. Immunostaining of BPDE-DNA adducts were carried out in embryos exposed to BPDE *in vitro* and BaP through the father *in vivo*. Staining of BPDE-DNA adducts in embryos inside an agarose clot gave poor results for unknown reasons. Due to the time limits of this master, results for paternal transfer of BPDE-DNA adducts to embryo DNA and 2 and 4 cell stages of embryos are therefore absent.

3.3 The Pig-a assay for measuring somatic mutations (*in vivo*)

The Pig-a assay for detection of *in vivo* somatic mutations was established at the MIKT lab with the purpose of later studying environmental mutagens, including BaP, with potential toxic effects on male germ cells. Experiments were performed using red blood cells isolated from small blood samples in mice. A fluorescent RNA/DNA probe (Syto13) and a phycoerythrin (PE) labelled antibody to the CD24 marker was used to separate mutated (CD24 negative) and non-mutated (CD24 positive) reticulocytes (RETs, Syto13 positive) and mature red blood cells (RBCs, Syto13 negative). In this assay, an increased mutation frequency is measured as an increase in CD24 negative cells.

3.3.1 Dose-respons analysis of unlabelled "mutant mimics"

In order to examine the performance of the Pig-a assay, isolated red blood cells were incubated with the CD24 antibody and mixed with a dilution series of unlabelled red blood cells. The latter cells are referred to as "mutant mimics". The number of "mutant mimic" cells pr. 10^5 was estimated by manual cell counting (chapter 2.7.1). Figure 3.9 shows cytograms obtained by flow cytometry for the sample containing red blood cells to which different number of "mutant mimic" cells were added. The cells with a mutant phenotype was localised in the Q1 (RETs) or Q3 (RBCs) quadrants of the cytograms, and figure 3.9 shows a clear increase in amount of mutated RBCs, with increasing number of mutant mimics added.

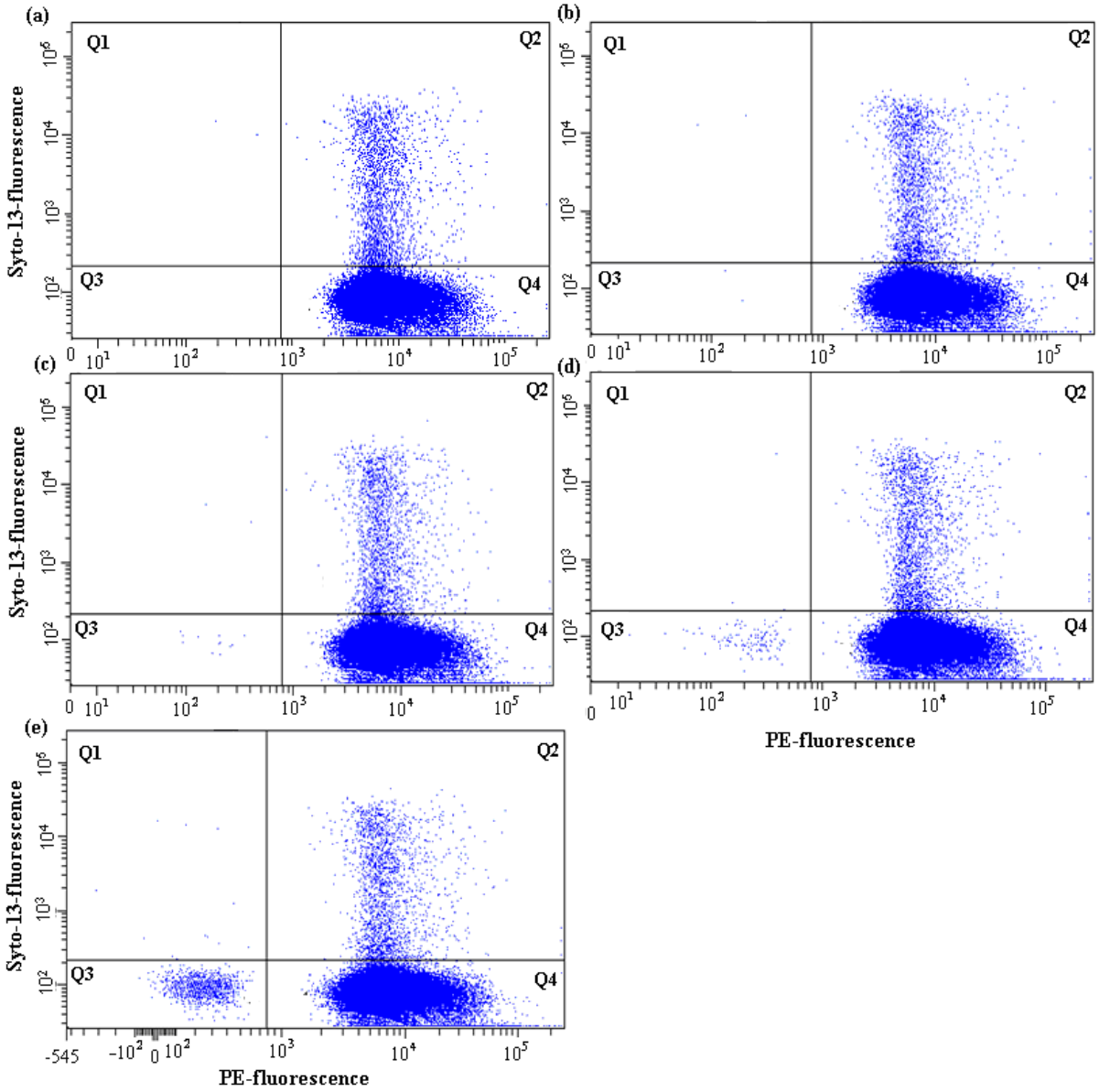

Figure 3.9 Cytograms showing a dose-response experiment with "mutant mimics". One sample containing red blood cells incubated with anti-CD24-PE were allocated and added non-labelled red blood cells from a dilution series. **(a)** Red blood cells labelled with anti-CD24-PE and Syto13 (negative control cells) **(b)** 10^5 labelled red blood cells added an estimated amount of 2.5 "mutant" cells **(c)** 10^5 labelled red blood cells added an estimated amount of 25 "mutant" cells **(d)** 10^5 labelled red blood cells added an estimated amount of 250 "mutant" cells **(e)** 10^5 labelled red blood cells added an estimated amount of 2500 "mutant" cells.

Table 3.3 shows the number of cells from the dose-response experiment with "mutant mimics" that were localised in the four quadrants (Q1, Q2, Q3, and Q4) from the cytograms in figure 3.9. The pig-a assay was able to separate cells with a mutated phenotype from the rest of the cell population. The flow cytometer detected a ten fold increase in the amount of "mutant mimic" RBC (Q3), which corresponded well to the ten folds increased concentration of added "mutant cells". The mutated RETs (Q1) showed a background level

of false positive (mutated) cells in the control sample (a). The levels of mutated RETs did also not increase with increased concentration of "mutant mimic" RETs. This indicates that the assay was not detecting the mutated RETs (Q1) as well as the mutated RBC (Q3).

Table 3.3 Results from the dose-response experiment with "mutant mimics", showing the number of cells detected in each of the four quadrants of the cytograms (figure 3.9). The two columns to the left shows the estimated number of un-labelled cells that were added to 10^5 labelled cells, together with the number of cells that the Pig-a assay and flow cytometer detected as mutants. The amount of cells in Q1 and Q3 quadrants (mutated RETs and RBCs) are increasing with higher amount of "mutant mimic" cells added. Quadrant Q2 and Q4 shows labelled cells in the blood population. Data are obtained by flow cytometry and BD FACSDiva software (v 6.1.2).

Sample	Q1 (mutated RETs)	Q2 (non-mutated RETs)	Q3 (mutated RBCs)	Q4 (non-mutated RBCs)	Estimated number of "mutant mimic" cells added to each sample (pr. 10^5 cells)	Number of "mutant mimic" cells detected by the flow cytometer (pr. 10^5 cells)
(a)	7	2237	0	94039	0	7
(b)	7	2098	2	94002	2.5	9
(c)	5	2067	12	94137	25	17
(d)	10	2123	127	94084	250	137
(e)	15	2092	1095	92912	2500	1110

3.3.2 Visualisation of platelets and lymphocytes in flow diagrams

Platelets and lymphocytes were visualised in forward and side scatter cytograms to examine the localisation of these compared to the red blood cells. This was to decrease the possibility of contamination of these cell types in samples with red blood cells during flow analysis. Figure 3.10 shows cytograms obtained by flow cytometry for samples containing platelets and lymphocytes. An allophycocyanin (APC) labelled antibody for platelets (CD_{42}d-APC) was used to identify the localisation of platelets in the cytogram and staining with Syto13 of all cells made it possible to distinguish lymphocytes from red blood cells.

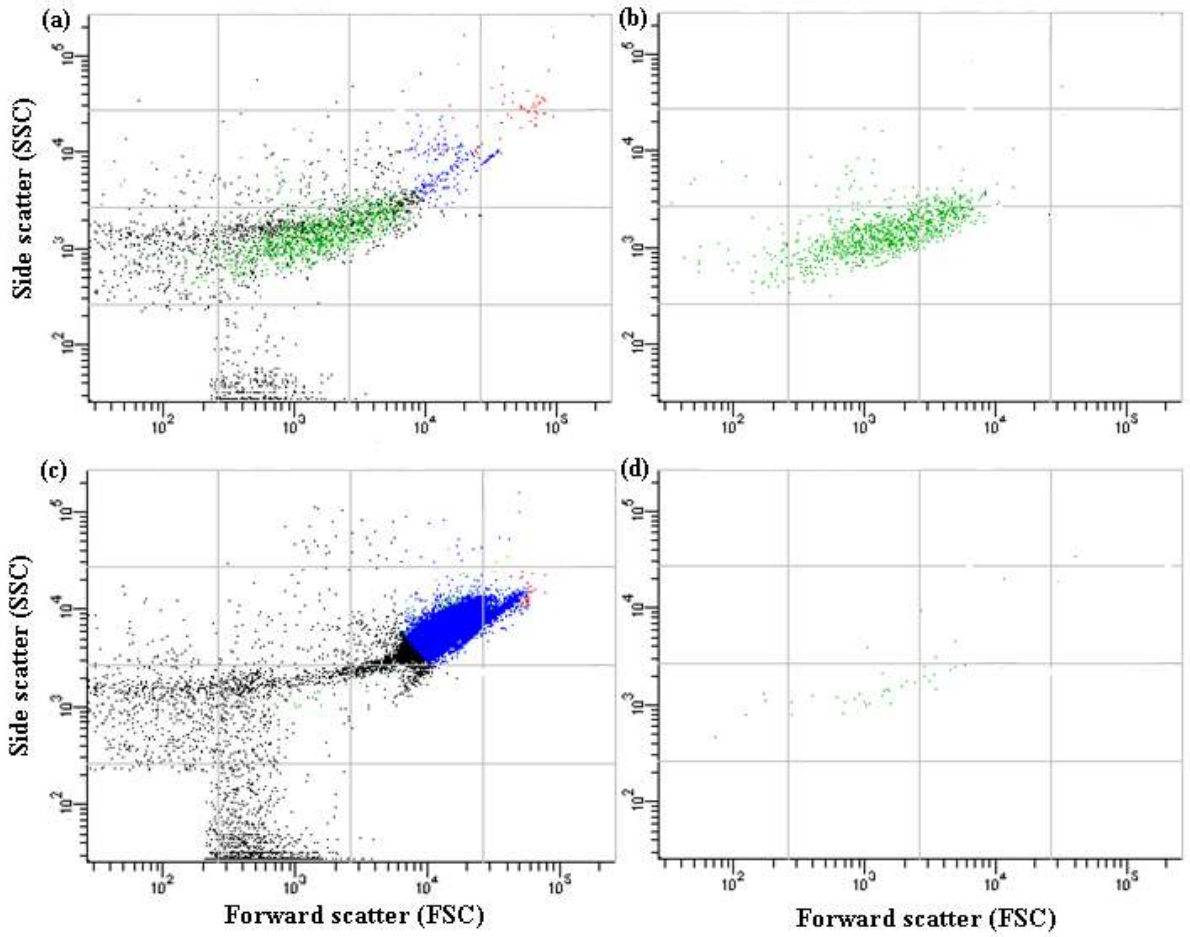

Figure 3.10 Forward and side scatter plots obtained by flow cytometry showing blood samples pooled from four unexposed control mice. Lymphocytes are shown in red, platelets in green and red blood cells in blue. These cell populations were identified in separate histograms (not shown) due to APC-positively (platelets) and Syto13 staining (high in lymphocytes). **(a)** Lymphocytes and platelets isolated from red blood cells. Cells were labelled with antibody for platelets (CD_{42}d-APC) and Syto13 **(b)** Same sample as (a), only platelets are shown **(c)** Red blood cells isolated from whole blood and labelled with antibody for platelets (CD_{42}d-APC) and Syto13 **(d)** Same sample as (c), only platelets are shown.

Figure 3.10 (a) and (b) shows that the main population of platelets was localised below the red blood cells. The lymphocytes were localised mainly above the red blood cells as shown in figure 3.10 (a). This information allowed us to more precisely set the gate used in subsequent experiments to avoid contamination of platelets and lymphocytes. Figure 3.10 (c and d) shows that platelets and lymphocytes were present in a minor amount in the sample of isolated red blood cells that had followed the normal pig-a procedure.

3.4 The performance of the Pig-a assay in response to (ENU) mutagenesis

The number of mutated RETs and mature RBCs in blood samples from mice was analysed by the Pig-a assay after exposure to the model mutagen N-ethyl-N-nitrosourea (ENU). This experiment was performed as a positive control to benchmark the performance of the Pig-a assay in our lab compared to performance in Litron associated labs. Mice were divided into three treatment groups. These were unexposed control (n=2), vehicle (solvent) (n=4) and ENU exposed (n=6). The results from analyses pre-exposure (before treatments), two weeks and five weeks after exposure are presented in this master thesis. Mutated RETs are shown in quadrant Q1 of the cytograms and mutated RBCs are shown in quadrant Q3. Figure 3.11 shows blood samples from one of the animals in the ENU exposed group following Pig-a analysis, pre-exposure, week 2 and week 5 after exposure.

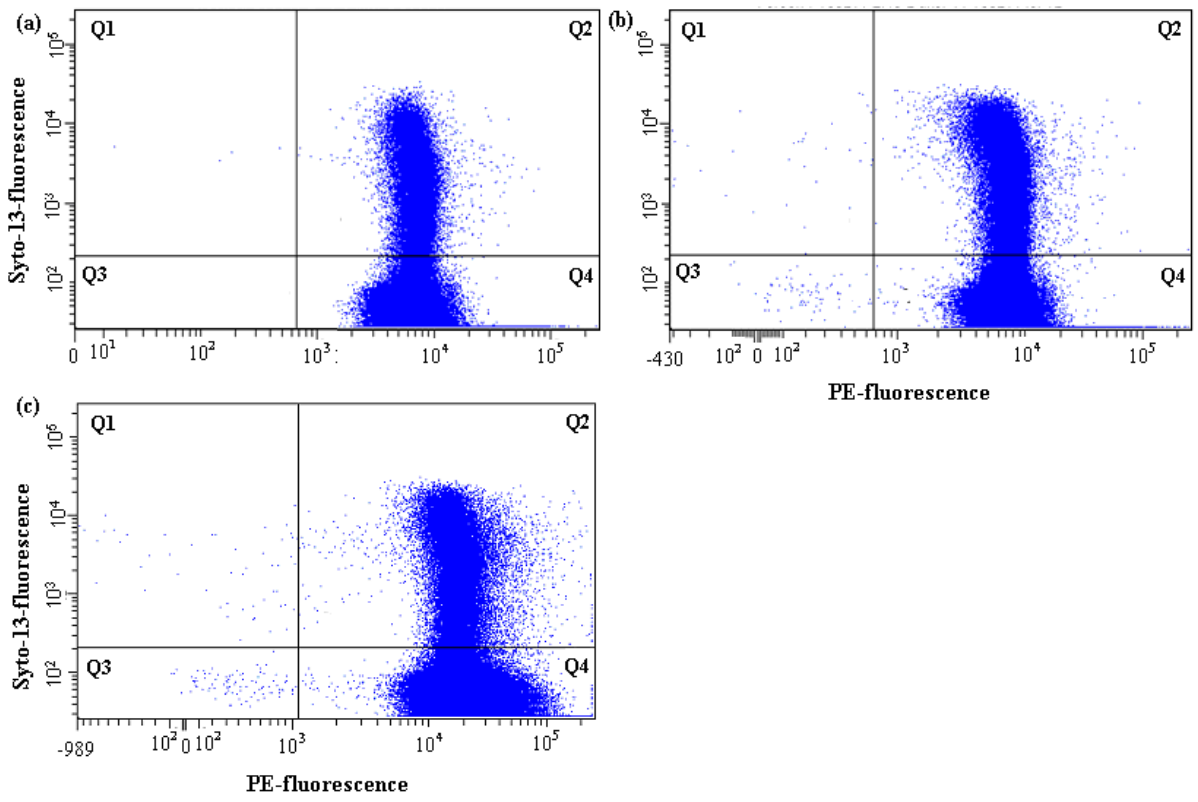

Figure 3.11 Cytograms obtained by flow cytometry showing blood samples from a mouse following the Pig-a assay. Syto13-fluorescence on the y-axis indicates RNA content, while PE-fluorescence on the x-axis indicates CD24 staining. **(a)** Pre-exposure Pig-a analysis of one mice from the ENU group **(b)** Same mouse two weeks after ENU-exposure **(c)** Same mouse five weeks after ENU-exposure.

Table 3.4 shows the mean values of cells in the cytograms (Q1, Q2, Q3 and Q4) from the whole experiment with ENU exposed mice, including control and solvent treated animals. The data was obtained by Pig-a analysis and flow cytometry on blood samples collected pre-exposure, two weeks and five weeks after exposure. Data showed that the amount of mutated RETs (Q1) was generally variable, and high for all treatment groups pre-exposure. This indicates a high background of false positive (mutated) RETs. The amount of mutated RBCs (Q3) was more stable and showed low background of mutated cells in all treatment groups pre-exposure. Mutated RBCs in ENU-exposed animals were increasing following time after exposure, which indicates that the assay is relatively sensitive for detecting mutated RBCs.

Table 3.4 Mean number of cells in each quadrant of cytograms from unexposed (n=2), solvent (n=4) and ENU (n=6) exposed animals. Pig-a analysis was performed for every blood sample pre-exposure, week 2 and week 5 after treatments. Q1 and Q3 represent mean values of mutated RETs and RBCs, respectively, and the standard deviations are calculated for these values. Quadrant Q2 and Q4 are non-mutated cells in the blood populations. Total amount of cells counted for each sample was approximately 10^5 cells. Data was obtained by BD FACSDiva software (v 6.1.2).

	Treatment	Q1 (mutated RETs)	Q2	Q3 (mutated RBCs)	Q4
Pre-exposure	**Unexposed**	57.5 (SD17.7)	37054	1.5 (SD 2.1)	931473
	Solvent	74 (SD 21.0)	38759	1.5 (SD 0.6)	940834
	ENU	43.8 (SD 30.5)	36050	3.5 (SD 2.6)	934023
Week 2	**Unexposed**	9 (SD 1.4)	31828	2 (SD 0)	906098
	Solvent	16.3 (SD 5.6)	34091	2.8 (SD 3.5)	911539
	ENU	76.7 (SD 20.7)	57253	74.7 (SD 17.7)	916467
Week 5	**Unexposed**	74 (SD 21.2)	45860	36 (SD 48.0)	930156
	Solvent	122 (SD 20.6)	37889	1.5 (SD 1.7)	910060
	ENU	133.8 (SD 10.8)	42701	98.5 (SD 45.9)	926419

3.4.1 Analysis of mutated reticulocytes (RETs) after ENU exposure of mice

The number of mutated RETs was analysed by the Pig-a assay in samples pre-exposure (before exposure to ENU), two weeks and five weeks after exposure in order to examine the performance of the assay. Figure 3.12 shows the number of mutated RETs in mice after different treatments (unexposed, vehicle and ENU) over a time course of five weeks.

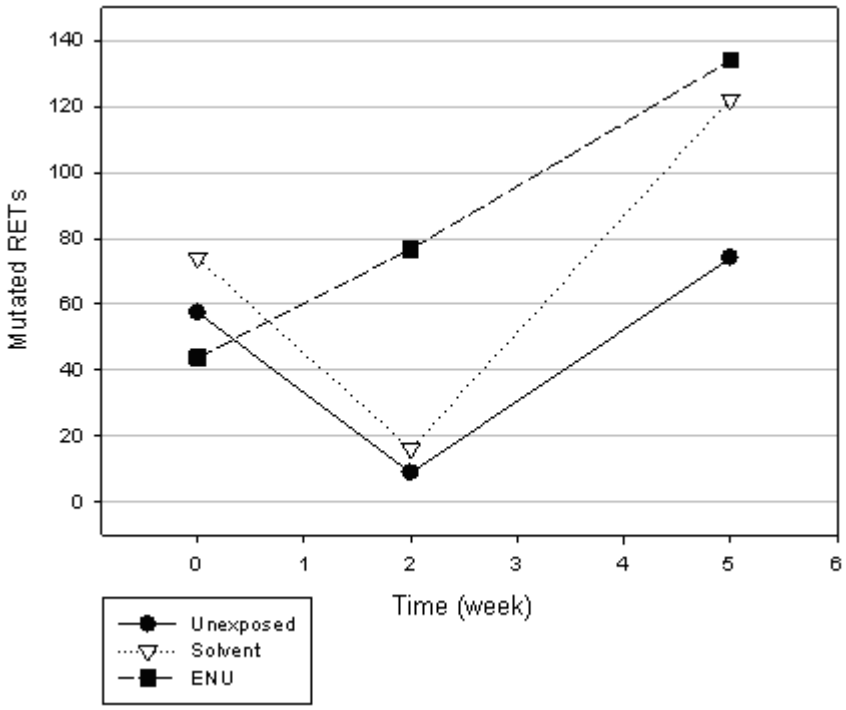

Figure 3.12 Mutation load in reticulocytes (RETs) of mice from pre-exposure to five weeks after administration analysed by the Pig-a assay. The time course curve shows the number of mutated RETs pr. 10^5 counted cells in unexposed mice (n=2), solvent treated mice (n=4) and ENU exposed mice (n=6) from analysis. Data from table 3.6 are used to make the plot.

The amount of mutated RETs was considerably higher than expected for all treatment groups pre-exposure. The figure shows a clear time-dependent increase of mutated RETs in the ENU exposed animals. The amount of mutated RETs in the unexposed and solvent treated mice had a similar trend with a decrease in mutated cells from pre-exposure to week two and an increase in mutated cells from week two to week five. The high number of mutated RETs pre-exposure and generally variable amount of mutations in the control and vehicle treated mice shows that the analysis of mutated RETs needs to be optimised. No further statistical analyses was therefore conducted.

3.4.2 Analysis of mutated mature red blood cells (RBCs) after ENU exposure of mice

The number of mutated RBCs was analysed by the Pig-a assay in samples from pre-exposure, week two and week five in order to examine the performance of the assay. Figure 3.13 shows the number of mutated RBCs in mice after different treatments over a time course of 5 weeks.

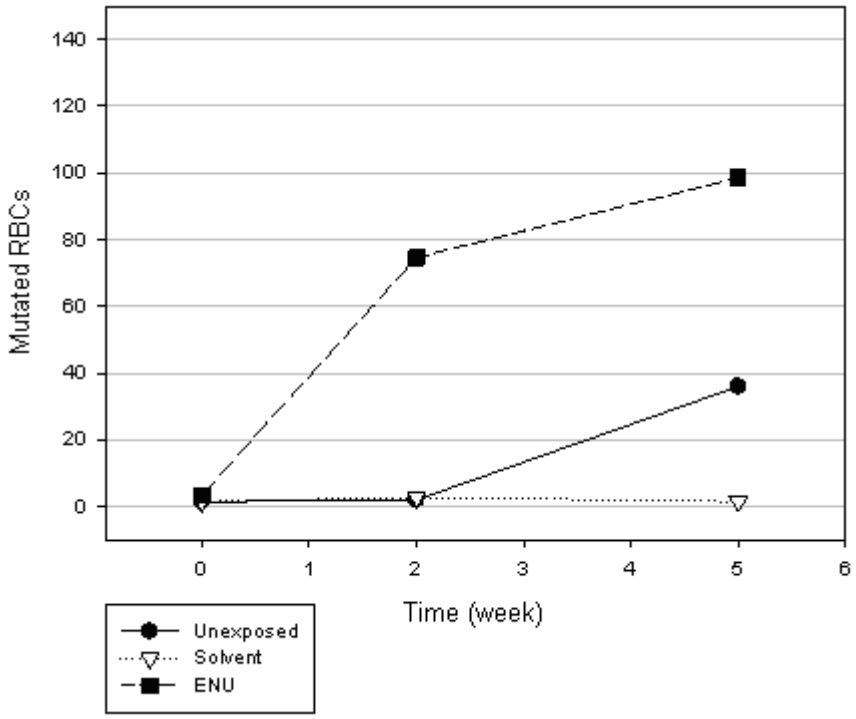

Figure 3.13 Mutation load in mature red blood cells (RBCs) of mice from analyses pre-exposure to five weeks after administration analysed by the Pig-a assay. The time course curve shows the number of mutated RBCs pr. 10^5 counted cells in unexposed mice (n=2), solvent treated mice (n=4) and ENU exposed mice (n=6). Data from table 3.6 are used to make the plot.

Figure 3.13 shows a clear time-dependent increase of mutated RBCs in the ENU exposed animals. The solvent treated animals had a generally low mutation load, while the unexposed animals showed an increase in the amount of mutated RBCs after five weeks. However, the unexposed group only consisted of two animals. The observed increase in mutated mature RBCs was comparable to results obtained in other labs. Statistical analyses were performed on the data to verify that the observed induction of mutations by ENU was statistically significant.

Data for the mutated mature RBCs was normally distributed ($p>0.649$) and meet the requirements for a one-way ANOVA. There were statistical significant differences ($p<0.001$) in amount of mutations following the time course curve. A Fisher LSD (least significant difference method) post hoc test was then conducted and showed a statistical significant increase in mutated RBCs from ENU exposed animals at pre-exposure compared to week 2 ($p<0.001$) and week 5 ($p<0.001$) after exposure. There were no statistical significant increase in the amount of mutations from week two to week five ($p=0.168$).

Data from vehicle and ENU exposed mice were compared, in order to examine if there were statistical significant differences in mutations between these two treatments. The unexposed animals were not included due to the low number of animals ($n=2$). Data from samples pre-exposure and week two in vehicle treated animals were not normally distributed ($p<0.005$), and the non-parametric Mann-Withney test was therefore conducted to compare data in the two groups. There were statistical significant differences between vehicle and ENU exposure at week 2 ($p=0.01$) and at week 5 ($p=0.01$) in the amount of mutated RBCs. There were no statistical significant difference between vehicle and ENU exposed animals in the amount of mutations at pre-exposure ($p=0.267$).

4. Discussion

As indicated in the introduction, the genomic integrity of human cells is constantly influenced by environmental mutagens. The effects of these compounds on both somatic and germ cells have gained increased attention during the last decades. It is suggested that these compounds contribute to the decreased fertility observed in couples in the industrialised world. In this project, the aim was to study the effects of the environmental toxicant BaP, on the DNA in male germ cells. As described in chapter 1.7, BaP is distributed to several tissues where metabolism converts BaP into metabolites that may have toxic effects on human cells. Many of these metabolites have ability to react with the DNA, including radical cations and PAH-0-quionones. The most deleterious metabolite is considered to be the ultimate carcinogen BaP-7,8-diol-9,10-epoxide (BPDE) (Conney 1982; Sims *et al*., 1974). The low repair capacity in sperm cells at later stages of the spermatogenesis contributes to a possible transmission of BPDE-DNA adducts to embryonal DNA following fertilisation (Zenzes *et al*., 1999b). Furthermore, a study on human surplus embryos from IVF treatment have suggested that paternally transmitted BPDE-DNA adducts also can persist past the first embryonic cleavage divisions (Zenzes *et al*., 1999b).

4.1 Testicular toxicity of BaP

In this study, BaP was administered by i.p. to animals as a single dose of 150 mg/kg/bw. This dose was below an acute LDlo dose at 500 mg/kg/bw found for mice after i.p injection (Epstein *et al.*, 1972). In dominant lethality studies of mice it has been shown that paternal BaP exposure to i.p. doses of 100 and 500 mg/kg/bw in the 1-2 weeks preceding fertilisation induced increased rate of embryo losses (Generoso *et al*., 1982; Shukla and Taneja 2001). The sperm cells used in our IVF experiments was exposed to BaP *in vivo* for 4 days prior to IVF. The fertilisation rate in these experiments was only slightly reduced by BaP exposure (Ryan 2011, unpublished). This indicates that BaP-exposed sperm cells are able to fertilise the oocyte, although BaP is highly embryo-toxic.

Mice in the SCSA experiment were sacrificed ten days after exposure. The passage of spermatozoa through the epididymis takes approximately ten days in both mice and humans (Moore 1998; Oakberg and Diminno 1960; Rowley *et al*., 1970). Thus, sperm cells were located between the rete testis and caput epididymis when exposed to BaP. These cells are

elongated and have a reduced repair capacity because of the condensed nature of chromatin. Accordingly, BPDE-DNA adducts levels were shown to be high both four and sixteen days after BaP-exposure in mice (Olsen *et al*., 2010). Sperm cells collected from the cauda epididymis ten days after BaP-exposure in the SCSA experiments were therefore assumed to have a high level of DNA damage. The lack of DNA repair in sperm, suggests that human males that are exposed to a relatively high doses of BaP via for instance continuously high intake of cigarette smoke or extensive occupational exposure may accumulate BPDE-DNA adducts in their sperm DNA. This may affect their fertility potential, and is supported by the observed association between smoking and reduced fertility (Irvine *et al*., 2000; Künzle *et al*., 2003; Vine 1996).

The doses and exposure route used in the lethality studies and in the experiments of the present master are high compared to what a human population normally are exposed to. A realistic exposure scenario is low doses over a long period of time (chronic exposure). Sub-acute and chronic studies of BaP-exposure reveal effects on testosterone levels in addition to BaP-induced DNA damage (Inyang *et al*., 2009). The benefit of using a single high dose of BaP is the opportunity to specifically measure effects of exposure of early to middle spermatozoa, a maturation stage that is associated with the induction of dominant lethality (Generoso *et al*., 1982; Shukla and Taneja 2001). In addition, statistical significant results can be obtained with a reduced number of animals compared to a low-dose exposure scenario. The effect of genotoxic chemicals is assumed to be linear with the dose. A high dose of BaP can therefore be used to extrapolate low dose effects.

4.2 DNA integrity of BaP exposed sperm as measured by the SCSA

The SCSA was used in the present master in order to examine if the assay could detect BaP-induced DNA damage in sperm cells from mice. This was based on the knowledge that BaP is a DNA disturbing toxicant that induces embryo lethality following paternal exposure (Generoso *et al*., 1982; Sims *et al*., 1974; Verhofstad *et al*., 2010; Xue and Warshawsky 2005). Advantages with the SCSA are that the assay is well-proven, extensively used and is based on flow cytometry, which is a valuable tool for measuring thousands of cells in short time. The SCSA is also inexpensive and relatively easy to perform. The assay measure pre-existing or denaturation-induced single or double stranded breaks in the DNA, but are unable to detect the cause of the strand breaks.

4.2.1 The SCSA indicated no difference in DNA damage between treatment groups

In the present BaP-experiment, no statistical significant differences in the degree of DNA damage expressed as mean Alpha t and % DFI was observed between sperm cells from mice after different treatments (control, vehicle and BaP). Previous SCSA experiments have shown that smoking men and men exposed to air pollution had elevated level of DNA damage expressed as % DFI in sperm cells compared to controls (Potts *et al*., 1999; Rubes *et al.*, 2010). However, it is not confident that BaP in particular causes DNA damage in form of strand breaks. Our study indicates that BaP does not cause this kind of damage. There are numerous other compounds in air pollution and cigarettes smoke than BaP, and this together with long-term exposure of humans may give a completely different result in the SCSA than measurements of BaP alone.

There were a few animals that showed increased % DFI values (table 3.2). This was observed in one of the animals in the oil treated $Ogg1^{wt}$ group (32.59%) and another in the BaP exposed $Ogg1^{wt}$ group, with the high value of 70.57 % DFI. The latter animal also gave high values in the mean Alpha t parameter compared to the other animals in the experiment. Because of the enhanced responses in these two animals, the mean values and standard deviations (SD) were increased for the % DFI parameter in these groups. Even if the genetic background in these mice is similar, it is expected that animals experience different stress level caused by external factors, and hence may respond differently to exposure. The results indicate that these animals were more susceptible to exposure than the other animals, which is generally accepted in human populations as well. The SCSA is a method with high sensitivity, and human mistakes may also occur. Inaccuracy in the acid denaturation step or a delay during the flow analyses could be plausible reasons for some elevated values in the result. However, this type of bias would have been discovered during the analysis. Previous pilot experiments with the SCSA performed at the MIKT-lab have shown that a denaturation time of 60 seconds instead of 30 seconds gave only a slight increase in % DFI, and not as high as up to 70 % which is shown in the BaP treated $Ogg1^{wt}$ animal in this study. Since this was a biological experiment it is not accurate to eliminate these data from the result even if they may look like outliers, and the statistical analyses were therefore performed with these data. A higher number of animals in the experimental groups would have been useful to

confirm if the observed enhanced values were characteristic for these kinds of experiments or random.

% DFI is believed to be the most sensitive SCSA parameter (Evenson and Jost 2000), and this was confirmed in the preliminary SCSA experiment with a dose-response analysis of sperm cells after DNase exposure. The % DFI parameter reached a saturated level after a dose of 0.2 U/ml DNase, while the mean Alpha t value in the same experiment increased in a fairly linear way following higher doses (figure 3.1). This indicates that % DFI potentially is a good parameter for studying genotoxic compounds, although the parameter may be unsuited in some toxicological animal experiments. A highly sensitive parameter could easily reach saturation, and this has been observed in an earlier master thesis at the MIKT-lab, where the % DFI parameter easily reached saturation in sperm cells exposed to acrylamid (Shahzadi 2008, unpublished). Since BaP did not generate increased DNA damage measured as strand breaks in the present project, and % DFI is a sensitive parameter, this further indicate that this kind of damage is not present in the sperm cells after BaP-exposure.

4.2.2 Effects of BaP on sperm DNA damage in Ogg1$^{-/-}$ mice

In studies of exposure to specific compounds in experimental animals, the use of transgenic mice is often valuable. Knock out of desirable genes can be used to increase the knowledge of cellular mechanisms, and increase the relevance of animal studies to humans. The Ogg1$^{-/-}$ mice used in the present BaP-experiment were deficient in repair of the oxidative DNA lesion 8-oxoG, due to a knock out of the OGG1 gene for DNA glycosylase (Klungland *et al.*, 1999). Human testicular cells have a lower degree of repair capacity of oxidative DNA-lesions such as 8-oxoG than mice (Olsen *et al*., 2003). Hence, these Ogg1$^{-/-}$ mice are often used as a model for human testicular toxicity studies. A lower repair capacity may result in a higher background level of oxidative DNA lesions in sperm from Ogg1$^{-/-}$ mice compared to Ogg1$^{+/+}$, possibly rendering them more sensitive to additional damage. The extent of DNA damage was therefore assumed to be similar or higher in the Ogg1$^{-/-}$ animals compared to Ogg1$^{+/+}$ (or Ogg1^{wt}). However, BaP exposed Ogg1$^{-/-}$ mice rather had a slightly lower mean value compared to BaP exposed Ogg1^{wt} mice for the % DFI parameter (figure 3.5). There were no statistical significant differences between the two groups in the % DFI parameter. This indicates that a deficiency in repair of 8-oxoG did not generate any higher level of DNA

damage compared to mice with a higher repair capacity ($Ogg1^{wt}$), at least as was measureable by the SCSA.

The data from the % High green parameter demonstrated no statistical significant differences between treatment groups in the wild type animals. However, animals in the BaP-exposed $Ogg1^{-/-}$ group showed statistical significant lower mean values compared to the groups with wild type mice (figure 3.6). Sperm cells in the High green parameter are cells with a higher stainability of dsDNA by acridine orange (AO). These cells are believed to be immature sperm cells without fully protamine condensed chromatin, which allows a higher accessibility of the nucleic dye (Evenson and Jost 2000). The reasons for statistical significant lower levels for these sperm cells in the BaP exposed $Ogg1^{-/-}$ mice are unclear.

The oxidation of protamine thiols plays an important role in sperm maturation (Pfeifer *et al*., 2001). A potential explanation may thus be that the combination of BaP-exposure and a decreased repair capacity induce a moderate oxidative stress that promotes the condensation of sperm chromatin. This could lower the amount of immature cells in the cauda epididymis. Alternately, the decreased repair capacity may also result in a higher level of apoptosis in sperm cells from the BaP exposed $Ogg1^{-/-}$ mice. If this apoptosis was selective towards immature cells due to their weaker chromatin configuration, a lower total amount of immature cells could be present in a sperm sample. Furthermore, the % High green parameter is not as precise as the other SCSA parameters because measurements of cell doublets have been observed (Evenson and Jost 2000). Cell doublets are a concept in flow cytometric analysis where two cells are physically attached to each other or pass through the laser beam so close that they are detected as a single event by the cytometer. The cell doublets normally comprise a very small percentage of the total population, and should probably be present in the other groups of mice as well. It would be interesting to observe if the % High green parameter was reduced in the control and vehicle $Ogg1^{-/-}$ mice as well, or if BaP-exposure was the reason for a reduced value in the BaP exposed $Ogg1^{-/-}$ mice. However, this was not possible to examine in this project due to the erroneous genotyping mentioned in chapter 3.1.2, and this short coming makes it difficult to achieve the aim of comparing the two genotypes.

4.2.3 Limitations in the SCSA for measuring BaP-induced DNA damage

Sperm DNA damage is difficult to measure due to the highly compact nature of sperm DNA. Although the SCSA is widely used and measure single and double stranded DNA breaks with great efficiency, the results from this study indicate that BaP-exposure of early and middle spermatozoa do not make the chromatin in sperm cells more unstable, and the damage is thus not measurable by the SCSA. Studies have shown that BaP give a high amount of BPDE-DNA adducts in sperm (Olsen *et al*., 2010; Sipinen *et al*., 2010), meaning that these adducts were present in the chromatin of BaP exposed mice. The induction of embryo lethality stresses the need for an alternative assay that can reveal BaP-induced sperm damage. However, the SCSA results suggest that embryo toxicity induced by paternal BaP exposure is related to DNA adduct formation and not to secondary formation of DNA strand breaks in paternal DNA. This is in contrast to acrylamid that also has shown to induce dominant lethality, but where both DNA-adducts and DNA breaks is considered to play a part (Marchetti and Wyrobek 2005; Brevik, manuscript in preperation).

4.3 Establishment of an immunostaining procedure for BPDE-DNA adducts

One of the aims for this master project was to set up an immunological method suited for staining of BPDE-DNA adducts. The ultimate goal was to use this method to examine if sperm BPDE-DNA adducts persist in pre-implantation embryos after paternal exposure to BaP. Immunostaining techniques has previously detected BPDE-DNA adducts in other tissues, including both oocytes and sperm cells (Zenzes *et al*., 1998; Zenzes *et al*., 1999a; Zhang *et al*., 1998). Successful staining of BPDE-DNA adducts in embryos after paternal BaP-exposure has also been performed with surplus embryo from IVF treatments (Zenzes *et al*., 1999b). Zenzes study of paternal transfer of BPDE-DNA adducts was performed on a small sample size and indirect exposure of the mother could have occurred. A part of the aim for this master was to establish a more robust method that could be applied to larger number of embryos and under controlled exposure conditions.

Immunostaining of BPDE exposed hepatoma cells *in vitro* confirmed that the procedure worked, with clear staining of BPDE-DNA adducts (figure 3.8). The use of clots for capturing embryos before staining was believed to give a more efficient staining procedure without need for mouth pipetting in every stage. Since embryos on slides were easily lost,

capture in clots was also believed to reduce this problem. Experiments with oocytes in fibrinogen clots on slides are performed earlier with other immunostaining procedures (Hunt *et al.*, 1995; Shahzadi 2008, unpublished). Because of the denaturation step in the procedure for staining BPDE-DNA adducts, fibrinogen clots were dissolved and we concluded that these clots was unsuited. Subsequently, agarose clots were tried and these were able to capture embryos and did tolerate the denaturation step. However, the results were poor for staining of embryos after BaP-exposure both *in vivo* and *in vitro* together with *in vitro* exposed oocytes. Testicular somatic cells were also exposed to BPDE as a positive control to test the procedure, and there were no staining of BPDE-DNA adducts in testicular cells as well. Since the same procedure gave efficient staining of adducts in hepatoma cells at an earlier stage, there are really no logical explanation for why the procedure suddenly did not work. We concluded that there was a methodological failure. This failure where not resolved, due to the time limit of this master thesis. The main focus for the immunostaining part of this master became testing of the method. Although the results were poor, a method for capturing embryos in agarose is now established at the MIKT-lab and the procedure for immunostaining for BPDE-adducts has been optimised.

A successful staining of BPDE-DNA adducts in embryos would have indicated whether exposure to BaP *in vivo* to male mice could give DNA adducts that are transferred to embryonal DNA following fertilisation. It could also give information of whether known BPDE-DNA adducts were present in later stages of the embryo. For a further link to humans, this could have indicated that a smoking father have potential to transfer BaP-induced adducts and disturb a healthy embryonal development of his offspring, as suggested by studies by Zenzes (Zenzes *et al*., 1999b).

4.4 Promising results for the somatic mutation assay Pig-a

Establishment of the Pig-a assay at the MIKT-lab was one of the aims for this project. This work has been performed with support from the Litron laboratories, and continuous improvements increase the sensitivity of the assay. The pilot experiments in the present master project has provided knowledge about the assay qualities, and been a part of establishing a protocol for the Pig-a assay at the MIKT-lab. Several laboratories are using the prototype kit provided by Litron with mutual solutions for comparison of results, and the Pig-a assay has proved to be promising. The Pig-a assay has shown to be relatively quick to

perform, it takes approximately one day from collecting blood samples to completed flow analysis, in a sample size with blood from ten animals. Since the acquired volume of withdrawn blood from each animal is relatively small, animals are not very affected and the assay can be used in combination with long-term exposures in evaluation of chemicals. *In vivo* mutation assay are needed, and the Pig-a assay could be included into 28-days repeated dose standard toxicological studies of chemicals. However, the Pig-a assay only measure mutations in a single gene whose sensitivity to various types of DNA damage has not yet been well defined. Since the Pig-a gene is located on the X chromosome it is expected to identify only a part of the mutations that can be detected with an autosomal reporter gene (Dobrovolsky *et al*., 2010). The assay is also relatively new, and limited data have been generated on the fact that all GPI marker deficient cells have mutations in the Pig-a gene. Pig-a mutations in other tissues than blood are also presently not well established. This study has shown that the assay was sensitive and well repeatable. It was also shown that the assay had some background level of false positive mutated reticulocytes (RETs).

4.4.1 Pilot experiments

The dose-response analysis with a mixture of an increasing amount of unlabelled "mutant mimic" cells (CD24 negative) and labelled cells (CD24 positive) indicated that the assay was able to detect cells with a mutant phenotype. This was best detected in mutated mature red blood cells (RBCs), with a correct detection of a ten fold increase in mutated cells in the dilution series (table 3.3). The amounts of mutated RETs were variable and showed a background of false positive cells in the control sample (table 3.3). In mutation assays that use samples with red blood cells, the key parameter to examine is the amount of mutated RETs. RETs are young and recently produced in the bone marrow (chapter 1.15), while the erythrocytes are older and already circulating in the blood pool. Erythrocytes may thus been through a selection of healthy cells and apoptosis of mutated ones, which could provide an incorrect picture of the actual mutated number of cells in a sample caused by the compound tested. In contrast, RETs are assumed to contain all the mutated and non-mutated cells. To be able to measure effects in RETs, the chemicals tested needs to reach and affect cells in the bone marrow. This limitation is also true for the micronucleus assay.

Labelling of platelets and lymphocytes gave information about localisation of these cells in Pig-a flow cytograms. This experiment was performed due to the observed amount of false positive RETs. We wanted to examine if some of the platelets or lymphocytes was still

present after the red blood cell preparation during the Pig-a procedure, and possibly was detected as false positives. Due to different sizes of the various mammalian blood cells together with antibody (labelling of platelets) and Syto13 labelling (nucleic acid dye), we were able to establish the localisation of these in the cytogram compared to the red blood cells. The small platelets were displayed below the red blood cells, while the larger lymphocytes were displayed above (figure 3.10a). This experiment confirmed that only a small amount of platelets and lymphocytes were present in a sample with isolated red blood cells (figure 3.10 b), and are probably not the reason for the repeated level of false positive RETs observed. However, it is important to be aware of this when making conclusions of results from the assay. Establishment of where platelets and lymphocytes are localised, makes the gating for future Pig-a experiments more stringent and reliable, and contamination of samples for Pig-a analyses can more easily be avoided.

4.5 Performance of the Pig-a in response to ENU-treatment in mice

The Pig-a experiment with ENU exposure to mice, was conducted as a positive control for the assays performance in our lab, compared to other similar experiments. Earlier experiments with performance of the Pig-a assay using different mutagens, including ENU, has shown an increased frequency of mutated cells (Miura *et al*., 2008; Phonethepswath *et al*., 2008; Phonethepswath *et al*., 2010). ENU-exposure of mice in our project gave a statistical significant increase in number of mutated RBCs detected by the Pig-a assay, following a time period of five weeks. However, the results for mutated RETs were variable and indicated the detection of false positive cells. The assay detected a relatively high amount of mutated RETs pre-exposure (before treatments) in all animals (figure 3.12). The mutation load in animals at this time is expected to be low. The analysis two weeks after exposure showed that amount of mutations in control animals was decreased. In the Pig-a analysis pre-exposure, the technique with preparation of all blood samples may not have been incorporated well enough, and the gating performed in the calibration standard may have been performed more liberal in this analysis. This could give a higher amount of RETs measured as mutants pre-exposure, and explain the decrease in amount of mutations analysed in week two. Since this experiment was a part of establishing the Pig-a assay, further statistical analyses on the clearly unstable measurements of RETs was not conducted. The aim was to increase the knowledge of the assay for further studies. Results from other laboratories (Miura *et al*., 2009) have shown that the mutations in RETs occur earlier in time

(one week) than mutations in RBCs. Furthermore, the mutation frequency was shown to be higher in RETs than in RBCs, suggesting a removal of mutated mature RBCs.

The measurements of mature red blood cells (RBCs) showed statistical significant differences from pre-exposure to both week two and week five, and no such difference from week two to week five (figure 3.13). This indicates that ENU generate a higher increase in mutations in the first two weeks, followed by a decrease in the rate of new mutations for the next three weeks. The mutation load pre-exposure in RBCs was very low (figure 3.13), which shows a low background of false positive RBCs compared to false positive RETs. Since the results from mutated RBCs showed a more satisfactory result, further statistical analysis was conducted. The result showed that ENU treated animals had a statistical significant higher amount of mutations than vehicle treated animals in both week two and week five. There were no statistical significant differences of mutation load between ENU and vehicle animals pre-exposure. The experiment indicated that the assay can measure mutations in RBCs with high sensitivity. The results of the analysis of mature RBCs was in agreement with other labs (Miura *et al*., 2009).

4.5.1 Improvement for the Pig-a assay and future relevance

It is currently ongoing work with improving the performance of the Pig-a assay, including experiments for reducing the amount of false positive RETs. The number of mutated cells in a blood sample is generally low, and by increasing the amount of cells that are counted by the flow cytometer for each sample, more reliable results could be achieved. Since the assay is using flow cytometry, gating can be made in the cytogram that only take RETs into account, since these are the most valuable cells to study in a mutation assay with red blood cells. Recently a new antibody with higher affinity towards the surface marker for the GPI-anchor has shown to reduce the amount of false positive RETs detected by the assay.

A future goal for the MIKT-lab regarding the Pig-a assay is a completely established assay that can be applied as a supplementary test to other studies. This assay will be examined for the possibility of using the mutation frequency in somatic cells as a proxy for the mutation frequency in germ cells. The ultimate goal would be analyses of human samples. This is also needed in order to examine if the assay is functional in humans. If this proves to be the case, the assay could be applied in the work with establishment of genotoxicity data in human biomonitoring.

4.6 Conclusions

BaP-exposure of male mice *in vivo* did not generate enhanced levels of DNA damage in sperm cells analysed by the SCSA. This indicates that the SCSA is an unsuited method for examination of BPDE-DNA adducts although it is a well used and established method in humans. Furthermore, the results indicated that BaP exposure does not induce secondary DNA strand breaks in sperm cells. A decreased value of sperm cells in the % High green parameter was observed in BaP-exposed $Ogg1^{-/-}$ mice compared to wild type animals. Whether this decrease was due to the genotype in general or the combination of BaP-exposure and genotype was not possible to determine in this study, because control and vehicle treated mice were absent for the $Ogg^{-/-}$ genotype.

Establishment of a method for immunostaining of BPDE-DNA adducts in embryo, was technically challenging. Hepatoma cells exposed to a high dose of BPDE *in vitro* gave detectable adducts and confirmed that the procedure worked. We managed to establish a method for capturing embryos inside clots of agarose, however, the staining for BPDE-DNA adducts in these embryos after exposure both *in vitro* and *in vivo* were poor. The study of paternal transfer of BPDE-DNA adducts to embryo DNA is incomplete and we were not able to proceed to further staining of adducts in second and four cell stages of the embryo. The reason for this is believed to be methodological, and the problem was not solved do to the time limits of this master. Despite poor results in this part of the project, we have gained knowledge of the procedure and have excluded several approaches in the development of the method. This will be a significant advantage in further studies with staining of BPDE-DNA adducts in embryos.

The establishment of the Pig-a assay has showed that the assay is promising and has great sensitivity for detection of mutant mature red blood cells (RBCs). This was proved in a positive control with ENU-exposed mice, and a dose-response experiment with “mutant mimics”. These experiments have also indicated that the assay needs improvement regarding the sensitivity for detection of mutated reticulocytes (RETs). The assay seems promising for measuring somatic mutations, and it is now an established protocol for the assay at the MIKT-lab that is under current improvements. This includes separate analysis of mutated RETs and the use of an antibody with higher affinity towards the GPI-anchor marker. The amount of cells examined for each sample is also increased. The Pig-a assay has potential for regulatory toxicology and in the study of environmental mutagens.

4.7 Future work

Measurements of sperm DNA-integrity is complicated due to the highly compact DNA in sperm. Since the SCSA showed poor results for detection of BaP-induced DNA damage, other assays are needed for this purpose. Measurements of DNA damage in mitochondrial DNA in sperm cells, instead of nuclear DNA is one method that are under consideration at the MIKT lab (Ryan 2011, unpublished). Preparation for further studies on immunostaining of embryos is under current consideration at the MIKT-lab to answer the questions of DNA adduct persistence in pre-implantation embryos. The Pig-a assay is presently under development and improvement. A future study on mutagenic effect of BaP in somatic cells would be of great interest and a study is planned to compare the mutation frequencies in somatic and germ line cells following BaP exposure.

5. Reference list

Adami, H.O., Bergstrom, R., Mohner, M., Zatonski, W., Storm, H., Ekbom, A., Tretli, S., Teppo, L., Ziegler, H., Rahu, M. (1994). Testicular cancer in nine northern European countries. *Int J Cancer* **59**, 33-38.

Ahmadi, A., and Ng, S.C. (1999). Fertilizing ability of DNA-damaged spermatozoa. *J Exp Zool.* **284**, 696-704.

Anastas, P.T., and Williamson, T.C. (1996). Green Chemistry: An Overview. In *Green Chemistry* **626** ed., pp. 1-17. American Chemical Society.

ATSDR (1995). Toxicological profile for polycyclic aromatic hydrocarbons (PAHs)(Update). (U.S.Department of Health and Human Services. Atlanta, Georgia, U.S.)

Baek, S.O., Field, R.A., Goldstone, M.E., Kirk, P.W., Lester, J.N., and Perry, R. (1991). A review of atmospheric polycyclic aromatic hydrocarbons: Sources, fate and behavior. *Water, Air, & Soil Pollution* **60**, 279-300.

Baird, W. M., Hooven, L.A., and Mahadevan, B. (2005). Carcinogenic polycyclic aromatic hydrocarbon-DNA adducts and mechanism of action. *Environ Mol Mutagen.* **45**, 106-114.

Barratt, C.L., Aitken, R.J., Bjorndahl, L., Carrell, D.T., de, B.P., Kvist, U., Lewis, S.E., Perreault, S.D., Perry, M.J., Ramos, L., Robaire, B., Ward, S., and Zini, A. (2010). Sperm DNA: organization, protection and vulnerability: from basic science to clinical applications-a position report. *Hum Reprod.* **25**, 824-838.

Bavister, B.D. (2002). Early history of in vitro fertilization. *Reproduction* **124**, 181-196.

Bedford, J.M. (1994). The status and the state of the human epididymis. *Hum Reprod.* 9, 2187-2199.

Bellve, A.R., Millette, C.F., Bhatnagar, Y.M., and O'Brien, D.A. (1977). Dissociation of the mouse testis and characterization of isolated spermatogenic cells. *J Histochem. Cytochem.* **25**, 480-494.

Boffetta, P., Jourenkova, N., and Gustavsson, P. (1997). Cancer risk from occupational and environmental exposure to polycyclic aromatic hydrocarbons. *Cancer Causes Control* **8**, 444-472.

Borg, C.L., Wolski, K.M., Gibbs, G.M., and O'Bryan, M.K. (2010). Phenotyping male infertility in the mouse: how to get the most out of a 'non-performer'. *Hum Reprod. Update* **16**, 205-224.

Boström, C.E., Gerde, P., Hanberg, A., Jernstrom, B., Johansson, C., Kyrklund, T., Rannug, A., Tornqvist, M., Victorin, K., and Westerholm, R. (2002). Cancer risk assessment, indicators, and guidelines for polycyclic aromatic hydrocarbons in the ambient air. *Environ Health Perspect* **110** Suppl 3, 451-488.

Bryce, S.M., Bemis, J.C., and Dertinger, S.D. (2008). In vivo mutation assay based on the endogenous Pig-a locus. *Environ Mol Mutagen.* **49**, 256-264.

Campbell, A.C., and Reece, J.B. (2005). Animal reproduction, in *Biology* 7 ed., pp. 964-986. Pearson Education, Inc., San Fransisco.

Chang, M. C. (1959). Fertilization of rabbit ova in vitro. *Nature* **184** (Suppl 7), 466-467.

Chary, P., Latham, G.J., Robberson, D.L., Kim, S.J., Han, S., Harris, C.M., Harris, T.M., and Lloyd, R.S. (1995). In vivo and in Vitro Replication Consequences of Stereoisomeric Benzo[a]pyrene-7,8-dihydrodiol 9,10-Epoxide Adducts on Adenine N6 at the Second Position of N-ras Codon 61. *Journal of Biological Chemistry* **270**, 4990-5000.

Cheng, K.C., Cahill, D.S., Kasai, H., Nishimura, S., and Loeb, L.A. (1992). 8-Hydroxyguanine, an abundant form of oxidative DNA damage, causes G----T and A----C substitutions. *J Biol Chem* **267**, 166-172.

Conney, A.H. (1982). Induction of microsomal enzymes by foreign chemicals and carcinogenesis by polycyclic aromatic hydrocarbons: G. H. A. Clowes Memorial Lecture. *Cancer Res* **42**, 4875-4917.

Culp, S.J., and Beland, F.A. (1994). Comparison of DNA adduct formation in mice fed coal tar or benzo[a]pyrene. *Carcinogenesis* **15**, 247-252.

D'Occhio, M.J., Hengstberger, K.J., and Johnston, S.D. (2007). Biology of sperm chromatin structure and relationship to male fertility and embryonic survival. *Animal Reproduction Science* **101**, 1-17.

Dabestani, R., and Ivanov, I.N. (1999). A Compilation of Physical, Spectroscopic and Photophysical Properties of Polycyclic Aromatic Hydrocarbons. *Photochemistry and Photobiology* **70**, 10-34.

Dadoune, J.P. (2003). Expression of mammalian spermatozoal nucleoproteins. *Microsc. Res Tech* **61**, 56-75.

De Bont, R., and van Larebeke, N. (2004). Endogenous DNA damage in humans: a review of quantitative data. *Mutagenesis* **19**, 169-185.

De Jonge, C., and Barratt, C. (2006). Sperm maturation in the human epididymis, in *The Sperm Cell* 1 ed., pp. 72-107. Cambridge University Press, New York.

Delbes, G., Hales, B.F., and Robaire, B. (2010). Toxicants and human sperm chromatin integrity. *Mol Hum Reprod.* **16**, 14-22.

Devanesan, P.D., Higginbotham, S., Ariese, F., Jankowiak, R., Suh, M., Small, G.J., Cavalieri, E.L., and Rogan, E.G. (1996). Depurinating and stable benzo[a]pyrene-DNA adducts formed in isolated rat liver nuclei. *Chem Res Toxicol* **9**, 1113-1116.

Dobrovolsky, V.N., Miura, D., Heflich, R.H., and Dertinger, S.D. (2010). The in vivo Pig-a gene mutation assay, a potential tool for regulatory safety assessment. *Environ Mol Mutagen.* **51**, 825-835.

Epstein, S.S., Arnold, E., Andrea, J., Bass, W., and Bishop, Y. (1972). Detection of chemical mutagens by the dominant lethal assay in the mouse. *Toxicol Appl Pharmacol* **23**, 288-325.

Erenpreiss, J., Spano, M., Erenpreisa, J., Bungum, M., and Giwercman, A. (2006). Sperm chromatin structure and male fertility: biological and clinical aspects. *Asian J Androl* **8**, 11-29.

Evenson, D., and Jost, L. (2000). Sperm chromatin structure assay is useful for fertility assessment. *Methods Cell Sci* **22**, 169-189.

Evenson, D.P., Darzynkiewicz, Z., and Melamed, M. R. (1980). Comparison of human and mouse sperm chromatin structure by flow cytometry. *Chromosoma* **78**, 225-238.

Festing, M.F., and Altman, D.G. (2002). Guidelines for the design and statistical analysis of experiments using laboratory animals. *ILAR. J* **43**, 244-258.

Gasko, O., and Danon, D. (1974). Endocytosis and exocytosis in membrane remodelling during reticulocyte maturation. *Br J Haematol.* **28**, 463-470.

Gaspari, L., Chang, S.S., Santella, R.M., Garte, S., Pedotti, P., and Taioli, E. (2003). Polycyclic aromatic hydrocarbon-DNA adducts in human sperm as a marker of DNA damage and infertility. *Mutat. Res* **535**, 155-160.

Gelboin, H.V. (1980). Benzo[alpha]pyrene metabolism, activation and carcinogenesis: role and regulation of mixed-function oxidases and related enzymes. *Physiol Rev* **60**, 1107-1166.

Geminard, C., de, G.A., and Vidal, M. (2002). Reticulocyte maturation: mitoptosis and exosome release. *Biocell* **26**, 205-215.

Generoso, W.M., Cain, K.T., Hellwig, C.S., and Cacheiro, N.L. (1982). Lack of association between induction of dominant-lethal mutations and induction of heritable translocations with benzo[a]pyrene in postmeiotic germ cells of male mice. *Mutat. Res* **94**, 155-163.

Giwercman, A., and Giwercman, Y.L. (2011). Environmental factors and testicular function. *Best Practice & Research Clinical Endocrinology & Metabolism* **25**, 391-402.

Godschalk, R.W., van Schooten, F.J., and Bartsch, H. (2003). A critical evaluation of DNA adducts as biological markers for human exposure to polycyclic aromatic compounds. *J Biochem Mol Biol* **36**, 1-11.

Goth-Goldstein, R., and John Burki, H. (1980). Ethylnitrosourea-induced mutagenesis in asynchronous and synchronous Chinese hamster ovary cells. *Mutation Research/Fundamental and Molecular Mechanisms of Mutagenesis* **69**, 127-137.

Halliwell, B. (1991). Reactive oxygen species in living systems: Source, biochemistry, and role in human disease. *The American Journal of Medicine* **91**, S14-S22.

Hecht, S.S. (2003). Tobacco carcinogens, their biomarkers and tobacco-induced cancer. *Nat Rev Cancer* **3**, 733-744.

Heller, C.G., and Clermont, Y. (1963). Spermatogenesis in man: an estimate of its duration. *Science* **140**, 184-186.

Henderson, A.R. (2006). Testing experimental data for univariate normality. *Clinica Chimica Acta* **366**, 112-129.

Holstein, A.F., Schulze, W., and Davidoff, M. (2003). Understanding spermatogenesis is a prerequisite for treatment. *Reprod. Biol Endocrinol.* **1**, 107.

Hotaling, J.M., and Walsh, T.J. (2009). Male infertility: a risk factor for testicular cancer. *Nat Rev Urol.* **6**, 550-556.

Hunt, P., LeMaire, R., Embury, P., Sheean, L., and Mroz, K. (1995). Analysis of chromosome behavior in intact mammalian oocytes: monitoring the segregation of a univalent chromosome during female meiosis. *Hum Mol Genet.* **4**, 2007-2012.

IARC. (1973). Certain Polycyclic Aromatic Hydrocarbons and Heterocyclic Compounds (Update 1998). Vol **3**.

IARC. (2011). Agents classified by the IARC monographs. Vol **1-102**.

Inyang, F., Ramesh, A., Kopsombut, P., Niaz, M.S., Hood, D.B., Nyanda, A.M., and Archibong, A.E. (2009). Disruption of testicular steroidogenesis and epididymal function by inhaled benzo(a)pyrene. *Reproductive Toxicology* **17**, 527-537.

Irvine, D.S., Twigg, J.P., Gordon, E.L., Fulton, N., Milne, P.A., and Aitken, R.J. (2000). DNA integrity in human spermatozoa: relationships with semen quality. *J Androl* **21**, 33-44.

Jaroudi, S., and SenGupta, S. (2007). DNA repair in mammalian embryos. *Mutat. Res* **635**, 53-77.

Jeffrey, A.M. (1985). DNA modification by chemical carcinogens. *Pharmacology & Therapeutics* **28**, 237-272.

Ji, B.T., Shu, X.O., Linet, M.S., Zheng, W., Wacholder, S., Gao, Y. T., Ying, D. M., and Jin, F. (1997). Paternal cigarette smoking and the risk of childhood cancer among offspring of nonsmoking mothers. *J Natl. Cancer Inst.* **89**, 238-244.

Jørgensen, N., Asklund, C., Carlsen, E., and Skakkebaek, N.E. (2006). Coordinated European investigations of semen quality: results from studies of Scandinavian young men is a matter of concern. *Int J Androl* **29**, 54-61.

Kawagoe, K., Takeda, J., Endo, Y., and Kinoshita, T. (1994). Molecular cloning of murine pig-a, a gene for GPI-anchor biosynthesis, and demonstration of interspecies conservation of its structure, function, and genetic locus. *Genomics* **23**, 566-574.

Kemper, A.R., Hayes, R.J., and Bogdanffy, S.M. (2008). Metabolism: A Determinant of Toxicology, in *Principles and Methods of Toxicology* (A.W.Hayes, Ed.), 5 ed., pp. 103-178. Informa Healthcare USA, Inc., New York.

Kidd, S.A., Eskenazi, B., and Wyrobek, A.J. (2001). Effects of male age on semen quality and fertility: a review of the literature. *Fertility and Sterility* **75**, 237-248.

Kim, K.B., and Lee, B.M. (1997). Oxidative stress to DNA, protein, and antioxidant enzymes (superoxide dismutase and catalase) in rats treated with benzo(a)pyrene. *Cancer Lett.* **113**, 205-212.

Klungland, A., Rosewell, I., Hollenbach, S., Larsen, E., Daly, G., Epe, B., Seeberg, E., Lindahl, T., and Barnes, D.E. (1999). Accumulation of premutagenic DNA lesions in mice defective in removal of oxidative base damage. *Proc Natl. Acad. Sci U S A* **96**, 13300-13305.

Knuckles, M.E., Inyang, F., and Ramesh, A. (2001). Acute and subchronic oral toxicities of benzo[a]pyrene in F-344 rats. *Toxicol Sci* **61**, 382-388.

Künzle, R., Mueller, M.D., Hαnggi, W., Birkhαuser, M.H., Drescher, H., and Bersinger, N.A. (2003). Semen quality of male smokers and nonsmokers in infertile couples. *Fertility and Sterility* **79**, 287-291.

Larsen, E., Kwon, K., Coin, F., Egly, J.M., and Klungland, A. (2004). Transcription activities at 8-oxoG lesions in DNA. *DNA Repair (Amst)* **3**, 1457-1468.

Lesko, S.A., and Lorentzen, R.J. (1985). Benzo[a]pyrene dione-benzo[a]pyrene diol oxidation-reduction couples; involvement in DNA damage, cellular toxicity, and carcinogenesis. *J Toxicol Environ Health* **16**, 679-691.

Lewtas, J. (2007). Air pollution combustion emissions: characterization of causative agents and mechanisms associated with cancer, reproductive, and cardiovascular effects. *Mutat. Res* **636**, 95-133.

Lindahl, T., and Wood, R.D. (1999). Quality control by DNA repair. *Science* **286**, 1897-1905.

Lovell, D.P., and Omori, T. (2008). Statistical issues in the use of the comet assay. *Mutagenesis* **23**, 171-182.

Low, M.G. (1989). Glycosyl-phosphatidylinositol: a versatile anchor for cell surface proteins. *FASEB J* **3**, 1600-1608.

MacKenzie, K.M., and Angevine, D.M. (1981). Infertility in mice exposed in utero to benzo(a)pyrene. *Biol Reprod.* **2**4, 183-191.

Marchetti, F., and Wyrobek, A.J. (2005). Mechanisms and consequences of paternally-transmitted chromosomal abnormalities. *Birth Defects Res C Embryo. Today* **75**, 112-129.

Mattison, D.R., White, N.B., and Nightingale, M.R. (1980). The effect of benzo(a)pyrene on fertility, primordial oocyte number, and ovarian response to pregnant mare's serum gonadotropin. *Pediatr Pharmacol (New York)* **1**, 143-151.

Meier, U. (2006). A note on the power of Fisher's least significant difference procedure. *Pharmaceut. Statist.* **5**, 253-263.

Miller, K.P., and Ramos, K.S. (2001). Impact of cellular metabolism on the biological effects of benzo[a]pyrene and related hydrocarbons. *Drug Metab Rev* **33**, 1-35.

Miura, D., Dobrovolsky, V.N., Kasahara, Y., Katsuura, Y., and Heflich, R.H. (2008). Development of an in vivo gene mutation assay using the endogenous Pig-A gene: I. Flow cytometric detection of CD59-negative peripheral red blood cells and CD48-negative spleen T-cells from the rat. *Environ Mol Mutagen.* **49**, 614-621.

Miura, D., Dobrovolsky, V.N., Kimoto, T., Kasahara, Y., and Heflich, R.H. (2009). Accumulation and persistence of Pig-A mutant peripheral red blood cells following treatment of rats with single and split doses of N-ethyl-N-nitrosourea. *Mutat. Res* **677**, 86-92.

Moore, H.D. (1998). Contribution of epididymal factors to sperm maturation and storage. *Andrologia* **30**, 233-239.

Nagy, A., Gertsenstein, M., Vintersten, K., and Behringer, R. (2003). Assisted reproduction, in *Manipulating the Mouse Embryo* (J.Inglis and J.Cuddihy, Eds.), 3 ed., pp. 565-597. Cold Spring Harbor Laboratory Press, New York.

Ni, Z.Y., Liu, Y.Q., Shen, H.M., Chia, S.E., and Ong, C.N. (1997). Does the increase of 8-hydroxydeoxyguanosine lead to poor sperm quality? *Mutat. Res* **381**, 77-82.

Nielsen, T., Jørgensen, H.E., Larsen, J.C., and Poulsen, M. (1996). City air pollution of polycyclic aromatic hydrocarbons and other mutagens: occurrence, sources and health effects. *Sci Total Environ* **189-190**, 41-49.

Nikolaou, K., Masclet, P., and Mouvier, G. (1984). Sources and chemical reactivity of polynuclear aromatic hydrocarbons in the atmosphere -- A critical review. *Science of The Total Environment* **32**, 103-132.

Noveroske, J.K., Weber, J.S., and Justice, M. J. (2000). The mutagenic action of N-ethyl-N-nitrosourea in the mouse. *Mammalian Genome* **11**, 478-483.

Oakberg, E.F. (1956). Duration of spermatogenesis in the mouse and timing of stages of the cycle of the seminiferous epithelium. *Am J Anat.* **99**, 507-516.

Oakberg, E.F., and Diminno, R.L. (1960). X-ray sensitivity of primary spermatocytes of the mouse.int. *Int J Radiat. Biol* **2**, 196-209.

Oliva, R. (2006). Protamines and male infertility. *Hum Reprod. Update* **12**, 417-435.

Olsen, A.K., Andreassen, A., Singh, R., Wiger, R., Duale, N., Farmer, P.B., and Brunborg, G. (2010). Environmental exposure of the mouse germ line: DNA adducts in spermatozoa and formation of de novo mutations during spermatogenesis. *PLoS One* **5**, e11349.

Olsen, A.K., Duale, N., Bjørås, M., Larsen, C.T., Wiger, R., Holme, J.r.A., Seeberg, E.C., and Brunborg, G. (2003). Limited repair of 8–hydroxy–7,8–dihydroguanine residues in human testicular cells. *Nucleic Acids Research* **31**, 1351-1363.

Olsen, A.K., Lindeman, B., Wiger, R., Duale, N., and Brunborg, G. (2005). How do male germ cells handle DNA damage? *Toxicol Appl. Pharmacol* **207**, 521-531.

Parham, P. (2009). Antibody Structure and Generation of B-cell Diversity, in *The Immune System* (T.G.L.Garland Science, Ed.), 3 ed., pp. 95-122. New York.

Patel, V.P., and Lodish, H.F. (1984). Loss of adhesion of murine erythroleukemia cells to fibronectin during erythroid differentiation. *Science* **224**, 996-998.

Pelkonen, O., and Nebert, D.W. (1982). Metabolism of polycyclic aromatic hydrocarbons: etiologic role in carcinogenesis. *Pharmacol Rev* **34**, 189-222.

Penning, T.M. (2004). Aldo-keto reductases and formation of polycyclic aromatic hydrocarbon o-quinones. *Methods Enzymol.* **378**, 31-67.

Perreault, S.D. (1992). Chromatin remodeling in mammalian zygotes. *Mutat. Res* **296**, 43-55.

Peruzzi, B., Araten, D.J., Notaro, R., and Luzzatto, L. (2010). The use of PIG-A as a sentinel gene for the study of the somatic mutation rate and of mutagenic agents in vivo. *Mutat. Res* **705**, 3-10.

Pfeifer, G.P., Denissenko, M.F., Olivier, M., Tretyakova, N., Hecht, S.S., and Hainaut, P. (2002). Tobacco smoke carcinogens, DNA damage and p53 mutations in smoking-associated cancers. *Oncogene* **2**1, 7435-7451.

Pfeifer, H., Conrad, M., Roethlein, D., Kyriakopoulos, A., Brielmeier, M., Bornkamm, G. W., and Behne, D. (2001). Identification of a specific sperm nuclei selenoenzyme necessary for protamine thiol cross-linking during sperm maturation. *FASEB J* **15**, 1236-1238.

Phillips, D.H. (1999). Polycyclic aromatic hydrocarbons in the diet. *Mutat. Res* **443**, 139-147.

Phonethepswath, S., Bryce, S.M., Bemis, J.C., and Dertinger, S.D. (2008). Erythrocyte-based Pig-a gene mutation assay: demonstration of cross-species potential. *Mutat. Res* **657**, 122-126.

Phonethepswath, S., Franklin, D., Torous, D.K., Bryce, S.M., Bemis, J.C., Raja, S., Avlasevich, S., Weller, P., Hyrien, O., Palis, J., MacGregor, J.T., and Dertinger, S.D. (2010). Pig-a mutation: kinetics in rat erythrocytes following exposure to five prototypical mutagens. *Toxicol Sci* **114**, 59-70.

Plummer, J.L., Smith, B.R., Ball, L.M., and Bend, J.R. (1980). Metabolism and biliary excretion of benzo[a]pyrene 4,5-oxide in the rat. *Drug Metab Dispos.* **8**, 68-72.

Potts, R.J., Newbury, C.J., Smith, G., Notarianni, L.J., and Jefferies, T.M. (1999). Sperm chromatin damage associated with male smoking. *Mutation Research/Fundamental and Molecular Mechanisms of Mutagenesis* **423**, 103-111.

Qu, S.X., and Stacey, N.H. (1996). Formation and persistence of DNA adducts in different target tissues of rats after multiple administration of benzo[a]pyrene. *Carcinogenesis* **17**, 53-59.

Ramesh, A., Inyang, F., Hood, D.B., Archibong, A.E., Knuckles, M.E., and Nyanda, A.M. (2001). Metabolism, bioavailability, and toxicokinetics of Benzo([alpha])pyrenein F-344 rats following oral administration. *Experimental and Toxicologic Pathology* **53**, 275-290.

Ramlau-Hansen, C.H., Thulstrup, A.M., Aggerholm, A.S., Jensen, M.S., Toft, G., and Bonde, J.P. (2006). Is smoking a risk factor for decreased semen quality? A cross-sectional analysis. *Human Reproduction* **22**, 188-196.

Richter, C., Park, J.W., and Ames, B.N. (1988). Normal oxidative damage to mitochondrial and nuclear DNA is extensive. *Proceedings of the National Academy of Sciences* **85**, 6465-6467.

Richter, C. (1995). Oxidative damage to mitochondrial DNA and its relationship to ageing. *The International Journal of Biochemistry & Cell Biology* **27**, 647-653.

Riley, R.S., Ben-Ezra, J.M., Goel, R., and Tidwell, A. (2001). Reticulocytes and reticulocyte enumeration. *J. Clin. Lab. Anal.* **15**, 267-294.

Roth, R.A., and Vinegar, A. (1990). Action by the lungs on circulating xenobiotic agents, with a case study of physiologically based pharmacokinetic modeling of benzo(a)pyrene disposition. *Pharmacol Ther* **48**, 143-155.

Rowley, M.J., Teshima, F., and Heller, C.G. (1970). Duration of transit of spermatozoa through the human male ductular system. *Fertil. Steril.* **21**, 390-396.

Rubes, J., Rybar, R., Prinosilova, P., Veznik, Z., Chvatalova, I., Solansky, I., and Sram, R. J. (2010). Genetic polymorphisms influence the susceptibility of men to sperm DNA damage associated with exposure to air pollution. *Mutation Research/Fundamental and Molecular Mechanisms of Mutagenesis* **683**, 9-15.

Ryan, H. (2011) Adresseing sperm DNA integrity and ferilization;establishment of a PCR based method for detection of DNA damage (the MDDA assay). Ref Type:Thesis/Dissertation

Santella, R.M., Lin, C.D., Cleveland, W.L., and Weinstein, I.B. (1984). Monoclonal antibodies to DNA modified by a benzo[a]pyrene diol epoxide. *Carcinogenesis* **5**, 373-377.

Santella, R.M., Weston, A., Perera, F.P., Trivers, G.T., Harris, C.C., Young, T.L., Nguyen, D., Lee, B.M., and Poirier, M.C. (1988). Interlaboratory comparison of antisera and immunoassays for benzo[a]pyrene-diol-epoxide-I-modified DNA. *Carcinogenesis* **9**, 1265-1269.

Schuel, H. (2006). Tuning the oviduct to the anandamide tone. *J Clin Invest* **116**, 2087-2090.

Selkirk, J.K. (1977). Benzo[a]pyrene carcinogenesis: a biochemical selection mechanism. *J Toxicol Environ Health* **2**, 1245-1258.

Shahzadi, S. (2008). Betydning av paternell akrylamideksponering for utvikling av det befruktede egget. Ref Type:Thesis/Dissertation

Shukla, Y., and Taneja, P. (2001). Antimutagenic effect of black tea extract using 'rodent dominant lethal mutation assay'. *Toxicology* **168**, 269-274.

Sikka, S. C., Rajasekaran, M., and Hellstrom, W.J. (1995). Role of oxidative stress and antioxidants in male infertility. *J Androl* **16**, 464-468.

Sims, P., Grover, P.L., Swaisland, A., Pal, K., and Hewer, A. (1974). Metabolic activation of benzo(a)pyrene proceeds by a diol-epoxide. *Nature* **252**, 326-328.

Sipinen, V., Laubenthal, J., Baumgartner, A., Cemeli, E., Linschooten, J.O., Godschalk, R.W., van Schooten, F. J., Anderson, D., and Brunborg, G. (2010). In vitro evaluation of baseline and induced DNA damage in human sperm exposed to benzo[a]pyrene or its metabolite benzo[a]pyrene-7,8-diol-9,10-epoxide, using the comet assay. *Mutagenesis* **25**, 417-425.

Smithgall, T.E., Harvey, R.G., and Penning, T.M. (1988). Spectroscopic identification of ortho-quinones as the products of polycyclic aromatic trans-dihydrodiol oxidation catalyzed by dihydrodiol dehydrogenase. A potential route of proximate carcinogen metabolism. *J Biol Chem* **263**, 1814-1820.

Spectrum Laboratories. Chemical fact sheet. (CAS 50328). Florida.

Steptoe, P.C., and Edwards, R.G. (1978). Birth after the reimplantation of a human embryo. *Lancet* **2**, 366.

Sun, J.D., Wolff, R.K., and Kanapilly, G.M. (1982). Deposition, retention, and biological fate of inhaled benzo(a)pyrene adsorbed onto ultrafine particles and as a pure aerosol. *Toxicology and Applied Pharmacology* **65**, 231-244.

Szeliga, J., and Dipple, A. (1998). DNA adduct formation by polycyclic aromatic hydrocarbon dihydrodiol epoxides. *Chem Res Toxicol* **11**, 1-11.

Takeda, J., Miyata, T., Kawagoe, K., Iida, Y., Endo, Y., Fujita, T., Takahashi, M., Kitani, T., and Kinoshita, T. (1993). Deficiency of the GPI anchor caused by a somatic mutation of the PIG-A gene in paroxysmal nocturnal hemoglobinuria. *Cell* **73**, 703-711.

Takemura, H., Nagayoshi, H., Matsuda, T., Sakakibara, H., Morita, M., Matsui, A., Ohura, T., and Shimoi, K. (2010). Inhibitory effects of chrysoeriol on DNA adduct formation with benzo[a]pyrene in MCF-7 breast cancer cells. *Toxicology* **274**, 42-48.

Talbot, P., and Riveles, K. (2005). Smoking and reproduction: the oviduct as a target of cigarette smoke. *Reprod. Biol Endocrinol.* **3**, 52.

Tarantini, A., Maitre, A., Lefebvre, E., Marques, M., Rajhi, A., and Douki, T. (2011). Polycyclic aromatic hydrocarbons in binary mixtures modulate the efficiency of benzo[a]pyrene to form DNA adducts in human cells. *Toxicology* **279**, 36-44.

Vander, A., Sherman, j., and Luciano, D. (2001a). Circulation, in *Human Physiology* 8 ed., pp. 373-462. McGraw-Hill Companies, Inc., New York.

Vander, A., Sherman, j., and Luciano, D. (2001b). Reproduction, in *Human Physiology* 8 ed., pp. 636-679. McGraw-Hill Companies, Inc., New York.

Verhofstad, N., van Oostrom, C.T., van, B.J., van Schooten, F.J., van, S.H., and Godschalk, R.W. (2010). DNA adduct kinetics in reproductive tissues of DNA repair proficient and deficient male mice after oral exposure to benzo(a)pyrene. *Environ Mol Mutagen.* **51**, 123-129.

Verhofstad, N., van Oostrom, C.T., Zwart, E., Maas, L. M., van Benthem, J., van Schooten, F. J., van Steeg, H., and Godschalk, R. W. L. (2011). Evaluation of Benzo(a)pyrene-Induced Gene Mutations in Male Germ Cells. *Toxicological Sciences* **119**, 218-223.

Vine, M.F. (1996). Smoking and male reproduction: a review. *International Journal of Andrology* **19**, 323-337.

Wells, P.G., McCallum, G.P., Chen, C.S., Henderson, J.T., Lee, C.J., Perstin, J., Preston, T.J., Wiley, M.J., and Wong, A.W. (2009). Oxidative stress in developmental origins of disease: teratogenesis, neurodevelopmental deficits, and cancer. *Toxicol Sci* **108**, 4-18.

Weyand, E.H., and Bevan, D.R. (1986). Benzo(a)pyrene disposition and metabolism in rats following intratracheal instillation. *Cancer Res* **46**, 5655-5661.

Wolterbeek, B. (2002). Biomonitoring of trace element air pollution: principles, possibilities and perspectives. *Environmental Pollution* **120**, 11-21.

Xue, W., and Warshawsky, D. (2005). Metabolic activation of polycyclic and heterocyclic aromatic hydrocarbons and DNA damage: A review. *Toxicology and Applied Pharmacology* **206**, 73-93.

Yamazaki, H., Terada, M., Tsuboi, A., Matsubara, C., Hata, T., and Kakiuchi, Y. (1987). Distribution and binding pattern of benzo(a)pyrene in rat liver, lung and kidney constituents after oral administration. *Toxicological & Environmental Chemistry* **15**, 71-81.

Yang, J.J., Roy, T.A., Krueger, A.J., Neil, W., and Mackerer, C.R. (1989). In vitro and in vivo percutaneous absorption of benzo[a]pyrene from petroleum crude-fortified soil in the rat. *Bulletin of Environmental Contamination and Toxicology* **43**, 207-214.

Zenzes, M.T. (2000). Smoking and reproduction: gene damage to human gametes and embryos. *Hum Reprod. Update* **6**, 122-131.

Zenzes, M.T., Bielecki, R., and Reed, T.E. (1999a). Detection of benzo(a)pyrene diol epoxide-DNA adducts in sperm of men exposed to cigarette smoke. *Fertil. Steril.* **72**, 330-335.

Zenzes, M.T., Puy, L.A., and Bielecki, R. (1998). Immunodetection of benzo[a]pyrene adducts in ovarian cells of women exposed to cigarette smoke. *Mol Hum Reprod.* **4**, 159-165.

Zenzes, M.T., Puy, L.A., Bielecki, R., and Reed, T.E. (1999b). Detection of benzo[a]pyrene diol epoxide-DNA adducts in embryos from smoking couples: evidence for transmission by spermatozoa. *Mol Hum Reprod.* **5**, 125-131.

Zhang, Y.J., Weksler, B.B., Wang, L., Schwartz, J., and Santella, R.M. (1998). Immunohistochemical detection of polycyclic aromatic hydrocarbon-DNA damage in human blood vessels of smokers and non-smokers. *Atherosclerosis* **140**, 325-331.

Zhao, Y., Brezina, P., Hsu, C.C., Garcia, J., Brinsden, P.R., and Wallach, E. (2011). In vitro fertilization: Four decades of reflections and promises. *Biochim. Biophys. Acta* **1810**, 843-852.

Zhu, H., Li, Y.B., and Trush, M.A. (1995). Characterization of Benzo[a]pyrene Quinone-Induced Toxicity to Primary Cultured Bone Marrow Stromal Cells from DBA/2 Mice: Potential Role of Mitochondrial Dysfunction. *Toxicology and Applied Pharmacology* **130**, 108-120.

Zitzmann, M., Rolf, C., Nordhoff, V., Schrder, G., Rickert-Fuhring, M., Gassner, P., Behre, H. M., Greb, R.R., Kiesel, L., and Nieschlag, E. (2003). Male smokers have a decreased success rate for in vitro fertilization and intracytoplasmic sperm injection. *Fertility and Sterility* **79**, 1550-1554.

6. Appendix

6.1 Solutions and media

6.1.1 SCSA

DNase buffer

100ml ddH_2O

40mM Tris-HCl

10mM NaCl

6mM $MgCl_2$

10 mM $CaCl_2$

pH adjusted to 7.9 with 1M NaOH

0.1 % Triton Dnase buffer

100 µl Triton X-100

10 ml Dnase buffer

DNase

1mg/ml ddH_2O (200 U/ml)

TNE buffer, 10X

0.01 M Tris-HCl

0.15 M NaCl

1mM EDTA (disodium)

600 ml ddH_2O

Adjusted pH to 7.4 with 10 mM NaOH, stored at 4°C

TNE buffer, 1X

60ml TNE buffer (10X)

540ml ddH_2O

pH 7,4, stored at 4°C

Acid detergent solution

0.15 M NaCl

0.1 % Triton X-100

0.08 N HCl

500 ml ddH_20

Adjusted pH to 1.2 with 2N HCl, stored at 4° C

Citric acid buffer (0.1 M)

21.01 g citric acid monohydrate, 1 L ddH_20

Stored at 4 °C

Disodium hydrogen phosphate (Na_2HPO_4) buffer (0.2 M)

14.2 g Na_2HPO_4

500 ml ddH_20

Stored at 4 °C

Acridin orange (AO) stock solution (1.0 mg/ml)

5.5 mg Acridin orange

5.5 ml ddH_20

Protected from light and stored at 4°C

Staining buffer

185ml 0.1 M citric acid buffer

315ml 0.2 M Na_2HPO_4 buffer

186mg EDTA (disodium)

4.39g NaCl

Solved EDTA completely on magnetic stirrer

Adjusted pH to 6.0 with NaOH pellet

Stored at 4 °C

Acridin orange (AO) staining solution

100ml staining buffer in light-protected bottle

600 µl AO stock solution

Stored at 4 °C

AO equilibration buffer

400 µl acid detergent solution, 1.2 ml AO staining solution

6.1.2 Immunostaining

Tris Buffer (10mM Trizma base, 1 mM EDTA, 0.4 M NaCl)

10 mM Trizma base

1mM EDTA

0.4 M NaCl

1 L ddH_2O

Adjusted pH to 7.5 with NaOH, stored at 4 °C

Tris base solution
50 mM Trizma base, 1L dd-H_2O

Stored at 4 °C

Blocking solution

5 % BSA with 0.01 % Thimorosal

Stored at 4 °C

PBD (0.1 %)

1L PBS, 1mL Triton X100

Stored at 4 °C

Proteinase K

10 µg Proteinase K, 1 mL Tris buffer

Stored at 4 °C

6.1.3 Pig-a

Solutions used in the preliminary Pig-a experiments

Leukodepletion gradient (Nycoprep, Lymphoprep, Lympholyte)

Heparin in PBS (1:10)

Syto13 (0.157 µM in PBS)

AntiCD24-PE conjugated (1:20 in 2% FCS in PBS)

AntiCD42-APC conjugated (1:10 in 2% FCS in PBS)

Solutions used from Litrons prototype kit

Lympholyte

Anticoagulant solution

Buffered Salt Solution (BSS)

Working Antibody Solution (antiCD24-PE)

Working Nucleic Acid Dye Solution (Syto13)

6.2 Products and producers

Product	**Producer**
Acridin Orange	VWR International, USA
Acetone	VWR International, USA
Agarose	Sigma-Aldrich, Norway AS
Anti Coagulant Solution	Litron laboratories, USA
BD^{TM} cytometer setup and Tracking beads (Lot id 66656)	BD Bioscience, USA
Benzo(a)Pyrene	Sigma-Aldrich, Norway AS
Bovine serum albumin (BSA)	Sigma-Aldrich, Norway AS
BPDE	National Chemical laboratories, USA
Buffered Salt Solution (BSS).	Litron laboratories, USA
Calium chloride (CaCl)	Merck chemicals, USA
Citric acid monohydrate	Merck chemicals, USA
Corn Oil	Sigma-Aldrich, Norway AS
Dako cytomation fluorescence medium	Dako Norway
Dimethyl sulphoxide (DMSO)	Sigma-Aldrich, Norway AS
Disodium hydrogen phosphate (Na_2HPO_4)	Chemi-teknik AS, Norway
Distilled water (ddH2O)	NIPH, Norway
DNase	Roche Diagnostics, Norway AS
EDTA	VWR International, USA
Fibrinogen	Merck chemicals (Calbiochem), USA
Fetal calf serum (FCS)	Med Probe, Norway
Flow cytometer, BD LSR II	BD Bioscience, USA
HCG (Human Chorionic Gonadotropin)	Merck chemicals (Sereno), USA
Heparin	Pharma AS, Denmark
Hoechst 33342	Invitrogen, USA
HTF medium	EmbryoMax, Millipore, USA
Hyase	Vitrolife, Sweden
Hydrogen chloride (HCl)	Merck chemicals, USA
KSOM	EmbryoMax Millipore, USA
Lympholyte	Cedarlane labs, Canada
Lymphoprep	Medinor, Norway
M2 medium	Sigma-Aldrich, Norway AS
Magnesium chloride (MgCl)	Sigma-Aldrich, Norway AS
Methanol	Sigma-Aldrich, Norway AS
N-ethyl-N-nitrosourea (ENU)	Sigma-Aldrich, Norway AS

Nycoprep	Fresenius Kabi, Norway AS
Paraffin (liquid)	MediCult, Norway
Phosphate buffer solution (PBS)	Chemi-teknik AS, Norway
PMSG (Pregnant Mare Serum Gonadotropin)	Intervet (Folligon), Norway
Primary antibody mAb anti-5D11	Nordic BioSite AS, Norway
Primary antibody antiCD24-PE	eBioscience, Canada
CD42d-APC	eBioscience, Canada
Proteinase K	Sigma-Aldrich, Norway AS
Queens Advantage Protein PlusTM Fertilization (HTF) Medium	EmbryoMax, Millipore, USA
Rnase-it	Qiagen GmbH, Germany
RPMI medium 1640	Sigma-Aldrich, Norway AS
Secondary antibody donkey anti-mouse (Alexa:488)	Invitrogen, USA
Sodium chloride (NaCl)	Sigma Aldrich Norway AS
Sodium hydroxide (NaOH)	Merck chemicals, USA
Syto13	Invitrogen, USA
Thimorosal	Sigma Aldrich Norway AS
Triton-X100	VWR International, USA
Trizma base	Sigma-Aldrich, Norway AS
Trizma Hydrochloride, Tris-HCl	Sigma-Aldrich, Norway AS
Thrombin	Sigma-Aldrich, Norway AS
Tryphan blue	VWR International, USA
Trypsin	VWR International, USA
Working antibody solution	Litrons laboratories, USA
Working Nucleic dye Solution	Litrons laboratories, USA